Benemérita Universidad Autónoma de Puebla

Facultad de Ciencias Físico Matemáticas

Posgrado en Ciencias Matemáticas

The problems of construction of the reachable sets for stable oscillatory systems and its applications

Tesis presentada para obtener el grado de
Doctorado en Ciencias (Matemáticas)

Presenta:
Iryna Konovalenko

Director de Tesis:
Dr. Vladimir Alexandrov

Agosto de 2020, Puebla, Puebla.

DRA. LIDIA AURORA HERNÁNDEZ REBOLLAR
SECRETARIA DE INVESTIGACIÓN Y
ESTUDIOS DE POSGRADO, FCFM-BUAP
P R E S E N T E:

Por este medio le informo que la C:

IRYNA KONOVALENKO

estudiante del Doctorado en Ciencias (Matemáticas), ha cumplido con las indicaciones que el Jurado le señaló en el Coloquio que se realizó el día 30 de abril de 2020, con la tesis titulada:

"THE PROBLEMS OF CONSTRUCTION OF THE REACHABLE SETS FOR STABLE OSCILLATORY SYSTEMS AND ITS APPLICATIONS"

Por lo que se le autoriza a proceder con los trámites y realizar el examen de grado en la fecha que se le asigne.

A T E N T A M E N T E.
H. Puebla de Z, a 29 de junio de 2020.

DRA. PATRICIA DOMÍNGUEZ SOTO
COORDINADORA DEL POSGRADO
EN MATEMÁTICAS.

D*PDS/mtrv

Facultad
de Ciencias
Físico Matemáticas

Av. San Claudio y 18 Sur, edif. FM1
Ciudad Universitaria, Col. San
Manuel, Puebla, Pue. C.P. 72570
01 (222) 229 55 00 Ext. 7550 y 7552

DEDICATIONS

I would like to dedicate this work to my dear family.

"Труд и наука — выше этих двух сил нет ничего на земле."

Максим Горький

"Labor and science - above these two forces there is nothing on earth."

Maksim Gorky

ACKNOWLEDGEMENTS

First of all, I want to thank Dr. Vladimir Alexandrov for setting the problem "Reachable set and transitions in a bistable system", for all of your advice and support over the last 7 years, and also for being a great person and a great professional.

Dr. Carlos Guillén Galván, Dr. Lucía Cervantes Gómez, Dr. José Jacobo Oliveros Oliveros, Dra. María Blanca Bermúdez Juárez, Dr. Raúl Temoltzi Ávila thanks for reading this thesis, for your help in improving of this work and for all your time spent for me.

I would like to thank to the administration of Faculty of Physical and Mathematical Sciences for their help and understanding.

I want to thank CONACYT for all the economical support along these years.

CONTENT

INTRODUCTION **7**

1 BASIC THEOREMS AND SOME RESULTS ON THE ANALYSIS AND CONSTRUCTION OF THE REACHABLE SETS **10**

1.1 Reachable set: definition and properties 10

1.2 Application of reachable set for estimation of robust stability under permanent perturbation 18

1.3 Ellipsoidal estimates of the reachable set 31

1.4 Pixel method of construction of reachable sets for nonlinear systems 35

1.5 The conditional gradient method for solving the problem of finding the maximum deviation for two coordinates. . . 40

1.5.1 Example of applying conditional gradient method . 44

1.6 Lemma 1-2 by Demidovich 49

1.7 Application of the reachable sets for solution of the direct transition problem. 50

2 SYNTHESIS OF THE REACHABLE SETS FOR THE PERIODIC ATTRACTOR OF THE SECOND ORDER NONLINEAR SYSTEM **59**

2.1 Statement of the problem of construction of the reachable set in a neighborhood of a periodic attractor of a second-order nonlinear system 59

2.2 Algorithm of construction of the reachable set D_{t_1} in a neighborhood of a periodic attractor 68

2.3 An example of applying the method to the Van der Pol's system 71

2.4 Solution of the problem of inverse transition from the region of attraction of periodic attractor to the region of attraction of point attractor in bistable system 84

3 ANALYSIS AND SYNTHESIS OF THE MODEL OF HODGKIN-HUXLEY OF THE PRIMARY AFFERENT NEURON WITH MODIFICATIONS OF SOTO - ALEXANDROV 87

3.1 Analysis of the Model of Hodgkin - Huxley with modifications of Soto-Alexandrov of the second order. Application of the theorem of Andronov-Leontovich. . . . 87

3.2 Analysis of the Model of Hodgkin-Huxley with modifications of Soto-Alexandrov of the third order 95

3.3 Solution of the problem of inverse transition for model of the second order 106

4 FUNCTIONAL SCHEME OF GALVANIC CORRECTOR OF THE VESTIBULAR APPARATUS 120

CONCLUSIONS 130

Appendices 130

Appendix A First Lyapunov value 130

BIBLIOGRAPHY 131

INTRODUCTION

Reachable sets play a fundamental role in the theories of robust stability and the optimal control. The analysis of reachable sets gives a possibility to solve a wide class of problems related to the study of dynamic models in various fields of natural science. Specifically, such analysis is widely used in rocket science [57], construction of automotive autopilots [26] or neural networks [73]. Therefore, researching and constructing the reachable sets is an actual problem nowadays.

The majority of existing methods of constructing reachable sets can be grouped into two classes:

- analytical construction of reachable sets of linear systems with constant or variable coefficients ([5], [29], [38], [50], [57], [70], [71], [75]);

- numerical calculation of reachable sets for nonlinear systems (different numerical algorithms [26], [33], [55], [60], [61], [63], [64], [73], [74] and methods implemented as Matlab toolboxes: CORA [17], HyPro [49]).

This work provides an algorithm which is a symbiosis of these two methods. On the one hand, this algorithm is a new method for constructing reachable sets for linear systems with variable coefficients. On the other hand, it is possible to obtain an approximation of the reachable set for a nonlinear system. The sequence of reachable sets for a linear system, constructed in the neighborhood of the periodic attractor of a nonlinear system, is an approximation of the reachable set of nonlinear system. The approximation can be obtained with any desired numerical accuracy by increasing the number of sequence elements and the quantity of boundary points for each element. It turns out that the

proposed method requires less computational resources and reachable set is properly constructed using a personal computer in contrast with other numerical methods, which mainly dedicated to use the cluster parallel computing.

The algorithm gives the approximation of the reachable sets in the neighborhood of the limit cycle for the perturbed nonlinear Van der Pol system and for the nonlinear modified model of Hodgkin-Huxley. Moreover, the constructed reachable set for the modified Hodgkin-Huxley system is used to solve the problem of the inverse transition between periodic and point attractors.

Chapter 1 of this work presents a brief overview of the reachable sets theory for linear systems with constant coefficients constructed in the neighborhood of a point attractor (estimates of the reachable sets, methods of construction and applications of these sets for practice). In addition to the already known definitions and theorems, in Chapter 1 we introduce the new definition and properties of the reachable set for a linear system with periodic coefficients constructed in the neighborhood of a periodic attractor.

Chapter 2 describes the algorithm of constructing a reachable set of a linear system with periodic coefficients in the presence of a permanent acting perturbation and gives an illustrative example. This linear system corresponds to a nonlinear perturbed system, which has a periodic attractor when perturbation is equivalent to zero function. The linear system is constructed in the neighborhood of a periodic attractor of a nonlinear system and moves along an asymptotically orbitally stable limit cycle. In addition, using the constructed reachable set we solve the inverse transition problem in a bistable system. That is, the transition from the region of attraction of a periodic attractor to the region of attraction of a point attractor.

The theoretical results described in Chapters 1 and 2 are applied to solve practical problems in Chapter 3. Specifically, we analyze and compare the behavior of the modified Hodgkin-Huxley models of second and third order. Besides, the reachability set in the neighborhood of the point attractor of the third order system is estimated and the problem of the inverse transition in the second order system is solved.

Chapter 4 represents the functional scheme of a galvanic corrector of the human vestibular apparatus and its practical realization. It also contains a brief description of the experiment conducted using this device in the Laboratory of Mathematical Modeling and Dynamic Systems at Department of Applied Mechanics and Control of Moscow State University in October of 2018. By using the constructed galvanic stimulator it is possible to solve two important problems. The first one is the galvanic imitation of a vestibule-ocular reflex on the stand of a reference type with tilt angles that do not allow the dynamic simulation of the vestibule-ocular reflex [40]. The other one is the problem of improvement of the quality of pilot gaze stabilization in extreme flight situations [67].

BASIC THEOREMS AND SOME RESULTS ON THE ANALYSIS AND CONSTRUCTION OF THE REACHABLE SETS

1.1 Reachable set: definition and properties

Consider a space $\Omega(E^n)$ consisting of all non empty compact subsets of space E^n.

The algebraic sum of two non empty compact sets $F, G \in \Omega(E^n)$ is the set

$$F + G = \{x = f + g : \ f \in F, \ g \in G\}.$$

The sum $F + G$ of two sets $F, G \in \Omega(E^n)$ is also a nonempty closed and bounded set [29].

The operation of an algebraic sum for any sets $F, G \in \Omega(E^n)$ is commutative, associative, and there is a zero element $\{0\}$ in space $\Omega(E^n)$.

The product of a set $F \in \Omega(E^n)$ by a number λ is called a set

$$G = \lambda F = \{g = \lambda f : \ f \in F\}.$$

The product of a set $F \in \Omega(E^n)$ by a number λ is a non empty closed and bounded set. The operation of multiplication is associative and has a neutral multiplicative element $\{1\} \in \Omega(E^n)$.

Thus, the space $\Omega(E^n)$ is not a linear space with operations of the algebraic sum of two sets and multiplication by a number. Not every element $F \in \Omega(E^n)$ has an inverse element $-F$. Distribution law is not always true, that is, it is not always true

$$(\alpha + \beta)F = \alpha F + \beta F, \ \alpha, \beta \in \mathrm{R}.$$

In the space $\Omega(E^n)$ we introduce the Hausdorff metric, or the distance $d(F,G)$ between the two sets $F,G \in \Omega(E^n)$ as:

$$d(F,G) = \min\{r \geqslant 0 :\ F \subset G + S_r(0),\ G \subset F + S_r(0)\},$$

where $S_r(0)$ is a sphere with the radius f and center in the point 0.

Function $d(F,G)$ satisfies all axioms of distance (the proof is given by [29]).

Consider a controlled object whose behaviour is described by a linear system of differential equations:

$$\dot{x} = Ax + bv. \tag{1}$$

Here A is a constant matrix, b is a vector of absence or presence of control in the system. The set of initial conditions $M_0 \in \Omega(E^n)$. The class of admissible controls V consists of all Lebesgue integrable on a time interval $I = [t_0, t_1]$ functions $v(t)$, that is $v(t) \in V,\ V \in \Omega(E^n)$.

Definition. ***Reachable set*** $D(t)$ *at time* t *is defined as the set of all points of the phase space* E^n*, which can be reachable in the time interval* $[t_0, t_1]$ *from all possible points of the initial set* M_0 *by the trajectories of solutions (1) with all possible admissible controls* $v(t)$*.*

Thus, a reachable set $D(t)$ consists of all points of the form $\{x(t)\}$, where $x(t)$ — solution of the equation (1) with initial condition $x(t_0) \in M_0$ and with admissible control $v(t)$ (Fig. 1). Reachable set depends on the matrix A, functional set of controls V, set of initial states M_0 and the time interval $[t_0, t_1]$.

Properties of the reachable set:

Property 1'. Reachable set $D(t)$ can be presented in the form

$$D(t) = e^{(t-t_0)A}M_0 + \int_{t_0}^{t} e^{(t-s)A}bV\,ds, \tag{2}$$

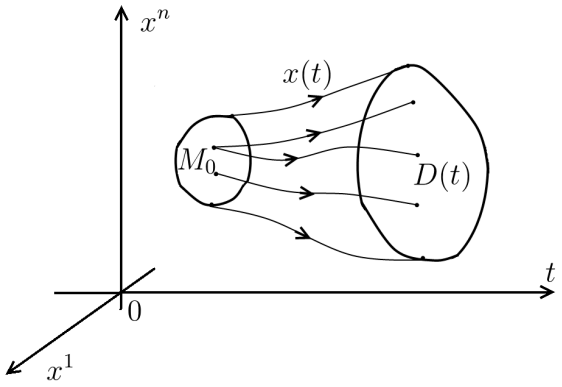

Fig. 1: Reachable set $D(t)$.

where $e^{(t-t_0)A}M_0$ is the image of the set M_0 under a linear transformation $e^{(t-t_0)A}$. Under the integral sign implied the multi valued mapping, which is obtained for all $s \in [t_0, t]$ as the image of the set V under a linear transformation $e^{(t-s)A}$.

Property 2'. The reachable set is a non-empty compact subset of the phase space E^n, i.e. $D(t) \in \Omega(E^n)$.

Property 3'. If the set of initial conditions M_0 is convex, then the reachable set $D(t)$ is convex also.

Property 4'. The support function of the reachable set is

$$c(D(t), \psi) = c(M_0, e^{(t-t_0)A^*}\psi) + \int_{t_0}^{t} c(bV, e^{(t-s)A^*}\psi)ds.$$

The *support function* $c(D(t), \psi)$ of the reachable set $D(t)$ is understood as the scalar function of the vector argument $\psi \in E^n$ determined by the condition

$$c(D(t), \psi) = \max_{x \in D(t)} \langle x, \psi \rangle .$$

Here $\langle x, \psi \rangle$ - scalar product of vectors $x = (x^1, ..., x^n)$ and $\psi =$

$(\psi^1, ..., \psi^n)$, given by the formula:

$$\langle x, \psi \rangle = \sum_{i=1}^{n} x^i \psi^i.$$

Property 5'. Let τ — length of time interval $[t_0, t]$, i.e. $\tau = t - t_0$. Then the reachable set $D(t)$ depends only on the length of interval τ and has form

$$D(t) = e^{\tau A} M_0 + \int_0^{\tau} e^{sA} bV ds.$$

Property 6'. The support function $c(D(t), \psi)$ as the function of the length of interval $\tau = t - t_0$ has form

$$c(D(t), \psi) = c(M_0, e^{\tau A^*} \psi) + \int_0^{\tau} c(bV, e^{sA^*} \psi) ds.$$

Property 7'. Reachable set $D(t)$ is continuously dependent on the argument t, i.e. multi valued transition $D(\cdot) : I \to \Omega(E^n)$ is continuous in the Hausdorff metric.

Demonstrations of properties 1'-7' are presented in the work [29].

Consider a linear dynamical system:

$$\dot{x} = A(t)x + B(t)v(t), \tag{3}$$

where $A(t)$ and $B(t)$ are $(n \times n)$ time-varying matrices. Here the space of controls is the function space $L_p(t_0, t_1)$ for various values of p, $1 \leqslant p \leqslant \infty$ and arbitrary finite intervals of time (t_0, t_1):

$$v \in V \subset L_p(t_0, t_1). \tag{4}$$

ASSUMPTIONS. The following assumptions are being used further:

1. Every element of the matrix $A(t)$ is integrable on each finite time interval (t_0, t_1).

2. If the admissible controls for a given problem are elements of the $L_p(t_0, t_1)$ space, then every element of the matrix $B(t)$ is an element of the $L_{p'}(t_0, t_1)$ space, where

$$p' \geqslant \frac{p}{p-1}.$$

3. $L_1(t_0, t_1)$ denotes that space of measures which make up the bounded linear functionals on $L_\infty(t_0, t_1)$. It means, that space $L_1(t_0, t_1)$ contains not only the Lebesgue integrable functions on (t_0, t_1), but also the symbolic or generalized function $\delta(t-\tau)$, where $t_0 < \tau < t_1$, commonly referred to as the "delta-function" or "Dirac function":

$$\delta(t-\tau) = \int_{-\infty}^{\infty} \delta(\tau - x)\delta(x-t)dx = \begin{cases} +\infty, & t = \tau, \\ 0, & t \neq \tau. \end{cases}$$

4. If the admissible controls for a given problem are elements of the $L_1(t_0, t_1)$ space, then every element of the matrix $B(t)$ is continuous.

Definition. *(reachable state). Consider the system (3) with initial state $x(t_0) = x_0$ and admissible controls which satisfy relation (4) on every finite time interval (t_0, t_1) for a given control set V. The* ***state*** *$x_1 \in E^n$ is said to be* ***reachable*** *at time t_1 from $x(t_0) = x_0$ if there exists an admissible control and a time $t_1 \geqslant t_0$ such that the corresponding solution of system (3) at time t_1 coincides with x_1, i.e.,*

$$x(t_1) = \Phi(t_1, t_0)x_0 + \int_{t_0}^{t_1} \Phi(t_1, t)B(t)v(t)dt = x_1 \text{ for some } v \in V.$$

Definition. *(reachable set). The* ***reachable set*** *$D(t_1, x_0) \subset E^n$ at time t_1 for the system (3) with control constraint set V is defined as the set of all states $x \in E^n$ reachable at time t_1 from $x(t_0) = x_0$ by*

admissible controls:

$$D(t_1, x_0) = \left\{ x \in E^n : x = \Phi(t_1, t_0)x_0 + \int_{t_0}^{t_1} \Phi(t_1, t)B(t)v(t)dt,\ v \in V \right\}.$$

The set $D(t_1, x_0)$ *is a rigid translate of the set* $D(t_1, 0)$ *and denoted by* $D(t_1)$*:*

$$D(t_1) = \left\{ x \in E^n : x = \int_{t_0}^{t_1} \Phi(t_1, t)B(t)v(t)dt,\ v \in V \right\}. \qquad (5)$$

Property 1*. If the control set V are symmetric about the null function $v(t) \equiv 0$ on $[t_0, t_1]$, the reachable sets $D(t)$ are symmetric about the origin of E^n.

Property 2*. If system (1) is time-invariant, then the set $D(t_1)$ grows monotonically with t_1:

$$D(t_1) \subset D(t_2) \text{ for } t_1 \leqslant t_2.$$

Demonstrations of Properties 1*-2* are presented in [57].

Theorem (1)**.** *Consider system (3) with initial state* $x(t_0) = 0$ *and control set* $V = V_p$, $1 \leqslant p \leqslant \infty$, *and let the Assumptions 1-4 be satisfied. Then the reachable set* $D(t_1)$ *given by (5) is convex, compact, and grows strictly monotonically with* c_p *for all* p *in* $1 \leqslant p \leqslant \infty$.

Theorem (2)**.** *Consider system (3) with the matrices* A *and* B *constant, and let* λ_i, $i = 1, 2, ..., n$ *denote the eigenvalues of* A. *Let the initial state be* $x(t_0) = 0$, *the control set* $V = V_p$, $1 \leqslant p \leqslant \infty$, *and let the Assumptions 1-4 be satisfied. The infinite-time reachable set* $D(\infty)$ *is defined as*

$$D(\infty) = \lim_{t_1 \to \infty} D(t_1).$$

If $Re(\lambda_i) < 0$ *for all* $i = 1, 2, ..., n$, *then* $D(\infty)$ *is bounded for all* p *in* $1 \leqslant p \leqslant \infty$.

Proofs of the theorems 1-2 are given in the work [57].

Some results of this dissertation finding and using the reachability set for the system (1), constructed in the neighborhood of a point attractor (Sections 1.2 and 1.6). However, the most important and interesting results, obtained for the system in variations in the neighborhood of a periodic attractor. That is, for a system (3) that satisfies some additional conditions.

Consider the nonlinear dynamical system of the form:

$$\begin{cases} \dot{y} = f(y) + bv(t), \\ v(\cdot) \in V = \{v(\cdot) \in KC |\ |v(t)| \leqslant \delta_1 < 1,\ t \in (0, t_1 < \infty)\}, \end{cases} \tag{6}$$

which has the periodic solution $y^0(t+T) = y^0(t)$ with period T.

A system in variations constructed in the neighborhood of the limit cycle $y^0(t)$

$$\dot{x} = A(t)x + bv(t),\ x = y - y^0(t),\ A = \left(\frac{\partial f(y^0(t))}{\partial y_i} \right),\ i = 1, 2, \tag{7}$$

has a number of significant differences with the system (3).

1. The origin of the system (7) moves on the orbit of the limit cycle $y^0(t)$ with a period T, since the matrix $A(t+t) = A(t)$ is a T-periodic.

2. Further, the reachable set of system (7) in the neighborhood of a periodic attractor $y^0(t)$ will be found only for second-order systems.

3. Initial conditions are zero $x(t_0) = x_0 = 0$.

4. Initial time is $t_0 = 0$.

5. Matrix $B(t)$ of the system (3) is the constant matrix $b = (b_1, b_2)^T$, $b_1, b_2 \in \mathrm{R}$.

Definition. *The reachable set of the system (7), constructed in the neighborhood of the periodic attractor* $y^0(t)$ *of the nonlinear system (6), is the set of the form:*

$$D(t_1) = \left\{ x \in E^n : \; x = \int_0^{t_1} X(t_1) \cdot X^{-1}(s) b v(s) ds, \; v \in V \right\}, \qquad (8)$$

where matrix $X(t)$ *is a normalized fundamental matrix of solutions of the system (7) for* $v(t) \equiv 0$ *and* $X(0) = E_2$.

Property 1. If the set $V = \{v(\cdot) \in KC| \; |v(t)| \leqslant \delta_1 < 1, \; t \in (0, t_1 < \infty)\}$ is symmetric with respect to the zero function $v(t) \equiv 0$ for $t \in [0, t_1]$, then the reachable set $D(t_1)$ is also symmetric with respect to the origin of E^2.

Indeed, the maximum and minimum deviations of coordinates x_i, $i = 1, 2$, determined by the expressions

$$\max_{v \in V} x_i(t_1) = \delta_1 \int_0^{t_1} \left| e_i^T X(t_1) \cdot X^{-1}(s) b \right| ds,$$

$$\min_{v \in V} x_i(t_1) = -\delta_1 \int_0^{t_1} \left| e_i^T X(t_1) \cdot X^{-1}(s) b \right| ds,$$

are always symmetric about the origin.

Property 2. Set $D(t_1)$ is a non empty compact subset of E^2.

The normalized fundamental matrix of solutions $X(t)$ is continuous and non singular. Thus, its inverse matrix $X^{-1}(t)$ is continuous and non singular. Therefore the product of two continuous matrices $X(t) \cdot X^{-1}(t)$ is a continuous matrix also.

Therefore, the demonstration of the Property 2. goes from the formula (8) and the Theorem of non-emptiness and compactness of the integral of the multi-valued mapping [29].

Property 3. Set $D(t_1)$ is a continuously depends from t_1.

The Property 3. obviously follows from the formula (8).

Property 4. Set $D(t_1)$ is convex.

The system (7) satisfies Assumptions 1–4, therefore the Theorem (1) is also true for it.

Property 5. If $t_1 < t_2$ and $t_2 - t_1 = kT$ ($k \in \mathrm{N}$ and T is a period of $y^0(t)$), then

$$D(t_1) \subset D(t_2).$$

For $t = t_1$ and $t = t_2$ systems (7) become time-invariant. If $t_1 < t_2$ and $t_2 - t_1 = kT$ the origins of these systems are coincide. Thus, the Property 2* is satisfied. If the $t_1 < t_2$ and the difference $t_2 - t_1 \neq kT$, than Property 5 does not necessarily holds.

It should be emphasized, that the reachability problem consists from the finding set of all final reachable states $x(t_1)$, starting from a given initial state $x(t_0)$. By finding a set of reachability $D(t_1)$, can be solved the problems of robust stability (only for point attractors) and the transition problems in a bistable systems (for point and periodical attractors).

1.2 Application of reachable set for estimation of robust stability under permanent perturbation

Construction of reachable set can be applied for estimation of robust stability under permanent perturbation. If $D_\infty \to 0$ for $t \to \infty$, then system (1) is asymptotically stable, for example in [9], [14]. If reachable set $D_\infty = R^n$, then system (1) is not robustly stable. In all other cases we speak about the robust stability of the system (1) and use the estimation of this stability [1].

To construct the reachable set D_∞, first of all we need to solve the problem of maximum deviation.

The problem of the accumulation of perturbations, posed by Bulgakov, was the first among the extreme problems for system with

additive perturbation. In 1939, he set and solved the problem of the influence of the northern component of the speed of the ship on the perturbation of the gyro-compass [32]. The ship's speed was a piece-wise continuous function, limited in absolute value. In 1946, Bulgakov gave a complete solution to the problem of the maximum deviation of a linear system along one coordinate [31].

1.2.1. Consider the system of equations with a small perturbations

$$\frac{dx_i}{dt} = f_i(t, x_1, x_2, ..., x_n), \quad x_i(t_0) = x_{i0}. \tag{9}$$

Then, for a small range of t $(\bar{t}_0 \leqslant t \leqslant \bar{\bar{t}}_0)$ system (9) should be replaced by a perturbed system:

$$\frac{dx_i}{dt} = f_i(t, x_1, x_2, ..., x_n) + R_i(t, x_1, x_2, ..., x_n), \quad x_i(\bar{t}_0) = \tilde{x}_i(\bar{t}_0) \tag{10}$$

where all the $R_i(t, x_1, x_2, ..., x_n)$ are small in absolute value.

When $t \geqslant \bar{\bar{t}}_0$, the perturbations cease and we again revert to (9). However, the specific change of the initial values in $\bar{\bar{t}}_0$, $x_i(\bar{\bar{t}}_0) = \tilde{x}(\bar{\bar{t}}_0) + \delta_i$ $(i = 1, 2, ..., n)$, where $\tilde{x}_i(t)$ is the investigated solution of the system (9), and all the δ_i are small in absolute value for small $|R_i|$ (Fig. 2).

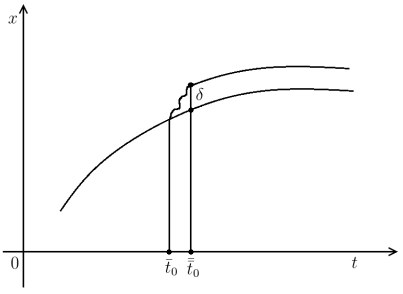

Fig. 2: Alike motions of the system for different initial conditions.

Therefore, the problem of a short-time perturbations reduces to the problem of initial perturbations, i.e. the problem of stability with respect to such short-time or instantaneous perturbations reduces to the problem of stability in the sense of Lyapunov [59], [72]. Hence, if perturbations are permanent, then system (9) must be replaced by the system (10) for all $t \geqslant t_0$ and a completely new problem of stability under permanent perturbations arises.

This problem has been investigated by I. Malkin and G. Duboshin [51].

It is possible to transform the investigated solution $y_i = \phi_i(t)$ $(i = 1, 2, ..., n)$ of the system $\frac{dy_i}{dt} = \Phi_i(t, y_1, ..., y_n)$ $(i = 1, 2, ..., n)$ into the trivial solution $x_i \equiv 0$ $(i = 1, 2, ..., n)$ of the transformed system (by a change of variables $x_i = y_i - \phi_i(t)$ $(i = 1, 2, ..., n)$). Therefore, we investigate the stability of the trivial solution $x_i \equiv 0$ $(i = 1, 2, ..., n)$ of the system (9).

Definition. *The trivial solution of the system (9) is called* ***stable with respect to permanent perturbations*** *if for every $\varepsilon > 0$ it is possible to choose $\delta_1 > 0$ and $\delta_2 > 0$ such that from the inequalities $\sum_{i=1}^{n} R_i^2 < \delta_1^2$ for $t \geqslant t_0$ and $\sum_{i=1}^{n} x_{i0}^2 < \delta_2^2$ it follows that*

$$\sum_{i=1}^{n} x_i^2(t) < \varepsilon^2 \quad for \quad t \geqslant t_0$$

where $x_i(t)$ $(i = 1, 2, ..., n)$ is the solution of the system (10) defined by the initial conditions $x_i(t_0) = x_{i0}$.

Theorem. ***(Malkin's theorem):*** *If for the system of equations (9) there exists a differentiable Lyapunov function $v(t, x_1, x_2, ..., x_n)$ which satisfies the following conditions in the neighborhood of the coordinate origin for $t \geqslant t_0$:*

1. *$v(t, x_1, x_2, ..., x_n) \geqslant w_1(x_1, x_2, ..., x_n) \geqslant 0$, $v(0, 0, ..., 0) = 0$, where*

w_1 *is a continuous function that vanishes only at the origin;*

2. *derivatives* $\frac{\partial v}{\partial x_s}$ $(s = 1, 2, ..., n)$ *are bounded in absolute value;*

3. *derivative* $\frac{dv}{dt} = \frac{\partial v}{\partial t} + \sum_{i=1}^{n} \frac{\partial v}{\partial x_i} f_i \leqslant -w_2(x_1, x_2, ..., x_n) \leqslant 0\,,$

where the continuous function $w_2(x_1, x_2, ..., x_n)$ *can vanish only at the origin, then the trivial solution of the system (9) is stable under permanent perturbations.*

The proof of the Malkin's theorem can be find in [37].

Consequence of the Malkin's theorem: *A stable equilibrium point* $x_i \equiv 0$ $(i = 1, 2, ..., n)$ *of the system*

$$\frac{dx_i}{dt} = \sum_{j=1}^{n} a_{ij} x_j + R_j(t, x_1, ..., x_n),\ (i = 1, ..., n) \tag{11}$$

is stable under permanent perturbations, if all the a_{ij} *are constant and the* R_i *satisfy the conditions of the Lyapunov theorem (that is* $|R_i| \leqslant N(\sum_{i=1}^{n} x_i^2)^{\frac{1}{2}+\alpha}$, $\alpha > 0$, N *is constant, and all the roots of the characteristic equation of the first-approximation system are distinct and negative). After changing of variables that reduce the linear parts of equation (11) to the canonical form, a Lyapunov function* $v = \sum_{i=1}^{n} y_i^2$ *satisfied all conditions of the Malkin's theorem; hence, the equilibrium point* $x_i \equiv 0$ *is stable under permanent perturbations.*

1.2.2. Consider dynamical system with small permanent perturbation in additional form:

$$\begin{cases} \ddot{x}_1 + 2\mu\dot{x}_1 + \lambda^2 x_1 = v(t), \\ v(\cdot) \in V = \{v(\cdot) \in KC|\ |v(t)| \leqslant \delta_1 < 1\}, \end{cases} \tag{12}$$

where $\delta_1 \equiv \text{const} \in (0, 1)\,,\ 0 < \mu < \lambda\,.$

The problem of finding the worst perturbation was solved in the

work [75] by considering the problem of minimization of the functional

$$\phi_0(x_1(t_1)) = x_1(t_1) \to \min_{|v(t)|\leqslant\delta_1} , \; x_2 = 0.$$

Using the Pontryagin Maximum Principle, could be obtained the expression for worst perturbation:

$$v^0(t) = \delta_1 \cdot sign(\dot{x}_1(t)).$$

Solving the problem of finding the maximum deviation on the half periods of the system oscillations, we obtain a similar expression for every next amplitude (comprehensive solution of the problem is presented in the master thesis [46]). Thus, solving successively the problem of finding the maximum deviation of amplitude, can be obtained a sequence of the amplitudes $\{\alpha_n\}$, n-th member of which has the following form:

$$\alpha_n = \frac{1}{\lambda^2}\left(\lambda^2 \cdot \alpha_{n-1} \cdot e^{-\frac{\pi\mu}{\omega}} + \delta_1(1 + e^{-\frac{\pi\mu}{\omega}})\right)$$

where $\omega = \sqrt{\lambda^2 - \mu^2}$ is frequency of self-oscillations of the system (12) with $v(t) \equiv 0$ for all $t \in [0, \infty)$.

The amplitude of self-oscillations α^*, corresponding to the limit cycle, obtained as the limit of the contraction mappings of Poincaré's, when axes x_1 is the section of Poincaré on the phase plan [36]:

$$\alpha^* = \frac{\delta_1}{\lambda^2}\left(\frac{1 + e^{-\frac{\pi\mu}{\omega}}}{1 - e^{-\frac{\pi\mu}{\omega}}}\right).$$

The section of Poincaré is line $\dot{x}_1 = 0$ (Fig. 3).

The limit cycle of self-oscillations of the system (12) can be find by solving the problem of maximum deviation in direct time [16], [9], here sign "$+$" corresponds the upper half of the cycle and "$-$" the lower half:

$$\begin{cases} x_1(t) = \pm\frac{\delta_1}{\lambda^2} \cdot \left[1 - \frac{2e^{-\mu t}}{1 - e^{-\frac{\pi\mu}{\omega}}}\left(\frac{\mu}{\omega}sin(\omega t) + cos(\omega t)\right)\right], \\ x_2(t) = \pm\delta_1 \cdot \frac{2e^{-\mu t}}{\omega(1 - e^{-\frac{\pi\mu}{\omega}})}sin(\omega t). \end{cases} \tag{13}$$

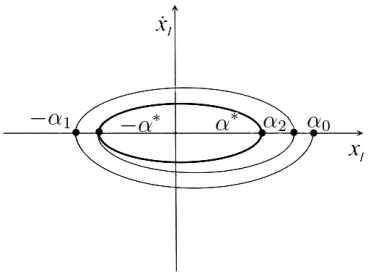

Fig. 3: Section of Poincaré $\dot{x}_1 = 0$.

Asymptotic orbital stability of this limit cycle is shown in [46].

Finding the limit of the contraction mappings of Poincaré (when Poincaré's section is the axis x_1 on the phase plane) gives the amplitude of oscillations corresponding to the limit cycle. Thus, the union of the set of points inside the cycle and the set of points on the cycle orbit gives reachable set D_∞.

The exact quality's estimation of robust stability can be found by construction of the reachable set D_∞ (for $t_1 \to \infty$) [58].

Consider the concept of **quality of robust stability** under permanent perturbations with zero initial conditions in case, when the dependence $\varepsilon = \varepsilon(\delta_1)$ is known [11], [7]:

$$\chi = \sup_{0<\delta_1<\delta_1^*} \frac{\varepsilon(\delta_1)}{\delta_1}, \tag{14}$$

where

$$\varepsilon = \max_{0\le t\le T} ||x(t, v^0(t))|| = \max_{0\le t\le T} \max_{1\le i\le 2} \{|x_i(t, v^0(t))|\},$$

$$v^0(t) = \delta_1 \cdot \mathrm{sign}(\dot{x}_1(t)),$$

T – period of movement on the cycle orbit.

The limit cycle describes the boundary of the reachable set, thus, the point which have the maximum distance from the origin belongs to this cycle.

According to the formulas obtained for this maximum distance by Zhermolenko in [15] there are different cases, where ε presented as the radius of the minimal circumscribed circle.

1. For $\mu^2 < \lambda^2 < \frac{1+e^{-\frac{\pi\mu}{\omega}}}{2}$:

$$r_{max1} = \frac{\delta_1}{\lambda^2}\left(\frac{1+e^{-\frac{\pi\mu}{\omega}}}{1-e^{-\frac{\pi\mu}{\omega}}}\right), \quad \chi_1 = \frac{1}{\lambda^2}\left(\frac{1+e^{-\frac{\pi\mu}{\omega}}}{1-e^{-\frac{\pi\mu}{\omega}}}\right). \tag{15}$$

2. For $\frac{1+e^{-\frac{\pi\mu}{\omega}}}{2} < \lambda^2 < 1$ or $1 < \lambda^2$:

$$r_{max2} = \frac{2\delta_1 e^{-\mu T_1} F(T_1)}{\omega\left(1-e^{-\frac{\pi\mu}{\omega}}\right)}, \quad \chi_2 = \frac{2e^{-\mu T_1} F(T_1)}{\omega\left(1-e^{-\frac{\pi\mu}{\omega}}\right)}, \tag{16}$$

where

$$F(T_1) = \sqrt{(\mu \sin\omega T_1 - \omega\cos\omega T_1)^2 + (\sin\omega T_1)^2}$$

and T_1 is the first positive root of the following equation

$$2e^{-\mu t}\left[\mu(1+\lambda^2)\sin\omega t + \omega(1-\lambda^2)\cos\omega t\right] = \omega(1-e^{\frac{-\pi\mu}{\omega}}).$$

Example

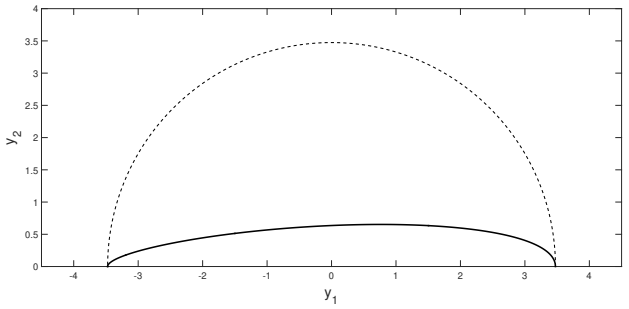

Fig. 4: Limit cycle (solid line) and its circumscribed circle (dotted line) for the first case with small λ.

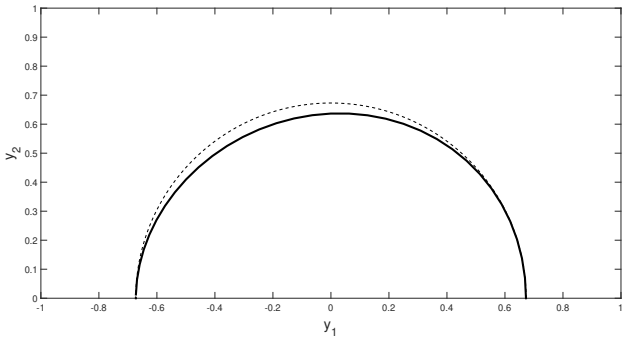

Fig. 5: Limit cycle (solid line) and its circumscribed circle (dotted line) for the second case with larger λ.

Fig. (4) present the upper half of the limit cycle for system (12) (solid line) and the circumscribed circle with radius r_{max1} (dotted line). The parameters of the calculation are $\mu = 0.1,\ \delta_1 = 0.1,\ \lambda_1 = 0.2$. The estimation of the robust stability $\chi_1 = 34,7396$.

Fig. (5) present analogical results, obtained for system (12) with parameters $\mu = 0.1,\ \delta_1 = 0.1,\ \lambda_1 = 0.95$. The estimation of the robust stability $\chi_2 = 6.75495$.

Theorem. *System (12) is robustly stable with the following quality estimation:* χ_1 *(15), if* $\mu^2 < \lambda^2 < \frac{1+e^{-\frac{\pi\mu}{\omega}}}{2}$ *;* χ_2 *(16), if* $\frac{1+e^{-\frac{\pi\mu}{\omega}}}{2} < \lambda^2 < 1$ *or* $1 < \lambda^2$.

1.2.3. Consider the case of linear dynamical system with permanent perturbation in additional and multiplicative forms:

$$\begin{cases} \ddot{x}_1 + 2\mu\dot{x}_1 + (1 + v(t))x_1 = v(t), \\ v(\cdot) \in V = \{v(\cdot) \in KC|\ |v(t)| \leqslant \delta_1 < 1\}, \end{cases} \tag{17}$$

where $\delta_1 \equiv \text{const} \in (0,1),\ \mu \equiv \text{const} \in (0, \sqrt{1-\delta_1})$.

The problem of the maximum deviation was solved in [70], by

finding the minimum of the functional:

$$\phi_0(x_1(t_1)) = x_1(t_1) \to \min_{|v(t)|\leqslant\delta_1} , \; x_2 = 0.$$

According to the Pontryagin Maximum Principle worst perturbation has form:

$$v^0(t) = \begin{cases} \delta_1, & \text{if } \dot{x}_1(t)[1 - x_1(t)] > 0, \\ -\delta_1, & \text{if } \dot{x}_1(t)[1 - x_1(t)] < 0. \end{cases} \tag{18}$$

Integrating system (17) in the inverse time $\tau = t_1 - t$ on the first half-interval with initial and boundary conditions $x_1(0) = -\beta_0$ (first maximum amplitude), $x_2(0) = 0$, and $x_1(\tau_1) = \alpha_0$ (initial amplitude), $x_2(\tau_1) = 0$, can be obtained the expression for the first maximum amplitude β_0:

$$\begin{aligned} \beta_0 &= \alpha_0 e^{-\frac{\pi\mu}{\omega_0}} + \tfrac{\delta_1}{1-\delta_1}(1 + e^{-\frac{\pi\mu}{\omega_0}}) = \\ &= A\alpha_0 + \tfrac{(1+A)\delta_1}{1-\delta_1}, \end{aligned} \tag{19}$$

where $A = e^{-\frac{\pi\mu}{\omega_0}}$, $\omega_0 = \sqrt{1 - \delta_1 - \mu^2}$.

Employing the procedure already described, continue to solve the boundary value problem for $\tau = t_2 - t$ with initial $x_1(0) = \alpha_1$ (second maximum amplitude), $x_2(0) = 0$ and boundary $x_1(\tau_2) = -\beta_0$ (first maximum amplitude), $x_2(\tau_2) = 0$ conditions. The maximum amplitude on the second half-interval α_1 is:

$$\begin{aligned} \alpha_1 &= \beta_0 e^{-\frac{\pi\mu}{\omega_1}} + \tfrac{\delta_1}{1+\delta_1}(1 + e^{-\frac{\pi\mu}{\omega_1}}) = \\ &= B\beta_0 + \tfrac{(1+B)\delta_1}{1+\delta_1}, \end{aligned} \tag{20}$$

where $B = e^{-\frac{\pi\mu}{\omega_1}}$, $\omega_1 = \sqrt{1 + \delta_1 - \mu^2}$.

Through an iterative process can be obtained two sequences $\{\alpha_n\}$ and $\{\beta_n\}$:

$$\begin{aligned} \beta_k &= A\alpha_k + \tfrac{(1+A)\delta_1}{1-\delta_1}, \\ \alpha_{k+1} &= B\beta_k + \tfrac{(1+B)\delta_1}{1+\delta_1}, \end{aligned} \tag{21}$$

where $k = 0, 1, 2, \ldots$.

Here the section of Poincaré will be the line $\dot{x}_1 = 0$ (Fig. 6).

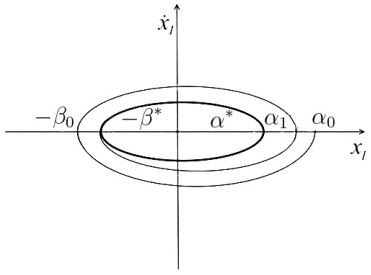

Fig. 6: Section of Poincaré $\dot{x}_1 = 0$.

When the restriction for initial conditions $\alpha_0 < 1$ and the restriction for (μ, δ_1) parameters of the system $\delta_1 < \frac{1-AB}{1+2B+AB}$ holds, the given sequences will be limited ($\alpha_k < 1$ for every $k = 0, 1, 2, \ldots$) and will have limits α^* and β^* [70].

According to the Theorem of a fix point, given in the work [23], sequence $\{\alpha_k\}$ converges to a value $\alpha^* \in R$ and $\{\beta_k\}$ converges to β^*, where:

$$\lim_{k\to\infty} \alpha_k = \alpha^* = \frac{\delta_1}{1-A\cdot B}\left(\frac{(1+A)B}{1-\delta_1} + \frac{1+B}{1+\delta_1}\right), \tag{22}$$

$$\lim_{k\to\infty} \beta_k = \beta^* = \frac{\delta_1}{1-A\cdot B}\left(\frac{1+A}{1-\delta_1} + \frac{(1+B)A}{1+\delta_1}\right). \tag{23}$$

Here $\beta^* > \alpha^*$, and the global orbitally stable limit cycle is located not symmetrically with respect to axis x_2 [2], in contrast to the previous example.

Solving the problem of the maximal deviation for system (17) with $v^0(t) = \delta_1 \cdot \mathrm{sign}(\dot{x}_1(t)[1 - x_1(t)])$ in the direct time t, will be obtained

the asymptotically stable limit cycle of the next form:

$$\begin{cases} x_1^+(t,\alpha^*) = \frac{\delta_1+(1-\delta_1)\alpha^*}{\omega_0\sqrt{1-\delta_1}}e^{-\mu t}\cos\left[\omega_0 t - \arctan\left(\frac{\mu}{\omega_0}\right)\right] - \frac{\delta_1}{1-\delta_1}, \\ x_1^-(t,\beta^*) = -\frac{\delta_1+(1+\delta_1)\beta^*}{\omega_1\sqrt{1+\delta_1}}e^{-\mu t}\cos\left[\omega_1 t - \arctan\left(\frac{\mu}{\omega_1}\right)\right] + \frac{\delta_1}{1+\delta_1}, \\ x_2^-(t,\alpha^*) = -\frac{\delta_1+(1-\delta_1)\alpha^*}{\omega_0}e^{-\mu t}\sin\omega_0 t, \\ x_2^+(t,\beta^*) = \frac{\delta_1+(1+\delta_1)\beta^*}{\omega_1}e^{-\mu t}\sin\omega_1 t, \end{cases} \tag{24}$$

where $\omega_0 = \sqrt{1-\delta_1-\mu^2}$, $\omega_1 = \sqrt{1+\delta_1-\mu^2}$ and α^*, β^* identified in (22), (23) respectively. The proof of the asymptotic orbital stability of this limit cycle obtained in [70].

System (17) is perturbed for every constant v. There is an open area S on the plane of parameters (δ_1, μ) (Fig. 7), where each point corresponds to the perturbed stable system. Construct a curve corresponding to the inequality (25):

$$\mu = \sqrt{\frac{1-\delta_1}{\gamma_0}}, \tag{25}$$

where $\gamma_0 = 1$.

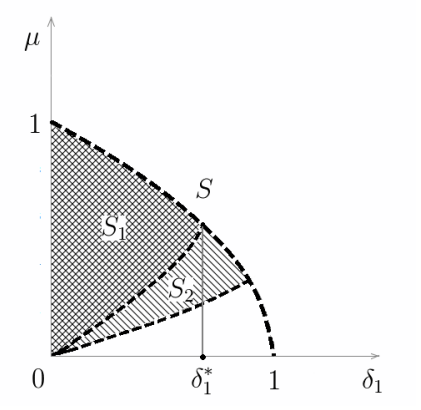

Fig. 7: The regions of the robust stability of the system (17).

There is an open subset $S_1 \cup S_2 \subset S$, where each point corresponds

to the perturbed homogeneous stable subsystem

$$\ddot{x}_1 + 2\mu\dot{x}_1 + (1 + v(t))x_1 = 0, \tag{26}$$

having one singular point $x_1 = \dot{x}_1 = 0$, which is absolutely stable [4].

Fig. 7 shows open area S_1, corresponding the inequality $\mu < \sqrt{1-\delta_1}$, doubly hatched, and area $\{S \setminus (S_1 \cup S_2)\}$ not hatched.

Mathematical model, that realizes self-oscillations of the system (17), is given by:

$$\ddot{x}_1 + (2\mu\dot{x}_1 - \delta_1 \mathrm{sign}n(\dot{x}_1)) + (1 + \delta_1 \mathrm{sign}(\dot{x}_1))x_1 = 0. \tag{27}$$

These self-oscillations - is sustained oscillations of dissipative dynamic system, which supported by the energy of a permanent perturbation. The period of oscillation is $\frac{\pi}{\omega_0} + \frac{\pi}{\omega_1}$. Thus, for a worst v^0 system (27) is a self-oscillating system.

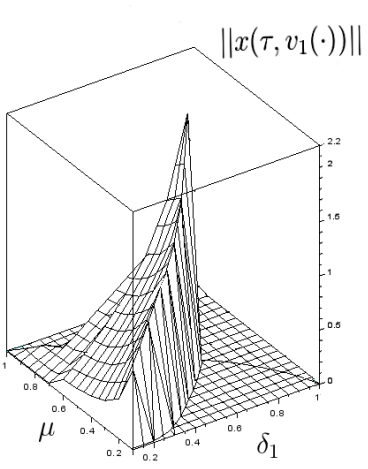

Fig. 8: Estimation of reachable set of the system (17).

Theorem. ***(sufficient condition)*** *If* $(\mu, \delta_1) \in S_1$, *then the*

system (17) is robustly stable with the estimation of quality χ*:*

$$\chi = \max\left\{\left(\frac{1+e^{-\frac{\pi\mu}{\sqrt{1-\mu^2}}}}{1-e^{-\frac{\pi\mu}{\sqrt{1-\mu^2}}}}\right), e^{-\frac{\mu}{\sqrt{1-\mu^2}}\arctan\frac{\sqrt{1-\mu^2}}{\mu}}\left(1+\frac{\left(1+e^{-\frac{\pi\mu}{\sqrt{1-\mu^2}}}\right)}{\left(1-e^{-\frac{\pi\mu}{\sqrt{1-\mu^2}}}\right)}\right)\right\}. \quad (28)$$

The estimation of the reachable set D_∞ *can be find by the maximal norm (Fig. 8):*

$$\max_{0\le\tau\le\tau_1(\delta_1^*)} ||x(\tau, v^0(\tau))|| = 2.2. \quad (29)$$

Proof of the theorem is given in the work [46].

We can say that this statement is similar to the consequence of Malkin's Theorem (please refer to [37]).

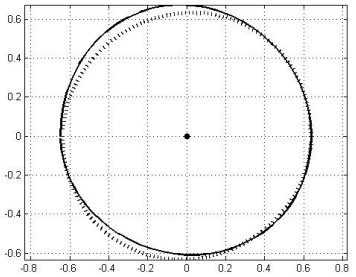

Fig. 9: Limit cycles for $\mu = 0,1$.

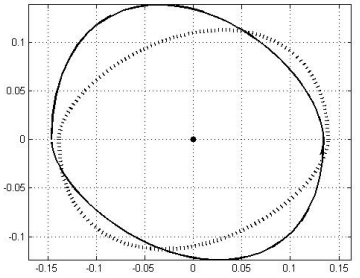

Fig. 10: Limit cycles for $\mu = 0,5$.

Example

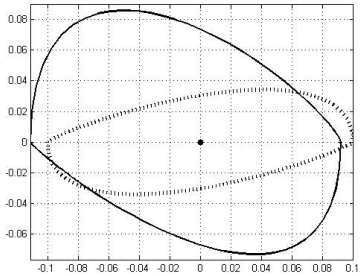

Fig. 11: Limit cycles for $\mu = 0,99$.

Compare the estimations of quality of the robust stability χ_1 (??) of the system (12) and the estimation χ (28) of the system (17) for different values μ.

For small δ_1: $\chi_1 = 6,39$, $\chi = 6,47$ if $\mu = 0,1$; $\chi_1 = 1,39$, $\chi = 1,46$ if $\mu = 0,5$; $\chi_1 = 1$, $\chi = 1$ if $\mu = 0,99$.

Comparisons of the limit cycles of systems (12) and (17) for different μ and for $\delta_1 = 0.1$ represented on the Fig. 9 - Fig. 11. Here the limit cycle of system (12) shown by dotted line and the limit cycle of system (17) shown by solid line.

Example 1 demonstrates a clear physical meaning: than larger dissipation forces of the system, than better estimation of the quality of robust stability. Consequently, the reachable sets D_∞ of both systems are smaller. Furthermore, the difference between reachable sets D_∞ of both systems grows with increase of the value μ.

1.3 Ellipsoidal estimates of the reachable set

L_2-norm. Restrict the system (1) by the L_2-norm:

$$\dot{x} = Ax + Bu, \quad x(0) = 0, \quad x \in R^n, \quad u \in R^m,$$
$$||u||_2^2 = \int_0^\infty u^T(t)u(t)dt \leqslant 1. \tag{30}$$

Function $u(t)$ can be interpreted as perturbation or as control (depends on the problem formulation).

Theorem. *Let the pair* (A, B) *be controllable, then* $D(t_1)$ *- ellipsoid:*

$$D(t_1) = \left\{x : \ x^T W_c^{-1}(t_1) x \leqslant 1\right\},$$

where matrix $W_c(t_1) > 0$ *has form:*

$$W_c(t_1) = \int_0^{t_1} e^{As} B B^T e^{A^T s} ds.$$

If A *stable, then* $D(\infty)$ *- ellipsoid*

$$D(\infty) = \left\{x : \ x^T W^{-1} x \leqslant 1\right\},$$

where $W > 0$ *- controllability gramian*

$$W = \int_0^{\infty} e^{As} B B^T e^{A^T s} ds,$$

i.e. solution of equation of Lyapunov

$$AW + WA^T = -BB^T.$$

Proof of the theorem presented in the work [58].

L_∞-norm. Present system (1) by the L_∞-norm:

$$\dot{x} = Ax + Bu, \quad ||u||_\infty = \sup_{t \geqslant 0} (u^T(t) u(t))^{1/2} \leqslant 1. \tag{31}$$

Let us characterize the sets $D(t_1)$ and $D(\infty)$ using the support function. Recall, that support function $c(X, \psi)$ for set $X \subset R^n$ and vector $\psi \in R^n$ has form:

$$c(X, \psi) = \max_{x \in X} \psi^T x.$$

A closed bounded set is uniquely restored by a support function. $X = \left\{x : \psi^T x \leqslant c(X, \psi), \ |\psi| = t_1\right\}$ - intersection of support half-spaces.

In this case, closure and convexity of $D(t_1)$ and $D(\infty)$ are obvious. Reachable set $D(t_1)$ is always bounded and reachable set D_∞ is bounded under suppose of stability of the system [58].

Sets $D(t_1)$ and $D(\infty)$, in general, not ellipsoids, but they are central-symmetric convex sets and it is conveniently approximate them by ellipsoids.

Consider case of the stable system and call ellipsoid

$$\xi = \left\{x : \ x^T Q x \leqslant 1\right\}$$

with center in the origin and matrix $Q > 0$ the *invariant ellipsoid*, if from $x(0) \in \xi$ follows that $x(t) \in \xi$ for all $t \geqslant 0$, where $x(t)$ satisfies system $\dot{x} = Ax + Bu, \ x(0) \in \xi, \ u^T(t)u(t) \leqslant 1$.

Introduce

$$V(x) = x^T Q x,$$

then

$$\dot{V}(x) = (Ax+Bu)^T Qx + x^T Q(Ax+Bu) = x^T(A^T Q + QA)x + 2u^T B^T Qx.$$

If $V(x) \leqslant 0$ for all x such that $V(x) \geqslant 1, \ u^T(t)u(t) \leqslant 1$, then trajectories of the system (1) could not left ellipsoid, because on it's bound $\dot{V}(x) \leqslant 0$, i.e. trajectories are directed inward ξ.

So, ξ will be the invariant ellipsoid, if from the inequalities:

$$x^T Q x \geqslant 1, \quad u^T u \leqslant 1,$$

follows

$$x^T(A^T Q + QA)x + 2u^T B^T Qx \leqslant 0.$$

According to the S-theorem [58], necessary and sufficient condition for the validity of this system of inequalities is the existence of such $\alpha \geqslant \beta \geqslant 0$ that

$$x^T(A^T Q + QA)x + \alpha x^T Q x - \beta u^T u + 2u^T B^T Qx \leqslant 0$$

for all $x,\ u$. In other words,

$$\begin{pmatrix} A^TQ + QA + \alpha Q & QB \\ B^TQ & -\beta I \end{pmatrix} \leqslant 0. \tag{32}$$

By the Schur's lemma [58] this is equivalent to the inequality

$$A^TQ + QA + \alpha Q + \beta^{-1}QBB^TQ \leqslant 0, \quad \beta > 0.$$

Multiplying left and right sides of the terms for $P = Q^{-1}$, obtain

$$PA^T + AP + \alpha P + \beta^{-1}BB^T \leqslant 0. \tag{33}$$

If for some $\alpha \geqslant \beta > 0$ we can find matrix $P > 0$, which satisfy the linear matrix inequality (33), then ellipsoid

$$\xi = \left\{x :\ x^TP^{-1}x \leqslant 1\right\}$$

will be invariant. Backward, all invariant ellipsoids are solutions of (33) for some $\alpha \geqslant \beta > 0$. We are interested in the minimal ellipsoid (i.e. from the matrices of the form μP, satisfies (33), we are interested in matrix with minimal μ). Thus, we need to use maximal β, which is equal to α. Moreover, inequality (33) can be replaced by equality:

$$PA^T + AP + \alpha P + \beta^{-1}BB^T = 0.$$

Theorem. *Let matrix A be stable, pair (A, B) be controllable and C be the full rank matrix (all rows and columns of it are linearly independent). Then reachable set $y(t)$ in the system*

$$\dot{x} = Ax + Bu, \quad x(0) = 0,$$

$$y = Cx, \quad u^Tu \leqslant 1, \quad 0 \leqslant t < \infty$$

contained in the ellipsoid $\xi = \left\{y :\ y^T(CPC^T)^{-1} \leqslant 1\right\}$, where $P = P(\alpha)$, $\alpha > 0$, - solution of the equation of Lyapunov

$$AP + PA^T + \alpha P + \alpha^{-1}BB^T = 0, \quad P > 0.$$

Moreover, solving the one-parameter problem of minimization

$$\min_{\alpha>0} tr\ CP(\alpha)C^T,$$

obtain the ellipsoid, which is minimal from the all ellipsoids, containing reachable set [58].

1.4 Pixel method of construction of reachable sets for nonlinear systems

Reachable set $D(t)$ depends on the next parameters:

- M_0 - set of initial conditions;
- t_0 - initial time moment;
- $t_1 > t_0$ - final moment of time;
- f - nonlinear function;
- $U = U_u$ - class of admissible controls.

Consider the Cauchy problem for controllable linear system:

$$\begin{cases} \dot{x} = Ax + u(t), \quad t_0 \leqslant t, \\ x(t_0) = x_0, \end{cases}$$

where function $u(t)$ is known.

Solution of this problem has form:

$$x(t) = e^{(t-t_0)A}x_0 + \int_{t_0}^{t} e^{(t-s)A}u(s)ds.$$

Thus, reachable set $D(t)$ can be presented as:

$$D(t) = D(t_0, t, M_0) = \bigcup_{x_0 \in M_0,\ u(\cdot)\in U} \left\{ e^{(t-t_0)A}x_0 + \int_{t_0}^{t} e^{(t-s)A}u(s)ds \right\},$$

or

$$D(t_0, t, M_0) = e^{(t-t_0)A}x_0 + \int_{t_0}^{t} e^{(t-s)A}U_u(s)ds.$$

The pixel method is associated with covering the area of the phase plane with a grid [55]. The grid is constructed as a partition of the considered area into squares. The reachable set is filled with square-shaped pixels. To appeal to the elements of the reachable set is necessary appeal to the elements of the characteristic matrix. Each element of the reachable set is associated with only one element of the matrix and on the contrary.

Algorithm. Characteristic matrix A corresponds to the reachable set $D(t_i)$ in each time t_i. Elements of this matrix a_{mn} determined using grid nodes λ_{mn}:

$$a_{mn} = \begin{cases} 1, & \text{if } \lambda_{mn} \in D(t_i), \\ 0, & \text{else.} \end{cases}$$

For the initial set, characteristic matrix is constructed the same: the set is divided into primitive squares, in the matrix for position i, j of the square placed 1, if square belongs to the set M_0, otherwise placed 0.

The values of the elements restores from matrix A of the set M_0 and substitutes into the formulas of solution of the Cauchy problem. The Cauchy problem solves by one of the methods: Euler's method, second-order Runge-Kutta method, fourth-order Runge-Kutta method. Thus, points of the reachable set are calculated at each time step [55].

Euler's Method.

Consider first-order system of differential equations

$$\begin{cases} \dot{x} = f(t, x), \\ x(t_0) = x_0, \end{cases} \tag{34}$$

where $x(t)$ denote the true solution to (34).

Approximate values are obtained for the solution at a set of grid points

$$x_0 < x_1 < ... < x_n < ...$$

and the approximate value at each x_n, is obtained by using some of the values obtained in previous steps.

An equal grid size $h > 0$ will be used to define the node points,

$$t_j = t_0 + jh, \quad j = 0, 1, ...$$

Euler's method is defined by

$$x_{n+1} = x_n + hf(t_n, x_n), \quad n = 0, 1, 2, ... \tag{35}$$

with $x_0 = x(t_0)$. Here formulas (35) can be obtained in 4 different ways: by a geometric viewpoint, Taylor series, numerical differentiation and numerical integration [24].

For reachable sets [55]

$$D(t_{i+1}) = D(t_{i+1}, D(t_i)) = \bigcup_{x(t_i) \in D(t_i)} \left\{ x(t_i) + \Delta_t \bigcup_{u \in U} f(t_i, x(t_i), u) \right\}.$$

Runge-Kutta methods.

The Runge-Kutta methods are closely related to the Taylor series expansion of $x(t)$, but no differentiation of f are necessary in the use of the methods. All Runge-Kutta methods can be written in the form

$$x_{n+1} = x_n + hF(t_n, x_n, h, f),$$

where F is the function, which depends on the order of the Runge-Kutta method [24].

The second-order formula of Runge–Kutta for reachable set is

$$D(t_{i+1}) = D(t_{i+1}, D(t_i)) =$$

$$= \bigcup_{x(t_i)\in D(t_i)} \left\{ x(t_i) + \Delta_t \bigcup_{u\in U} f(t_i + \frac{\Delta_t}{2}, x(t_i) + \Delta_t \frac{f(t_i, x(t_i), u)}{2}, u) \right\}.$$

The fourth-order formula of Runge–Kutta for reachable set is [55]

$$D(t_{i+1}) = D(t_{i+1}, D(t_i)) =$$

$$= \bigcup_{x(t_i)\in D(t_i),\ u\in U} \left\{ x(t_i) + \Delta_t \frac{k_1 + 2k_2 + 2k_3 + k_4}{6} \right\},$$

$$k_1 = f(t_i, x(t_i), u), \quad k_2 = f\left(t_i + \frac{\Delta_t}{2}, x(t_i) + \frac{1}{2}k_1, u\right),$$

$$k_3 = f\left(t_i + \frac{\Delta_t}{2}, x(t_i) + \frac{1}{2}k_2, u\right), \quad k_4 = f(t_i + \Delta_t, x(t_i) + k_3, u).$$

1. Example of mathematical pendulum.

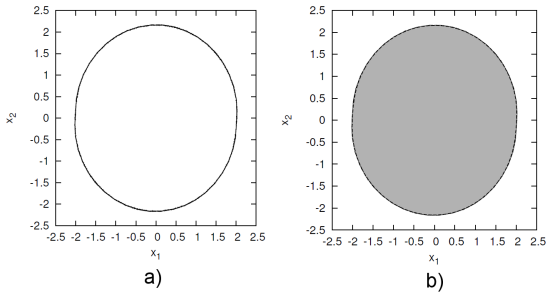

Fig. 12: a) Reachable set for the problem of mathematical pendulum; b) discrete approximation of the reachable set for the problem of mathematical pendulum.

Conditions of the problem:

- $t_1 > t_0$ - final moment of time;
- $A = \left(\begin{smallmatrix} 0 & 1 \\ -1 & 0 \end{smallmatrix}\right)$ - matrix of the system;
- $\left\{u \in E^2 :\ u_1 = 0,\ |u_2| \leqslant 1\right\}$ - control (vertical interval);
- $M_0 = \{\left(\begin{smallmatrix} 0 \\ 0 \end{smallmatrix}\right)\}$ - one-point set of initial conditions.

Parameters of the program:

- $x \in [-3,3],\ y \in [-3,3]$;
- $\Delta_x = \Delta_y = 0.003,\ \Delta_t = 0.15,\ \Delta_u = 0.05$;
- $t_0 = 0,\ t_1 = 3.3$.

Solution of the problem of finding the reachable set presented on the Fig. 12 ([55]).

2. Modified example of Lee-Markus model.

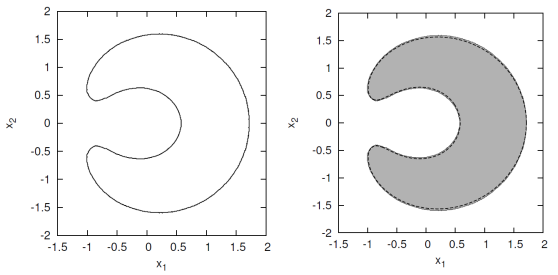

Fig. 13: a) Reachable set for the problem of Lee-Marcus model; b) discrete approximation of the reachable set for the problem of Lee-Marcus model.

The problem conditions are given in the work [48]:

- $t_1 > t_0$ - final moment of time;
- $\begin{cases} \dot{x}_1 = x_2 u_1 - x_1 u_2, \\ \dot{x}_2 = -x_1 u_1 - x_2 u_2; \end{cases}$
- $\left\{u \in E^2 :\ u_1^2 + 25u_2^2 \leqslant 1\right\}$ - control (ellipsoid);
- $M_0 = \{\binom{1}{0}\}$ - one-point set of initial conditions.

Parameters of the program:

- $x \in [-2, 2]$, $y \in [-2, 2]$;
- $\Delta_x = \Delta_y = 0.0083$, $\Delta_t = 0.3$, $\Delta_u = 0.16$;
- $t_0 = 0$, $t_1 = 2.7$.

Solution of the problem presented on the Fig. 13 ([55]).

1.5 The conditional gradient method for solving the problem of finding the maximum deviation for two coordinates.

Consider linear system (1), where $x^T = (x_1, x_2)$ and the control $u(t)$ presented as the perturbation $v(t)$ - piece-wise continuously differentiable function, limited by the absolute value

$$\begin{cases} \dot{x} = Ax + bv, \\ v(\cdot) \in V = \{v(\cdot) \in KC |\ |v(t)| \leqslant \delta_1 \text{ for } t \in (0, \infty),\ 0 < \delta_1 < 1\}. \end{cases} \tag{36}$$

It is necessary to find the maximum deviation in two coordinates x_1 and x_2 at the time t_1. The functional has form

$$J = x_1^2(t_1) + x_2^2(t_1). \tag{37}$$

Reachable set $D(t_1)$ of the points $\{x_1(t_1, v), x_2(t_1, v)\}$ corresponds to the set V. Finding the maximum of the functional (37) is equivalent to finding the most distant from the origin point of $D(t_1)$.

To find the worst perturbation in two coordinates, first we need to find the points

$$\max_{v \in V} x_1(t_1, v), \quad \max_{v \in V} x_2(t_1, v),$$

which are the maximum deviations of x_1 and x_2 coordinates correspondingly.

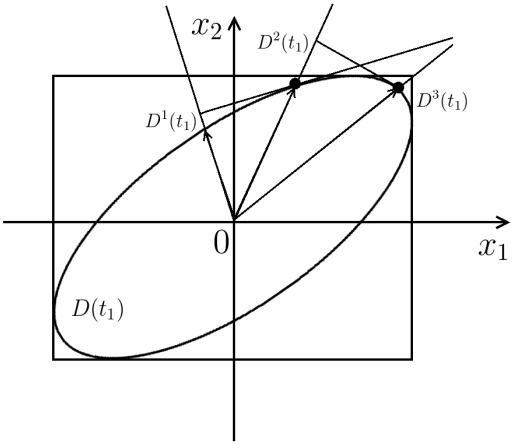

Fig. 14: Reachable set $D(t_1)$.

If $\max x_1 = \max x_2 = 0$, the system (36) is unperturbed and the problem is solved.

If $\max x_1 = 0$, the system (36) is unperturbed in x_1 and D_{t_1} is the interval in ordinate. If $\max x_2 = 0$, the system (36) is unperturbed in x_2 and D_{t_1} is the interval in abscissa.

If $\max x_1 \neq 0$, $\max x_2 \neq 0$, then (36) is perturbed in both coordinates. Then, finding $\min x_1$ and $\min x_2$, we have four different perturbations, which execute the projection of $D(t_1)$ on the axis ox_1 and ox_2. This points give possibility to construct the rectangle, containing $D(t_1)$.

To obtain the worst perturbation we shall apply the method of successive approximations .

Let us choose one of the obtained perturbations, denote it as $v^1(t)$ and find the maximum of the functional $\phi_0 = c_1^T x(t_1, v)$, where

$c_1 = \{x_1(t_1, v^1), x_2(t_1, v^1)\}$ is 2-dimensional vector. Geometrically, this is equivalent to finding the projection of the set $D(t_1)$ onto the direction c_1 (Fig. 14).

The maximum of the linear functional $c_1^T x(t_1, v)$ is unique. Therefore, the perturbation, corresponding to this maximum, we shall choose as next approximation of the worst perturbation. Thus, we have an iterative process, defined by the recurrence relation

$$\max_{v \in V} [x_1(t_1, v^n) x_1(t_1, v) + x_2(t_1, v^n) x_2(t_1, v)] =$$

$$= x_1(t_1, v^n) x_1(t_1, v^{n+1}) + x_2(t_1, v_{1n}) x_2(t_1, v^{n+1}) \tag{38}$$

or

$$\max_{z \in D(t_1)} z_n^T z = z_n^T z_{n+1}, \tag{39}$$

where $z_n = \{x_1(t_1, v^n), x_2(t_1, v^n)\}$. Because $z_n^T z_{n+1} = \max_{z \in D(t_1)} z^T z > z_n^T z_n$, then

$$|z_n||z_{n+1}| \cos(\angle z_n z_{n+1}) > |z_n||z_n|.$$

Consequently, $J(v^{n+1}) = |z_{n+1}|^2 > |z_n|^2 = J(v^n)$, i.e. sequence $\{J_n\}$ is increasing. Hence, the iterative method is convergent and allows us to find the maximum of the functional J.

If we shall obtain $z_n = z_{n+1}$ on the n-th step, then point $z^0 = z_n$ is stationary by the definition of the process (38). Perturbation $v^0(t)$, corresponding to the motion of the system to point z^0, satisfies (38), i.e.

$$\max_{v \in V} [x_1(t_1, v^0) x_1(t_1, v) + x_2(t_1, v^0) x_2(t_1, v)] = x_1^2(t_1, v^0) + x_2^2(t_1, v^0). \tag{40}$$

Thus, the iterative process described above allows us to find the perturbation, which satisfies the maximum principle (40). Geometrically

(40) means that line, drawn through a point z^0 and perpendicular to the vector z^0 is support line to the set $D(t_1)$ (Fig. 15).

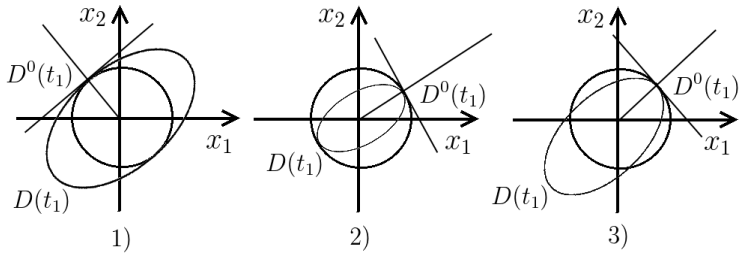

Fig. 15: Possible situations of the first step of the conditional gradient method.

The following situations are possible:

1. point z^0 is the point of local minimum of the boundary S of the set $D(t_1)$ in the sens of functional J (it is possible only on the first step, to avoid it we need to change the initial direction c_1);

2. point z^0 is the inflection point of the boundary S of the set $D(t_1)$ in the sens of functional J (to avoid it we need to change the initial direction c_1 in the direction of increase of the functional J);

3. point z^0 is the point of local maximum of the boundary S and the point of local maximum of the functional J (then point z^0 is the solution of the problem).

Therefore, using this method, we can get a perturbation v^0, that realizes local maximum of the functional $J(v)$ and the part of the boundary of reachable set $D(t_1)$. By using this method a few times, can be obtained the absolute maximum of the functional $J(v)$ and the worst perturbation v^0, that realizes this maximum [5].

1.5.1 Example of applying conditional gradient method

Consider a controlled system that describes the behavior of the pendulum:

$$\begin{cases} \ddot{x}_1 + x_1 = v(t), \\ v(\cdot) \in V = \{v(\cdot) \in KC || v(t)| \leqslant \delta_1 = 1\}. \end{cases}$$

Where by substituting $x_2 = \dot{x}_1$ can be obtained

$$\begin{cases} \dot{x}_1 = x_2, \\ \dot{x}_2 = -x_1 + v(t). \end{cases} \tag{41}$$

The set of reachability D_{t_1} for $0 \leqslant t_1 \leqslant \pi$ was found analytically by using the support function in [29] and presented on Figs. 16-17.

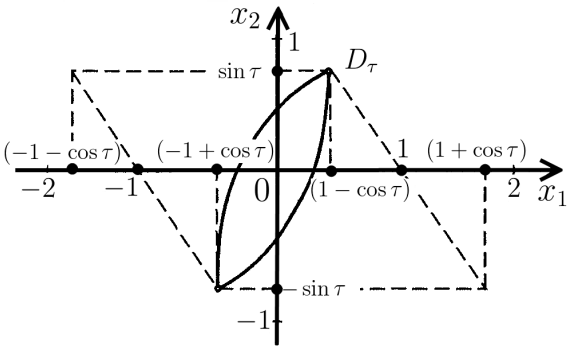

Fig. 16: Reachable sets, obtained analytically in [29].

Let us find the maximum deviations of the coordinates for the times $t_1 = \frac{\pi}{6}$ and $t_1 = \pi$. And then use the conditional gradient method to refine the points that limit the reachable set. Due to symmetry of reachable set D_{t_1} with respect to the origin of the system, it is sufficient to perform calculations only in the upper half-plane.

The normalized fundamental matrix of solutions of the system (41) for $v(t) \equiv 0$ and initial conditions $(1,0)^T$, $(0,1)^T$ has form

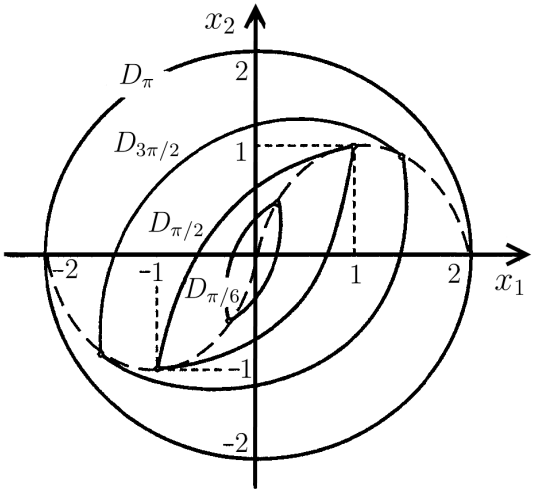

Fig. 17: Reachable sets, obtained in [29] for $D_{\pi/6}$, $D_{\pi/2}$, $D_{3\pi/2}$, D_π.

$$X(t) = \begin{pmatrix} \cos(t) & \sin(t) \\ -\sin(t) & \cos(t) \end{pmatrix}$$

and

$$X^{-1}(s) = \begin{pmatrix} \cos(s) & -\sin(s) \\ \sin(s) & \cos(s) \end{pmatrix}.$$

Then by (53) functions

$$x_1(t_1) = \int_0^{t_1} \sin(t_1 - s)v(s)ds,$$

$$x_2(t_1) = \int_0^{t_1} \cos(t_1 - s)v(s)ds,$$

are the solutions of the system (41).

Thus, the worst perturbations for maximum deviations of x_1 and x_2 coordinates are

$$v^0_{1max}(s) = \delta_1 \cdot \operatorname{sign}(\sin(t_1 - s))$$

$$v^0_{2max}(s) = \delta_1 \cdot \operatorname{sign}(\cos(t_1 - s))$$

The maximum deviations that can be achieved under the influence of the worst perturbations have form

$$\max x_1(t_1) = \delta_1 \int_0^{t_1} |\sin(t_1 - s)| ds =$$

$$= \delta_1 \left(-\cos(t_1) + 2\cos(t_1 - \pi) - ... \pm 2\cos(t_1 - \pi n) + 1\right)$$

and

$$\max x_2(t_1) = \delta_1 \int_0^{t_1} |\cos(t_1 - s)| ds =$$

$$= \delta_1 \left(\sin(t_1) - 2\sin(t_1 - \frac{\pi}{2}) + ... \pm 2\sin(t_1 - \pi n - \frac{\pi}{2})\right).$$

For $t_1 = \pi$**,** $\delta_1 = 1$.

The points of maximum deviations are $(2, 0)$ and $(0, 2)$, because:

$$\max x_1(\pi) = \int_0^{\pi} |\sin(\pi - s)| ds = 2,$$

$$x_2(\pi) = \int_0^{\pi} \cos(\pi - s) \cdot \text{sign}(\sin(\pi - s)) ds = \int_0^{\pi} \cos(\pi - s) ds = 0,$$

$$\max x_2(\pi) = \int_0^{\pi} |\cos(\pi - s)| ds = 2,$$

$$x_1(\pi) = \int_0^{\pi} \sin(\pi - s) \cdot \text{sign}(\cos(\pi - s)) ds = \int_0^{\pi/2} \sin(\pi - s) ds -$$

$$- \int_{\pi/2}^{\pi} \sin(\pi - s) ds = 0.$$

By the conditional gradient method we need to find the maximum of the functional $\phi_0 = c_j^T x(\pi, v)$. The initial value of the vector c_1^T can be any, for example $c_1^T = \{1, 1\}$. Thus, the functional

$$\phi_0 = 1 \cdot x_1(\pi, v_2) + 1 \cdot x_2(\pi, v_2) =$$

$$= \int_0^{\pi} \left(\sin(\pi - s) + \cos(\pi - s)\right) v_2(s) ds.$$

Then the perturbation on the next step takes the value

$$v_2(s) = \text{sign}\left(\sin(\pi - s) + \cos(\pi - s)\right) = \begin{cases} -1, & 0 < s < \frac{\pi}{4}, \\ 1, & \frac{\pi}{4} < s < \pi, \end{cases}$$

and

$$\phi_0 = \int_0^{\pi} |\sin(\pi - s) + \cos(\pi - s)| ds = 2\sqrt{2},$$

in the point $(\frac{2}{\sqrt{2}}, \frac{2}{\sqrt{2}})$, because

$$x_1(\pi, v_2(s)) = \int_0^{\pi} \sin(\pi - s) \cdot v_2(s) ds = \frac{2}{\sqrt{2}},$$

$$x_2(\pi, v_2(s)) = \int_0^{\pi} \cos(\pi - s) \cdot v_2(s) ds = \frac{2}{\sqrt{2}}.$$

Therefore, the vector c_2^T on the next step of the algorithm has form $c_2^T = \left\{\frac{2}{\sqrt{2}}, \frac{2}{\sqrt{2}}\right\}$. Accordingly vector c_2^T the functional ϕ_0 takes value

$$\phi_0 = \frac{2}{\sqrt{2}} \int_0^{\pi} (\sin(\pi - s) + \cos(\pi - s))\, v_3(s) ds,$$

whence

$$v_3(s) = \operatorname{sign}(\sin(\pi - s) + \cos(\pi - s)) = v_2(s).$$

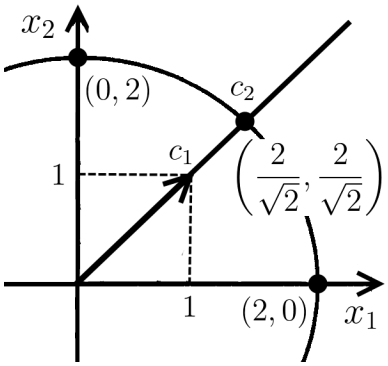

Fig. 18: Reachable set D_π.

Thus, at the second step of the algorithm we get to a stationary point $(\frac{2}{\sqrt{2}}, \frac{2}{\sqrt{2}})$ at which the functional ϕ_0 takes its maximum value $\max \phi_0 = 4$ (Fig. 18).

Continuing the algorithm for different values of the initial vector c_1^T, we will get the points lying on the circle $x_1^2 + x_2^2 = 4$, which is

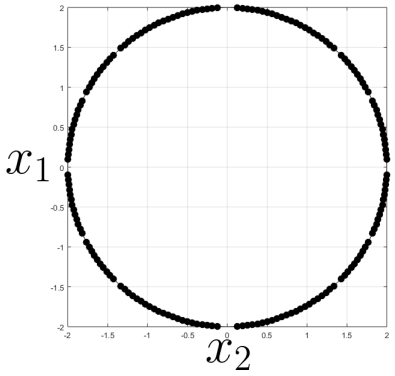

Fig. 19: Reachable set D_π.

completely coincide with the analytical description of the reachable set D_π in the work [29] (at the Fig. 19 were shown results, obtained for 100 different initial vectors c_1^T).

For $t_1 = \frac{\pi}{6}$, $\delta_1 = 1$.

The maximum deviation in only one coordinate have forms (x_1 and x_2 coordinates correspondingly):

$$x_1 = \int_0^{\pi/6} \sin(\frac{\pi}{6} - s) v_i(s) ds,$$

$$x_2 = \int_0^{\pi/6} \cos(\frac{\pi}{6} - s) v_i(s) ds,$$

where $v_i(s)$ is the worst perturbation, corresponding last step of the algorithm.

Using the conditional gradient method the results of the calculations of the maximum deviations in both coordinates at Fig. (20) were obtained (results were calculated for 100 different initial vectors c_1^T and presented as black points, black lines is the analytical results of Blagodatskikh constructed only for comparison).

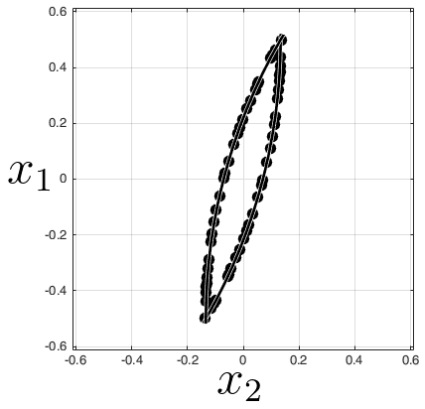

Fig. 20: Points, obtained by the conditional gradient method for $D_{\pi/6}$.

1.6 Lemma 1-2 by Demidovich

Lemma. ***1.*** *Let the periodic system*

$$\frac{dx}{dt} = P(t)x, \tag{42}$$

where $P(t) \in C(-\infty, +\infty)$ *and* $P(t+\omega) = P(t)$ $(\omega > 0)$ *has one Floquet multiplier* $\rho_1 = 1$ *and the absolute values of all other multipliers* $\rho_j (j = 2, ..., n)$ *less then one:*

$$|\rho_j| < 1 \text{ for } j \neq 1.$$

Then for system (42) exists a fundamental matrix of the special form

$$X(t) = \Phi_s(t) diag(E_1, e^{C_1 t}), \tag{43}$$

where $\Phi_s(t)$ *- real non-singular* ω*-periodic continuously differential* $(n \times n)$*-matrix,* $E_1 = 1$ *and* C_1 *- real continuous* $(n-1) \times (n-1)$*-matrix, all characteristic roots of it have negative real parts*

$$Re\lambda_j(C_j) < 0 \ (j = 1, ..., n-1).$$

Lemma. *2. Let $X(t)$ - real fundamental matrix of the system (42) of the form (43) and*

$$G(t,s) = \begin{cases} X(t)\,diag(0, E_{n-1})X^{-1}(s) \text{ for } t > s, \\ -X(t)\,diag(E_1, 0)X^{-1}(s) \text{ for } t < s, \end{cases}$$

Then vector-function:

$$y(t) = X(t)a + \int_0^\infty G(t,s)f(s)ds,$$

where a - an arbitrary constant vector with zero first coordinate, i.e.

$$(a, e_1) = 0, \ e_1 = colon(1, 0, ..., 0)$$

$$f(t) \in C\,[0,\infty)\,, \ \int_0^\infty ||f(t)||dt < \infty,$$

is the solution of non-homogeneous system

$$\frac{dy}{dt} = P(t)y + f(t),$$

which tends zero by $t \to \infty$: $y(\infty) = \lim\limits_{t\to\infty} y(t) = 0$.

The proofs of Lemma 1 and Lemma 2 are presented in the work [34].

1.7 Application of the reachable sets for solution of the direct transition problem.

The theory of bifurcations studies qualitative changes of trajectories in the phase space under some change of the parameters of the system. This definition is quite true when systems has simple dynamics. For systems with complicated chaotic dynamics (for example, for multidimensional systems whose invariant manifolds of saddle periodic trajectories intersect not transversal) there are "hidden parameters", the so-called modules, and there are infinitely many of

them. It is impossible to study completely the bifurcations of such systems [30].

Despite this, the theory of bifurcation is one of the most interesting and important sections of the theory of dynamical systems.

The first attempt to formulate the concept of phase space structure and its changes was made in 1937 by Andronov and Pontryagin [18]. They introduced a concept of the **rough system**, i.e. a system that does not change its qualitative properties under small perturbations. If small changes in these parameters lead to a change of topological structure of a dynamic system (system is not rough), then the topological structure of the system does not allow us to view physical phenomena. On the contrary, if the system is rough, then its structure may be directly related to the properties of this phenomena [30].

Andronov and Pontryagin proposed necessary and sufficient conditions of roughness for systems on a plane [18]. Two-dimensional system is rough if and only if:

- it has a finite number of equilibrium points, and they are all rough, i.e. do not have eigenvalues lying on the imaginary axis (roots $\lambda_{1,2} \neq \pm i\omega$ of the characteristic equation $\det|\lambda E_2 - A| = 0$);

- it has a finite number of limit cycles, and they are all rough, i.e. their second multiplier of Floquet is not equal to 1 (root $\rho_1 = 1$, $\rho_2 < 1$ of the characteristic equation $\det|\rho E_2 - A(t)| = 0$);

- there are no trajectories (separatrices) leaving from the same saddle equilibrium point and incoming into another or the same (no homoclinic and heteroclinic trajectories).

In the work [69], it was shown that transitions from region of attraction of one attractor to region of attraction of another under the

action of the small permanent perturbations are possible. It means, that the leaving from one area and the arriving to another area are possible motions of the system. For example, the pitching of the ship may result to the loss of stability, i.e. the transition from the region of oscillating motion to the region, corresponding the loss of stability and rolling-over the ship.

Formulation and solution of the problem of transition between different regions of attraction is widely used in applied and theoretical problems [69]:

- applications in physics and engineering (calculation of the cut-off frequency in the experimental simulation of noise acting on the nonlinear system, the engineering problem of loss of stability of the buckled column at random transverse load);

- shipbuilding (the problem of loss of stability of the vessel during the pitching in random seas);

- oceanography (the problem of the dynamics of coastal currents under the influence of wind at the wavy topography of ocean bottom);

- non-linear theory of control;

- theory of stochastic resonance;

- neurophysiology (the problem of asymmetric bistable model of auditory nerve fiber response, the problems of direct and inverse transitions in the model of primary afferent neuron of vestibular apparatus).

Consider a bistable rough system which has two attractors.

Assume that a bistable system:

$$\dot{y} = f^0(y), \qquad y \in G \subset R_2 \tag{44}$$

has an asymptotically orbitally stable limit cycle $y^0(t)$, inside of which there is a point attractor - a stable focus (y_1^0, y_2^0) and its region of attraction A^*. This region A^* is bounded by a limit cycle, asymptotically orbitally stable in inverse time. The region of attraction of the first limit cycle is $R_2 \setminus A^*$ (on Fig. 21 it is $R_2 \setminus A^* = C \cup B$).

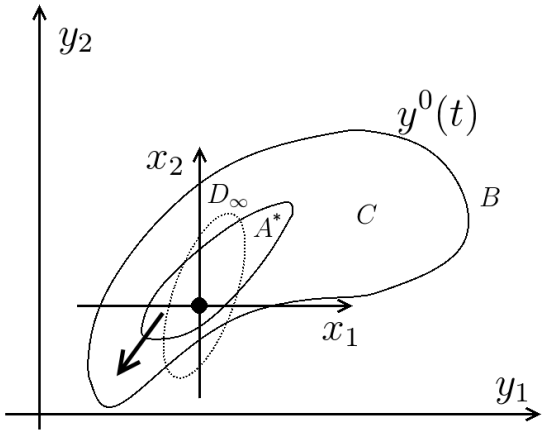

Fig. 21: Phase portrait of the bistable system (44). Point attractor is the origin of coordinate system (x_1, x_2); periodic attractor is the closed curve $y^0(t)$; A^* is the area of attraction of point attractor; $C \cup B$ is the area of attraction of periodic attractor; D_∞ is the reachable set, constructed in the neighborhood of a point attractor.

Suppose that the assumption of the existence of a closed orbit, which is the first attractor, is satisfied in the area $R_2 \setminus A^* = C \cup B$.

Thus, to solve the problem of the system's transition from the region of attraction of a point attractor to a region of attraction of an asymptotically orbitally stable limit cycle (problem of direct transition),

we need to add the perturbation to the system (44):

$$\begin{cases} \dot{y} = f^0(y) + bv, \\ v(\cdot) \in V = \{v(\cdot) \in KC |\ |v(t)| \leqslant \delta_1 \text{ for } t \in (0, \infty),\ 0 < \delta_1 < 1\}. \end{cases} \tag{45}$$

Further will be carried out the following algorithm:

1. From the nonlinear system (45), firstly, we make a transition to the linear system in variations

$$\dot{x} = Ax + bv(t), \tag{46}$$

by coordinates $x_i = y_i - y_i^0,\ i = 1, 2,\ A = \left(\frac{\partial f^0(y_1^0, y_2^0)}{\partial y_i}\right)$ and by perturbation $b = \left(\frac{\partial (f^0(y) + bv)}{\partial v}\right)$ in the neighborhood of stable point attractor (y_1^0, y_2^0).

2. For linear system in variations (46) we construct the reachable set D_∞ by solving the problem of maximum deviation (use stable limit cycle (13), results of paragraph 1.2.).

3. Then we need to compare the region of attraction of point attractor A^* of the nonlinear system (45) with reachable set D_∞ of the linear system in variations (46). The intersection of two closed sets A^* and D_∞ is not empty, because it contains at least one point - the focus, which belongs to both sets. However, if set D_∞ has points, that do not belong to A^*, then direct transition between the attractors of the system (45) is possible.

To find it we define the distance between these sets:

$$d(D_\infty, A^*) = \max_{x \in D_\infty} \min_{y \in A^*} \rho(x, y), \tag{47}$$

where ρ is the distance between points $x,\ y$. In this case the distance (47) is the analogue of the Hausdorff distance, which is called “directed”,

"non-symmetric" or "one-way", and correspondingly defined in [42], [65], [66]. Informally, two sets are close in the Hausdorff distance if every point of either set is close to some point of the other set.

If the distance (47) is positive, then we can confirm the possibility of transition under the influence of $v(t)$ from the region of attraction of a point attractor A^* to the region of attraction of the limit cycle $R_2 \setminus A^*$.

Example

The problem of direct transition in the Model of Hodgkin-Huxley with modifications of Soto-Alexandrov (system (61) presented in Chapter 4) was shown in [46] and [13].

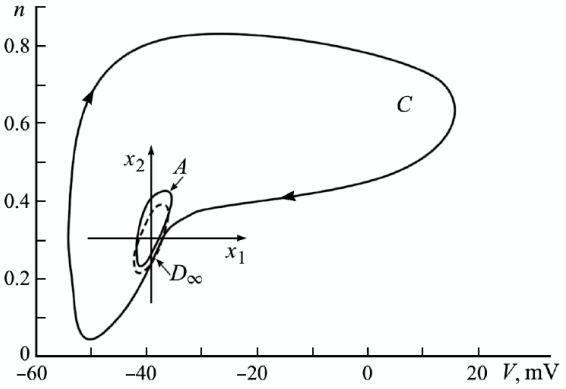

Fig. 22: Phase portrait of the bistable system (61).

Figure 22 illustrates two attractors of the system (61) for $I_{\text{syn}} = 0.99\ [\mu\text{A/cm}^2]$:

1. the stable focus with the attraction domain A^* obtained by constructing the limit cycle being asymptotically and orbitally stable in reverse time;

2. the globally and orbitally-stable limit cycle is the main attractor forming the relaxation self-excited oscillations (spikes).

Let us introduce the local coordinate system x_1, x_2 whose origin is in the stable focus (v^0, n^0), where $v^0 = -39$ mV and $n^0 = 0.3$ (Fig. 22):

$$\begin{cases} \dfrac{dv}{dt} = 0.245v - 12.698n + \gamma_0 P(t), \\ \dfrac{dn}{dt} = 0.013v - 0.305n, \\ P(\cdot) \in V = \{P(\cdot) \in KC| \ |v(t)| \leqslant \delta_1 < 1\}, \end{cases} \tag{48}$$

where $P(t)$ is perturbation, $\delta_1 = \frac{1}{2} I_{syn}$, γ_0 is a coefficients of presence of perturbation in the system $\gamma_0 = 0.2$.

In this coordinate system, we consider the points belonging to the reachable set D_∞ of the perturbed stable system (48).

Solving the Bulgakov problem, we come to the reachable set D_∞ illustrated in Fig. 22 by the dotted line. Parametric equations of this cycle are:

$$\begin{cases} n^+(t) = e^{-0.03t}(\alpha^* + 0.07\gamma_0)(0.1\sin(0.3t) + \cos(0.3t)) - 0.07\gamma_0; \\ n^-(t) = -e^{-0.03t}(\alpha^* + 0.07\gamma_0)(0.1\sin(0.3t) + \cos(0.3t)) + 0.07\gamma_0; \\ v^-(t) = -77.52e^{-0.03t}(\alpha^* + 0.07\gamma_0)(0.27\sin(0.3t) - 0.305\cos(0.3t)) - \\ \qquad -1.69\gamma_0; \\ v^+(t) = 77.52e^{-0.03t}(\alpha^* + 0.072\gamma_0)(0.27\sin(0.3t) - 0.305\cos(0.3t)) + \\ \qquad +1.69\gamma_0; \end{cases} \tag{49}$$

where $\alpha^* = \frac{0.07\gamma_0\left(1+e^{-\frac{\pi}{5}}\right)}{(1-e^{-\frac{\pi}{5}})}$ is the limit of maximal amplitude's sequences of oscillating coordinate $n(t)$.

Further, were found the points $M(x_1^0, x_2^0) \in D_\infty$, $x_1^0 = -42.131$, $x_2^0 = 0.239$; $N(y_1^0, y_2^0) \in A^*$, $y_1^0 = -41.761$, $y_2^0 = 0.273$ corresponding to the Hausdorff distance:

$$d(D_\infty, A^*) = d(M, N) = 0.372 > 0,$$

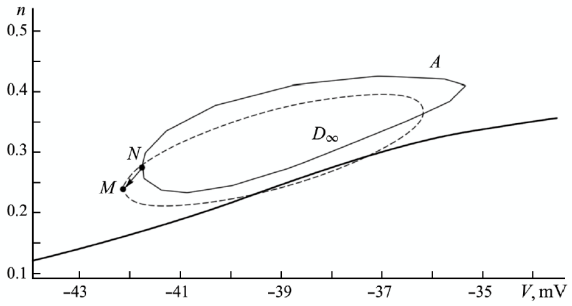

Fig. 23: Phase portrait of the bistable system (61).

which is a solution to the transition problem. According to the solution to this transition problem, the galvanic activity correction of the primary afferent neuron is a periodic function whose frequency is equal to the resonance frequency of the oscillatory system (61).

Since the Hausdorff distance in this case is strictly positive, then we can state the following: *under the action of a small permanent perturbation, system (61) is able to make the transition from the region of attraction of a point attractor into the region of attraction of the periodic attractor.*

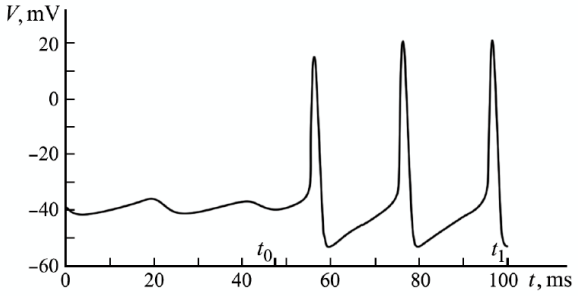

Fig. 24: Response of the system (61) for galvanic stimulation.

At the initial moment, system (61) is situated in the attraction domain A^* during the expectation of a mechanical stimulus. Since such

a stimulus is absent on the entry of the vestibular mechanoreceptor, the galvanic stimulation of the primary afferent neuron causes the activity of this neuron for $t \in [t_0, t_1]$ in the form of a spike packet (Fig. 24). The implementation of this activity corresponds to the correction of an inertial navigation system if additional information is available.

SYNTHESIS OF THE REACHABLE SETS FOR THE PERIODIC ATTRACTOR OF THE SECOND ORDER NONLINEAR SYSTEM

2.1 Statement of the problem of construction of the reachable set in a neighborhood of a periodic attractor of a second-order nonlinear system

Consider a nonlinear system under acting of permanent perturbation in the additive form:

$$\begin{cases} \dot{y} = f(y, v(t)) = \phi_0(y) + bv(t), \\ v(\cdot) \in V = \{v(\cdot) \in KC |\ |v(t)| \leqslant \delta_1 < 1 \text{ for } t \in (0, t_1 < \infty)\}, \end{cases} \tag{50}$$

where $y \in R^2$, b is the vector that determines absence/presence of permanent perturbation $v(t)$ in the system (50) (for example, in the Van der Pol's system $b = \binom{0}{1}$, in the model of Hodgkin-Huxley $b = \binom{1}{0}$).

The nonlinear system of differential equations (50) with $v \equiv 0$ has periodic solution $y^0(t+T) = y^0(t)$ with period of motion T.

To obtain a reachable set D_{t_1}, we will construct a system in variations by coordinates $x = y - y^0(t)$ and by perturbation $v(t)$ in the neighborhood of the periodic solution:

$$\dot{x} = A(t)x + bv(t), \text{ where } A(t+T) = A(t). \tag{51}$$

The coordinate origin of the system (51) will be located on the orbit of the periodic solution $y^0(t)$ and will move on it.

For system (51) and $v(t) \equiv 0$ we will find the normalized fundamental matrix of solutions $X_f(t)$. To obtain the first column of

the matrix $X_f(t)$, we shall integrate system

$$\dot{x} = A(t)x, \tag{52}$$

with initial conditions $x(0) = \binom{1}{0}$. As a next step, we shall obtain the second column of the matrix $X_f(t)$ by integrating system (52) with initial conditions $x(0) = \binom{0}{1}$.

Further on, the monodromy matrix $X_f(T)$ is obtained by substituting the values $t = T$ into $X_f(t)$.

Solution of the characteristic equation $\det(\rho E_2 - X_f(T)) = 0$ gives the eigenvalues ρ_1 and ρ_2, which are the Floquet multipliers.

Due to the fact that we are considering only systems with asymptotically stable in the sense of Poincaré limit cycle, according to the theory of Floquet $\rho_1 = 1$ and the theorem of Poincaré $0 < \rho_2 < 1$.

In general, the solution of the system (51) can be presented in the form

$$x(t) = \int_0^{t_1} X_f(t) X_f^{-1}(s) b v(s) ds.$$

However, one of the main ideas of our method is to present the solution $x(t)$ in a simpler form. To this end, we change the coordinate system of fundamental normalized matrix (x_1^f, x_2^f) to the new coordinate system (x_1^s, x_2^s) of the special fundamental matrix $X_s(t)$.

The question is, which direction of the coordinate axes (x_1^s, x_2^s) is more convenient and more expedient to choose?

If we assume that the system in variations does not have kinematic speed, then the direction of its axes will be the same as axes of initial nonlinear system

$$\Delta y_1 = x_1^f,$$

$$\Delta y_2 = x_2^f.$$

Note, in the new special system of coordinates the first x_1^s axis is

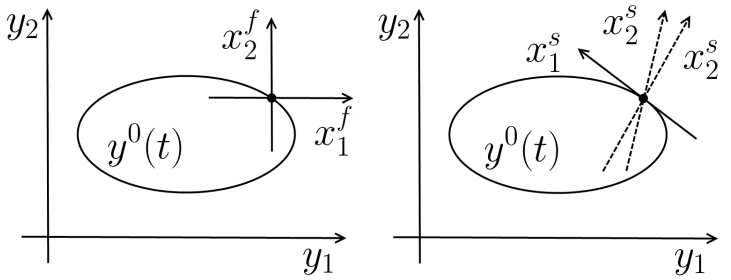

Fig. 25: Coordinate systems.

collinear to the velocity vector of the initial point in orbit. That is, it is tangent to the orbit of the limit cycle $y^0(t)$ in point $y^0(0)$. The second axis x_2^s can be any, but we choose a special coordinate system described in the work [34] (that is, the transition matrix to a special coordinate system should transform the monodromy matrix to its Jordan form). For example, for model of Van der Pol the second axis is perpendicular to the first axis, but in the model of Hodgkin-Huxley is not.

Thus, we are making the transition from the normalized fundamental matrix of solutions $X_f(t)$ to the special fundamental matrix of solutions $X_s(t)$:

$$X_s(t) = X_f(t) \cdot S.$$

According to [34] matrix S is not the only, but has to fulfill the conditions

$$(*) \qquad \det S \neq 0$$

and

$$(**) \qquad S^{-1} X_f(T) S = \begin{pmatrix} 1 & 0 \\ 0 & \rho_2 \end{pmatrix}.$$

One of the options to construct the matrix S is to use the eigenvectors s_1 and s_2 of the monodromy matrix $X_f(T)$ (it is obvious, that with this construction of the matrix $S = (s_1; s_2)$ conditions $(*)$,

$(**)$ are satisfied). However, it is possible to use another form of the matrix S, which will also satisfy the conditions $(*)$, $(**)$, but will be constructed using vectors that differ from the eigenvectors of the monodromy matrix $X_f(T)$.

The direction of the second axis x_2^s axis depends on the relative position of the vectors s_1 and s_2. Further in example of a Van der Pol' s model (Section 2.3), the vectors s_1 and s_2 will be orthogonal and the x_2^s axis will be the normal to the tangent of the orbit $y^0(t)$. On the contrary, in the example of modified model of Hodgkin-Huxley (paragraph 3.3) the angle between vectors s_1 and s_2 $\theta \approx 19°$, that is why the constructed new coordinate axes will be the affine.

Special fundamental matrix of solutions $X_s(t)$, according to the extension of the theorem of Floquet [34], can be presented in the form of the product of two matrices:

$$X_s(t) = \Phi_s(t) \cdot e^{\Lambda_s t},$$

where $\Phi_s(t)$ is T - periodic bounded (2×2) - matrix, $\Phi_s(t + T) = \Phi_s(t)$, $\Phi_s(0) = X_s(0)$; $\Lambda_s = \frac{1}{T}\mathrm{Ln}X_f(T)$ $\left(\text{if } n = 2 \text{ then } e^{\Lambda_s t} = \begin{pmatrix} 1 & 0 \\ 0 & e^{(\frac{1}{T}\ln\rho_2)\cdot t} \end{pmatrix}\right)$. We use a special matrix of solutions $X_s(T)$ because of the fulfillment of this property. Thus, the solution $x(t)$ of the system of equations (51) can be presented in a form that is shorter and simpler for numerical calculation (see the example of the van der Pol system in Section 2.3.).

The matrix S allows the transition from the coordinates of the linear system (52) $(x_1^f; x_2^f)$ to the new coordinates $(x_1^s; x_2^s)$.

According to [21], the solution of the equation in variations define curves, which do not depend on what coordinate system was used for their construction. Therefore, we have the full right to use the coordinate system constructed using the matrix S.

On the one hand, $X_s(t) = X_f(t) \cdot S$, on the other

$$X_s(t) = \Phi_s(t) \cdot \begin{pmatrix} 1 & 0 \\ 0 & e^{\left(\frac{1}{T}\ln\rho_2\right)t} \end{pmatrix}.$$

Where the matrix $\Phi_s(t)$ can be found as

$$\Phi_s(t) = X_f(t) \cdot S \cdot \begin{pmatrix} 1 & 0 \\ 0 & e^{-\left(\frac{1}{T}\ln\rho_2\right)t} \end{pmatrix}.$$

By Lemma 2. of [34], vector-function

$$x(t) = \int_0^{t_k} G(t,s)bv(s)ds, \quad (t_k = kT,\ v(s) \equiv 0 \text{ for } t_k < s) \tag{53}$$

with zero initial conditions $x(0) = (0,0)^T$ will be the solution of inhomogeneous linear system (51), where

$$G(t,s) = X_s(t) \cdot \begin{pmatrix} 0 & 0 \\ 0 & 1 \end{pmatrix} \cdot X_s^{-1}(s),\ s < t,$$

or

$$G(t,s) = \Phi_s(t) \cdot \begin{pmatrix} 0 & 0 \\ 0 & e^{\left(\frac{1}{T}\ln\rho_2\right)(t-s)} \end{pmatrix} \cdot \Phi_s^{-1}(s), \quad s < t.$$

Indeed,

$$x(t) = \int_0^{\infty} G(t,s)bv(s)ds = \int_0^{t_k} G(t,s)bv(s)ds + \int_{t_k}^{\infty} G(t,s)bv(s)ds =$$

$$= \int_0^{t_k} G(t,s)bv(s)ds,$$

because $v(s) \equiv 0$ for $s > t$.

In conclusion, we prove that this vector-function is a solution of the system (51). Firstly, we need to demonstrate two additional properties of matrix $G(t,s)$.

The complete form of the matrix $G(t,s)$ is [34]:

$$G(t,s) = \begin{cases} X_s(t) \cdot \begin{pmatrix} 0 & 0 \\ 0 & 1 \end{pmatrix} \cdot X_s^{-1}(s), & s < t, \\ -X_s(t) \cdot \begin{pmatrix} 1 & 0 \\ 0 & 0 \end{pmatrix} \cdot X_s^{-1}(s), & t < s. \end{cases}$$

Property 1.

$$G(t,t-0) - G(t,t+0) =$$

$$= X_s(t) \cdot \begin{pmatrix} 0 & 0 \\ 0 & 1 \end{pmatrix} \cdot X_s^{-1}(t-0) - \left(-X_s(t) \cdot \begin{pmatrix} 1 & 0 \\ 0 & 0 \end{pmatrix} \cdot X_s^{-1}(t+0) \right) =$$

$$= X_s(t) \left(\begin{pmatrix} 0 & 0 \\ 0 & 1 \end{pmatrix} + \begin{pmatrix} 1 & 0 \\ 0 & 0 \end{pmatrix} \right) \cdot X_s^{-1}(s) = X_s(t) \cdot X_s^{-1}(s) = E_2.$$

Property 2. (for $s < t_k$).

$$\dot{G}_t(t,s) = \dot{X}_s(t) \cdot \begin{pmatrix} 0 & 0 \\ 0 & 1 \end{pmatrix} \cdot X_s^{-1}(s) =$$

$$= A(t) \cdot X_s(t) \cdot \begin{pmatrix} 0 & 0 \\ 0 & 1 \end{pmatrix} X_s^{-1}(s) = A(t) \cdot G(t,s).$$

The differentiation of the function $x(t)$ by parameter t gives:

$$\dot{x}(t) = \left(\int_0^{t_k} G(t,s) bv(s) ds \right)_t' =$$

$$= \left(\int_0^t G(t,s) bv(s) ds + \int_t^{t_k} G(t,s) bv(s) ds \right)_t' =$$

$$= G(t,t-0) bv(s) + \int_0^t \dot{G}(t,s) bv(s) ds - G(t,t+0) bv(s) +$$

$$+\int_t^{t_k}\dot{G}(t,s)bv(s)ds=(G(t,t-0)-G(t,t+0))bv(s)+\int_0^{t_k}\dot{G}(t,s)bv(s)ds$$

$$=bv(s)+\int_0^{t_k}A(t)\cdot G(t,s)bv(s)ds=A(t)\cdot x(t)+bv(s).$$

Thus, the vector-function $x(t)=\int_0^{t_k}G(t,s)bv(s)ds$ is the solution of the inhomogeneous system (51) for any $t\in[0,t_k]$.

Remarkably, the vector-function $x(t)=\int_0^{t_k}G(t,s)bv(s)ds$ is the solution of the inhomogeneous system (51) only for some fixed time. It is impossible to show the same for $t\to\infty$. According to [34] improper integral $\int_0^{\infty}G(t,s)bv(s)ds$ is absolutely convergent only if $\int_0^{\infty}bv(s)ds<\infty$. However, for wide class of perturbation $v(\cdot)\in V=\{v(\cdot)\in KC|\ |v(t)|\leqslant\delta_1<1 \text{ for } t\in(0,\infty)\}$ a counterexample can be found. If $v(t)\equiv\delta_1$ for all $t\in(0,\infty)$, then

$$\int_0^{\infty}bv(s)ds=\int_0^{\infty}b\delta_1 ds=\infty. \tag{54}$$

Thus, it is impossible to prove that the vector function $x(t)=\int_0^{\infty}G(t,s)bv(s)ds$ shall be the solution for system (51) under acting of infinite perturbation.

Therefore, the statement of the robust stability problem for a periodic attractor is impossible for perturbation from the functional set $V=\{v(\cdot)\in KC|\ |v(t)|\leqslant\delta_1<1$ *for* $t\in(0,\infty)$*, i.e. acting infinitely.*

On account of (53):

$$x_1^s(t_1)=\int_0^{t_1}e_1^TG(t_1,s)bv(s)ds,$$

$$x_2^s(t_1)=\int_0^{t_1}e_2^TG(t_1,s)bv(s)ds.$$

These integrals take their maximum value if the function $v(s)$ changes its sign in the same way as the function $G(t_1,s)$. Therefore, the

worst perturbation formulas for coordinates x_1^s and x_2^s are given below:

$$\begin{aligned} v_{1max}^0(s) &= \quad \delta_1 \cdot \text{sign}(e_1^T G(t_1, s)b), \\ v_{1min}^0(s) &= - \quad \delta_1 \cdot \text{sign}(e_1^T G(t_1, s)b), \\ v_{2max}^0(s) &= \quad \delta_1 \cdot \text{sign}(e_2^T G(t_1, s)b), \\ v_{2min}^0(s) &= - \quad \delta_1 \cdot \text{sign}(e_2^T G(t_1, s)b). \end{aligned}$$

The coordinates of the points of maximum deviations can be calculated using the worst perturbations formulas v_{imax}, v_{imin}, $i = 1, 2$. Therefore,

1. The maximum deviation of x_1^s has coordinates:

$$\begin{aligned} \max x_1^s(t_1) &= \delta_1 \int_0^{t_1} |e_1^T G(t_1, s)b| ds, \\ x_2^s(t_1) &= \int_0^{t_1} e_2^T G(t_1, s) b v_{1max}^0(s) ds. \end{aligned}$$

2. The minimum deviation of x_1^s has coordinates:

$$\begin{aligned} \min x_1^s(t_1) &= -\delta_1 \int_0^{t_1} |e_1^T G(t_1, s)b| ds, \\ x_2^s(t_1) &= \int_0^{t_1} e_2^T G(t_1, s) b v_{1min}^0(s) ds. \end{aligned}$$

3. The maximum deviation of x_2^s has coordinates:

$$\begin{aligned} x_1^s(t_1) &= \int_0^{t_1} e_1^T G(t_1, s) b v_{2max}^0 ds, \\ \max x_2^s(t_1) &= \delta_1 \int_0^{t_1} |e_2^T G(t_1, s)b| ds. \end{aligned}$$

4. The minimum deviation of x_2^s has coordinates:

$$\begin{aligned} x_1^s(t_1) &= \int_0^{t_1} e_1^T G(t_1, s) b v_{2min}^0 ds, \\ \min x_2^s(t_1) &= -\delta_1 \int_0^{t_1} |e_2^T G(t_1, s)b| ds. \end{aligned}$$

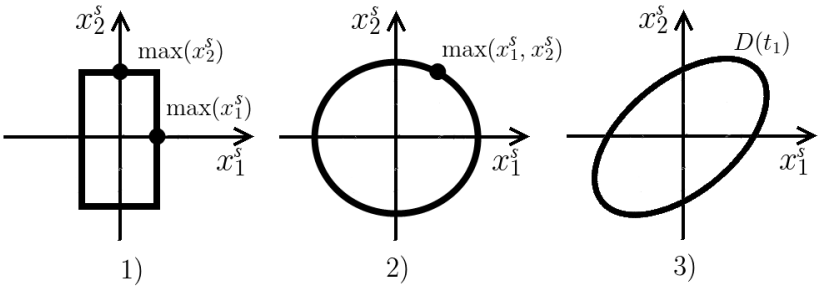

Fig. 26: Estimations of reachable set D_{t_1} $(t_1 < \infty)$.

By finding the minimum and maximum deviations of x_1^s and x_2^s can be constructed the estimations of the reachable set D_{t_1} $(t_1 < \infty)$.

- If for the system in variations we find only two maximum deviations of x_1^s and x_2^s coordinate, then the unimprovable estimation of the reachable set D_{t_1} $(t_1 < \infty)$ is a rectangle (Fig. 26. 1)).

- If will be found the maximum deviation in two coordinates (by using conditional gradient method), then the unimprovable estimation of the reachable set can be presented as a circle (Fig. 26. 2)).

- By the theorem from Section 1.3 for L_2-norm [58], the estimation of the reachable set D_{t_1} $(t_1 < \infty)$ is ellipsoid

$$D(t_1) = \left\{x : \ x^T W_c^{-1}(t_1) x \leqslant 1\right\},$$

where matrix $W_c(t_1) > 0$ and $W_c(t_1) = \int_0^{t_1} e^{As} B B^T e^{A^T s} ds$ (Fig. 26. 3)).

2.2 Algorithm of construction of the reachable set D_{t_1} in a neighborhood of a periodic attractor

According to the theory, presented in Section 2.1, a brief description of the method of construction of the reachable set in a neighborhood of a periodic attractor consists of the following steps.

Step 1. For nonlinear system (50) construct a system in variations by coordinates $x = y - y^0(t)$ and by perturbation $v(t)$ in the neighborhood of the periodic solution:

$$\dot{x} = A(t)x + bv(t), \text{ where } A(t) = \left(\frac{\partial \phi^0(y^0(t))}{\partial y_i}\right).$$

Step 2. For $v_1(t) \equiv 0$ find the normalized fundamental matrix $X_f(t)$

$$\dot{X}_f = A(t)X_f, \quad X_f(0) = E_2.$$

Calculate the monodromy matrix $X_f(T)$ and find the roots $\rho_1,\ \rho_2$ of the characteristic equation

$$\det(\rho E_2 - X_f(T)) = 0.$$

Here by to the theory of Floquet $\rho_1 = 1$ and the theorem of Poincaré $0 < \rho_2 < 1$.

Step 3. Find the matrix $S = (s_1; s_2)$ (where $S^{-1}X_f(T)S = \left(\begin{smallmatrix} 1 & 0 \\ 0 & \rho_2 \end{smallmatrix}\right)$) and make a transition to the special matrix $X_s(t)$

$$X_s(t) = X_f(t) \cdot S.$$

Step 4. Present special matrix $X_s(t)$ in the form

$$X_s(t) = \Phi_s(t) \cdot \begin{pmatrix} 1 & 0 \\ 0 & e^{\left(\frac{1}{T}\ln\rho_2\right)t} \end{pmatrix}$$

and find the T-periodical bounded matrix $\Phi_s(t)$ as

$$\Phi_s(t) = X_f(t) \cdot S \cdot \begin{pmatrix} 1 & 0 \\ 0 & e^{-\left(\frac{1}{T}\ln\rho_2\right)t} \end{pmatrix}.$$

Step 5. Find the worst perturbations

$$v^0_{1max}(s) = \delta_1 \cdot \mathrm{sign}(e_1^T G(t_1, s)b),$$

$$v^0_{2max}(s) = \delta_1 \cdot \mathrm{sign}(e_2^T G(t_1, s)b),$$

and maximum deviations

$$\max x_1^s(t_1) = \delta_1 \left| \int_0^{t_1} e_1^T G(t_1, s)b \; ds \right|,$$

$$\max x_2^s(t_1) = \delta_1 \left| \int_0^{t_1} e_2^T G(t_1, s)b \; ds \right|,$$

where

$$G(t, s) = \Phi_s(t) \cdot \begin{pmatrix} 0 & 0 \\ 0 & e^{\left(\frac{1}{T}\ln\rho_2\right)(t-s)} \end{pmatrix} \cdot \Phi_s^{-1}(s).$$

Step 6. Using conditional gradient method construct points of the boundary of D_{t_1} with the desired accuracy of calculation.

That is to find the maximum of the functional ϕ_0, where in the initial step

$$\phi_0^1 = a x_1^s(t_1, v^1) + b x_2^s(t_1, v^1)$$

and

$$v^1(s) = \delta_1 \mathrm{sign}(a x_1^s(t_1) + b x_2^s(t_1)),$$

where $c^T = (a, b)$ is any vector.

All further steps will have form

$$\phi_0^{n+1} = x_1^s(t_1, v^n) x_1^s(t_1, v^{n+1}) + x_2^s(t_1, v^n) x_2^s(t_1, v^{n+1})$$

and

$$v^{n+1}(s) = \delta_1 \mathrm{sign}(a \max x_1^s(t_1) + b \max x_2^s(t_1)).$$

When the equality

$$\max_{v \in V}[x_1^s(t_1, v^0)x_1^s(t_1, v) + x_2^s(t_1, v^0)x_2^s(t_1, v)] = (x_1^s)^2(t_1, v^0) + (x_2^s)^2(t_1, v^0)$$

satisfies, then point $(x_1^s(t_1, v^0), x_2^s(t_1, v^0))$ is the point of maximum deviation in two coordinates x_1^s and x_2^s. But the other points $(x_1^s(t_1, v^n), x_2^s(t_1, v^n))$ for all previous perturbations $v^n(s)$ lie on the boundary of the reachable set D_{t_1}.

Thus, by varying the value of the initial vector $c^T = (a, b)$, we can get a larger number of the boundary points of reachable set D_{t_1}. Consequently, the boundary of the reachable set D_{t_1} can be constructed with any accuracy we choose. It can be vary only by choosing the larger number of the initial vectors $c^T = (a, b)$. For example, in Section 2.3. different results of construction of the boundary of D_{t_1} presented for 100 and 2500 initial vectors. And for desired result in Section 3.3 we have used 250 000 initial vectors.

Thereby, we conclude that presented algorithm of constructing the boundaries of the reachable set can be applied only at a fixed time. The algorithm proposes a solution to the problem of constructing the reachability set of a linear system with periodic coefficients in the presence of a permanent acting perturbation. This linear system corresponds to a nonlinear perturbation system, which has a periodic attractor when perturbation is equivalent to zero function. A linear system is constructed in the neighborhood of a periodic attractor of a nonlinear system. The origin of the linear system moves along an asymptotically orbitally stable limit cycle. It means that the linear equations in variations have a matrix with periodic coefficients.

As the result of algorithm applying, finally can be obtained the sequence of reachable sets for linear system. However, the union of the elements of this sequence can be considered as an approximation of the

reachable set in the vicinity of the limit cycle of a nonlinear system. It should be noted that the number of sequence elements is selected by the researcher. Thus, the accuracy of the approximation of the reachability set for a nonlinear system is easy to vary.

2.3 An example of applying the method to the Van der Pol's system

Consider the nonlinear system of differential equations of Van der Pol under acting of permanent perturbation $v(t)$:

$$\begin{cases} \ddot{y}_1 + \mu(y_1^2 - 1)\dot{y}_1 + y_1 = v(t), \\ v(\cdot) \in V = \{v(\cdot) \in KC |\ |v(t)| \leqslant \delta_1 < 1,\ 0 \leqslant t \leqslant t_1 < \infty\}, \end{cases} \tag{55}$$

where small parameter $0 < \mu \ll 1$.

For $v(t) \equiv 0$ in a conservative system ($\mu = 0$) all critical points are centers (phase trajectories are closed), therefore oscillations with any amplitude are possible. The amplitude is determined by the initial conditions. In a non-conservative system ($\mu \neq 0$), qualitatively other phenomena are possible, for example, a stable limit cycle.

We introduce substitution $\dot{y}_1 = y_2$ and rewrite the system (55) in another form:

$$\begin{cases} \dot{y}_1 = f_1(y_1, y_2) & = \ y_2, \\ \dot{y}_2 = f_2(y_1, y_2, v(t)) & = -y_1 - \mu y_2(y_1^2 - 1) + v(t), \end{cases} \tag{56}$$

For $v(t) \equiv 0$ system (56) has one critical point $(y_1 = 0, y_2 = 0)$, which is unstable focus, because the roots of the characteristic equation are complex numbers with positive real parts:

$$A = \begin{pmatrix} \frac{\partial f_1(0,0)}{\partial y_1} & \frac{\partial f_1(0,0)}{\partial y_2} \\ \frac{\partial f_2(0,0)}{\partial y_1} & \frac{\partial f_2(0,0)}{\partial y_2} \end{pmatrix} = \begin{pmatrix} 0 & 1 \\ -1 & \mu \end{pmatrix},$$

$$\det(\lambda E_2 - A) = \lambda^2 - \mu\lambda + 1 = 0 \to \lambda_{1,2} = \frac{\mu}{2} \pm i\sqrt{1 - \frac{\mu^2}{4}},\ \frac{\mu}{2} > 0.$$

System (55) has stable limit cycle, accurate to μ^2 close to the circle $y_1^2 + \dot{y_1}^2 = 4$, constructed in coordinate system (y_1, y_2). Existence and stability of this cycle in the sense of Poincaré was shown in [22].

Let us demonstrate the asymptotic stability of the limit cycle using the theorem of Poincaré.

Theorem. *Limit cycle* $y^0(t+T) = y^0(t)$ *of the system*

$$\begin{cases} \dot{y}_1 = f_1(y_1, y_2), \\ \dot{y}_2 = f_2(y_1, y_2), \end{cases}$$

is asymptotically stable in the sense of Poincaré, if [34]

$$Re\,\lambda_2 = \frac{1}{T}\int_0^T \left(\frac{\partial f_1(y_1^0(t), y_2^0(t))}{\partial y_1} + \frac{\partial f_2(y_1^0(t), y_2^0(t))}{\partial y_2} \right) dt < 0.$$

For system (56) limit cycle $y_1^0(t) = 2 \cdot \cos(t),\ y_2^0(t) = -2 \cdot \sin(t)$ has period $T = 2\pi$, thus:

$$\lambda_2 = \frac{1}{2\pi}\int_0^{2\pi} \mu\left(1 - 4\cos^2(t)\right) dt = \frac{\mu}{2\pi} \cdot (-2\pi) = -\mu < 0.$$

Therefore, limit cycle $y_1^2 + \dot{y_1}^2 = 4$ accurate μ^2 is asymptotically stable in the sense of Poincaré.

Let us construct for system (56) system in variations by coordinates and by parameters $\dot{x} = A(t)x + bv(t)$ in the neighborhood of the periodic solution $(y_1^0(t) = 2\cos t,\ y_2^0(t) = -2\sin t)$, where

$$A(t) = \begin{pmatrix} \frac{\partial f_1(y_1^0(t), y_2^0(t))}{y_1} & \frac{\partial f_1(y_1^0(t), y_2^0(t))}{y_2} \\ \frac{\partial f_2(y_1^0(t), y_2^0(t))}{y_1} & \frac{\partial f_2(y_1^0(t), y_2^0(t))}{y_2} \end{pmatrix} = \begin{pmatrix} 0 & 1 \\ 8\mu\cos(t)\sin(t) - 1 & \mu(1 - 4\cos^2(t)) \end{pmatrix}.$$

The system in variations has the following form:

$$\begin{cases} \dot{x_1} = x_2, \\ \dot{x_2} = (8\mu\cos(t)\sin(t) - 1)x_1 + \mu(1 - 4\cos^2(t))x_2 + v(t). \end{cases} \tag{57}$$

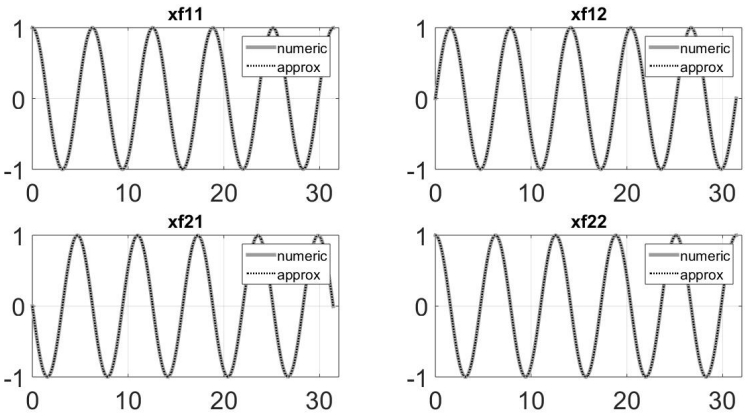

Fig. 27: Numeric solution and approximation of solution of (57) for $\mu = 0.0001$, 5 periods.

If system (57) is unperturbed ($v(t) \equiv 0$), then corresponding fundamental matrix of solutions $X_f(t) = \begin{pmatrix} x_{11}^f(t) & x_{12}^f(t) \\ x_{21}^f(t) & x_{22}^f(t) \end{pmatrix}$ can be obtained by integration of the system (57) with initial conditions $X_f(0) = \left(\begin{smallmatrix} 1 & 0 \\ 0 & 1 \end{smallmatrix}\right)$ accurate to μ^2, $\mu = 0.0001$.

Then we find the approximation of these functions.

In Fig. 27, the solid line shows the numerical results and dotted line approximation, which has an analytical form:

$$X_f(t) = \begin{pmatrix} e^{-\mu t}\cos(t) & \sin(t) \\ -e^{-\mu t}(\mu\cos(t) + \sin(t)) & \cos(t) \end{pmatrix}.$$

For $\mu = 0.0001$ the approximation calculation errors were obtained by the least squares method:

- for x_{11}^f error $\epsilon_1 = 1.55 \cdot 10^{-6}$,

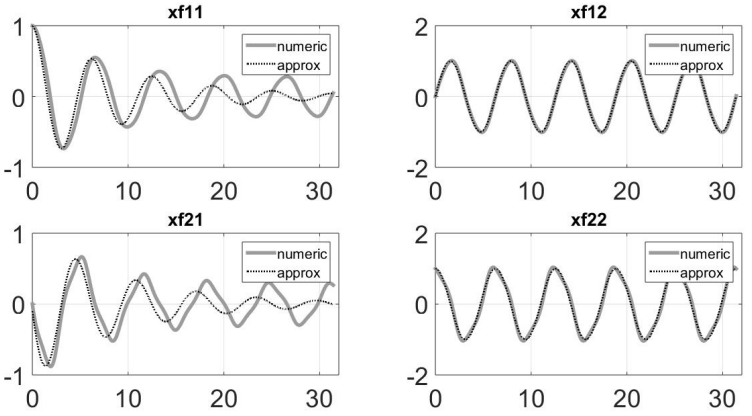

Fig. 28: Numeric solution and approximation of solution of (57) for $\mu = 0.1$ 5 periods.

- for x_{12}^f error $\epsilon_2 = 1.92 \cdot 10^{-6}$,
- for x_{21}^f error $\epsilon_3 = 9.9 \cdot 10^{-5}$,
- for x_{22}^f error $\epsilon_4 = 1.83 \cdot 10^{-5}$.

Errors of approximation grows proportionally with μ, for example for $\mu = 0.1$ errors obtained by the least squares method are:

- for x_{11}^f error $\epsilon_1 = 0.034$,
- for x_{12}^f error $\epsilon_2 = 1 \cdot 10^{-4}$,
- for x_{21}^f error $\epsilon_3 = 0.036$,
- for x_{22}^f error $\epsilon_4 = 6.6 \cdot 10^{-3}$ (Fig. 28).

The initial conditions of fundamental matrices calculated numerically and its approximation are closed to μ^2 also:

- numeric $X_f(0) = \left(\begin{smallmatrix} 1 & 0 \\ 0 & 1 \end{smallmatrix}\right)$;

- approximate $X_f(0) = \left(\begin{smallmatrix} 1 & 0 \\ -\mu & 1 \end{smallmatrix}\right) = \left(\begin{smallmatrix} 1 & 0 \\ -1\cdot 10^{-4} & 1 \end{smallmatrix}\right)$.

Monodromy matrix

$$X_f(2\pi) = \begin{pmatrix} 0.9993 & 0 \\ 0.0001 & 1 \end{pmatrix}$$

allows us to find the Floquet multipliers

$$\det(\rho E - X(2\pi)) = (\rho - 0.9993)(\rho - 1) = 0$$

$$\rightarrow \rho_1 = 1,\ \rho_2 = 0.9993 < 1.$$

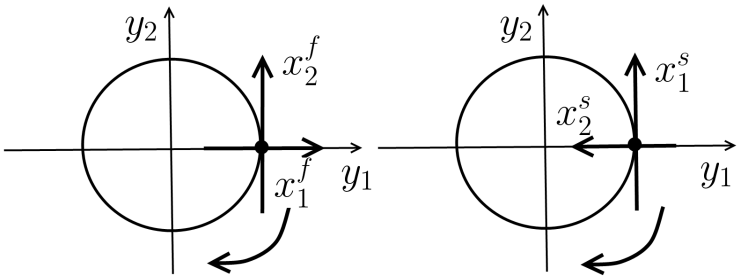

Fig. 29: Position of coordinate axes in nonlinear system and systems in variations.

Let us choose the matrix S such that the condition is satisfied:

$$S^{-1} \cdot X_f(2\pi) \cdot S = \left(\begin{smallmatrix} 1 & 0 \\ 0 & 0.9993 \end{smallmatrix}\right).$$

Thus, can be chosen matrix $S = (s^1; s^2) = \left(\begin{smallmatrix} 0 & -1 \\ 1 & 0 \end{smallmatrix}\right)$ where vectors s^1 and s^2 are orthogonal. Verification:

$$S^{-1}\cdot X_f(2\pi)\cdot S = \begin{pmatrix} 0 & 1 \\ -1 & 0 \end{pmatrix} \cdot \begin{pmatrix} 0.9993 & 0 \\ 0.0001 & 1 \end{pmatrix} \cdot \begin{pmatrix} 0 & -1 \\ 1 & 0 \end{pmatrix} = \begin{pmatrix} 1 & 0 \\ 0 & 0.9993 \end{pmatrix}.$$

The next step of the algorithm of construction of a reachable set D_{t_1} is the construction of fundamental special matrix $X_s(t)$, where

$$X_s(t) = X_f(t) \cdot S = \begin{pmatrix} \sin(t) & -e^{-\mu t}\cos(t) \\ \cos(t) & e^{-\mu t}(\mu\cos(t) + \sin(t)) \end{pmatrix}.$$

On the other hand, in [34] it has been proved that $X_s(t)$ matrix can be presented in the form of a product

$$X_s(t) = \Phi_s(t) \cdot \begin{pmatrix} 1 & 0 \\ 0 & e^{\left(\frac{1}{2\pi}\ln|\rho_2|\right)t} \end{pmatrix} = \begin{pmatrix} 1 & 0 \\ 0 & e^{(-\mu)t} \end{pmatrix}.$$

where

$$\Phi_s(t) = \begin{pmatrix} \Phi_{s11}(t) & \Phi_{s12}(t) \\ \Phi_{s21}(t) & \Phi_{s22}(t) \end{pmatrix}$$

is a bounded 2π-periodic matrix.

Which implies that

$$\Phi_s(t) = X_s(t) \cdot \begin{pmatrix} 1 & 0 \\ 0 & e^{(-\mu)t} \end{pmatrix}^{-1} =$$

$$= \begin{pmatrix} \sin(t) & -e^{(-\mu)t}\cos(t) \\ \cos(t) & e^{(-\mu)t}(\mu\cos(t) + \sin(t)) \end{pmatrix} \begin{pmatrix} 1 & 0 \\ 0 & e^{\mu t} \end{pmatrix} = \begin{pmatrix} \sin(t) & -\cos(t) \\ \cos(t) & \mu\cos(t) + \sin(t) \end{pmatrix}.$$

The inverse matrix of $\Phi_s(t)$ has form

$$\Phi_s^{-1}(s) = \frac{1}{(\mu\cos(s)\sin(s) + 1)} \begin{pmatrix} \mu\cos(s) + \sin(s) & \cos(s) \\ -\cos(s) & \sin(s) \end{pmatrix}.$$

The graphs of all 4 functions of matrix $\Phi_s(t)$ and the inverse matrix inv$\Phi_s(t)$ are presented in Figs. 30-31 correspondingly.

Using matrices $\Phi_s(t)$ and $\Phi_s^{-1}(s)$, can be calculated the matrix $G(t_1, s)$:

$$G(t_1, s) = \Phi_s(t_1) \cdot \begin{pmatrix} 0 & 0 \\ 0 & e^{(-\mu)(t_1 - s)} \end{pmatrix} \cdot \Phi_s^{-1}(s) =$$

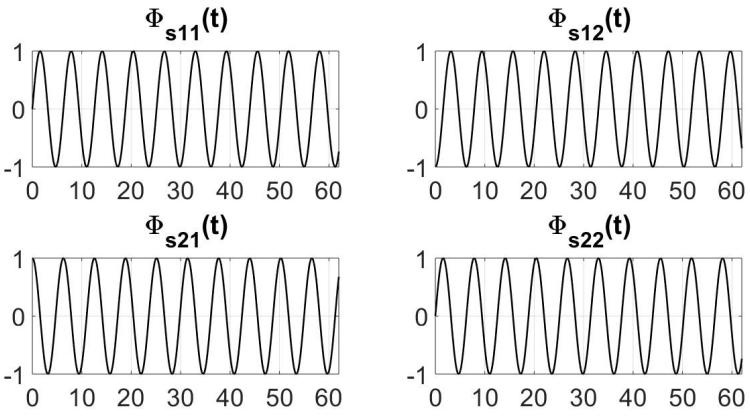

Fig. 30: Matrix $\Phi_s(t)$ for $\mu = 0.0001$, 10 periods.

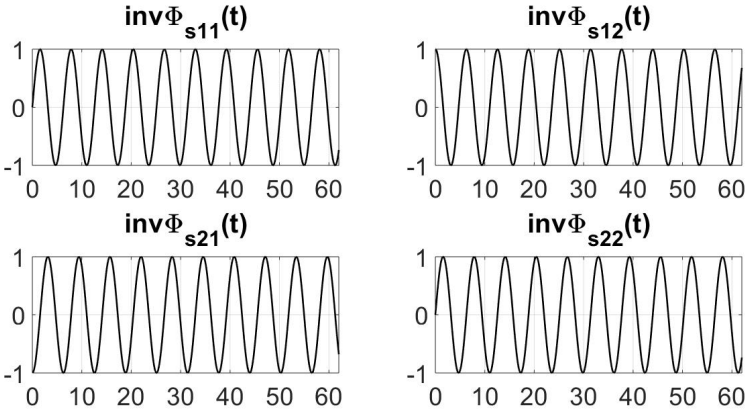

Fig. 31: Matrix $\text{inv}\Phi_s(t)$, inverse matrix of $\Phi_s(t)$ for $\mu = 0.0001$, 10 periods.

$$= \begin{pmatrix} \sin(t_1) & -\cos(t_1) \\ \cos(t_1) & \mu\cos(t_1)+\sin(t_1) \end{pmatrix} \cdot \begin{pmatrix} 0 & 0 \\ 0 & e^{(-\mu)(t_1-s)} \end{pmatrix} \times$$

$$\times \frac{1}{(\mu\cos(s)\sin(s)+1)} \begin{pmatrix} \mu\cos(s)+\sin(s) & \cos(s) \\ -\cos(s) & \sin(s) \end{pmatrix} =$$

$$= \begin{pmatrix} \frac{e^{-\mu(t_1-s)}\cos(t_1)\cos(s)}{(\mu\cos(s)\sin(s)+1)} & \frac{-e^{-\mu(t_1-s)}\cos(t_1)\sin(s)}{(\mu\cos(s)\sin(s)+1)} \\ \frac{-e^{-\mu(t_1-s)}\cos(s)(\mu\cos(t_1)+\sin(t_1))}{(\mu\cos(s)\sin(s)+1)} & \frac{e^{-\mu(t_1-s)}\sin(s)(\mu\cos(t_1)+\sin(t_1))}{(\mu\cos(s)\sin(s)+1)} \end{pmatrix}.$$

Then the worst perturbations are:

- for coordinate x_1^s

$$v_1^0(s) = \delta_1 \cdot \operatorname{sign}\left((1\ 0) \cdot (G(t_1,s)) \cdot \begin{pmatrix} 0 \\ 1 \end{pmatrix} \right) =$$

$$= \delta_1 \cdot \operatorname{sign}\left(\frac{e^{-\mu(t_1-s)}(-\cos(t_1))(\sin(s))}{\mu\cos(s)\sin(s)+1} \right);$$

- for coordinate x_2^s

$$v_2^0(s) = \delta_1 \cdot \operatorname{sign}\left((0\ 1) \cdot (G(t_1,s)) \cdot \begin{pmatrix} 0 \\ 1 \end{pmatrix} \right) =$$

$$= \delta_1 \cdot \operatorname{sign}\left(\frac{e^{-\mu(t_1-s)}(\mu\cos(t_1)+\sin(t_1))(\sin(s))}{\mu\cos(s)\sin(s)+1} \right).$$

Thus, the maximum deviations in coordinates x_1^s and x_2^s are

$$\max_{v\in V} x_1^s(t_1) = \delta_1 \int_0^{t_1} \left| \frac{e^{-\mu(t_1-s)}(-\cos(t_1))(\sin(s))}{(\mu\cos(s)\sin(s)+1)} \right| ds,$$

$$\max_{v\in V} x_2^s(t_1) = \delta_1 \int_0^{t_1} \left| \frac{e^{-\mu(t_1-s)}(\mu\cos(t_1)+\sin(t_1))(\sin(s))}{(\mu\cos(s)\sin(s)+1)} \right| ds.$$

An integrated function that depends on (t_1, s) can be expressed as the product of two functions, one of which depends on (t_1) and other on (s):

$$\max_{v\in V} x_1^s(t_1) = \delta_1 \left| e^{(-\mu)t_1}(-\cos(t_1)) \right| \cdot \int_0^{t_1} \left| \frac{e^{\mu s}(\sin(s))}{(\mu\cos(s)\sin(s)+1)} \right| ds, \quad (58)$$

$$\max_{v\in V} x_2^s(t_1) = \delta_1 \left| e^{(-\mu)t_1}(\mu\cos(t_1)+\sin(t_1) \right| \cdot \int_0^{t_1} \left| \frac{e^{\mu s}(\sin(s))}{(\mu\cos(s)\sin(s)+1)} \right| ds. \quad (59)$$

For time $t_1 = T = 2\pi$ and $\delta_1 = 0.1$ were calculated 4 worst perturbations corresponding $\max x_1^s$, $minx_1^s$, $\max x_2^s$ and $\min x_2^s$. Results presented in Figs 32-35.

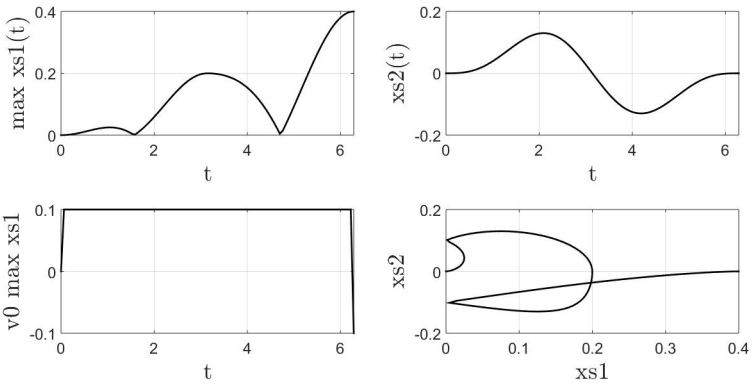

Fig. 32: 1) $\max x_1^s$; 2) x_2^s under acting of worst perturbation v^0 for $\max x_1^s$; 3) Worst perturbation v^0 for $\max x_1^s$; 4) Phase plane (x_1^s, x_2^s).

A more accurate boundary of the reachable set D_{t_1} is constructed due to the conditional gradient method.

The total period of oscillation of the system is divided by the number of points we have chosen. The distance between the points is the same and all of them are located on the orbit of the limit cycle. For

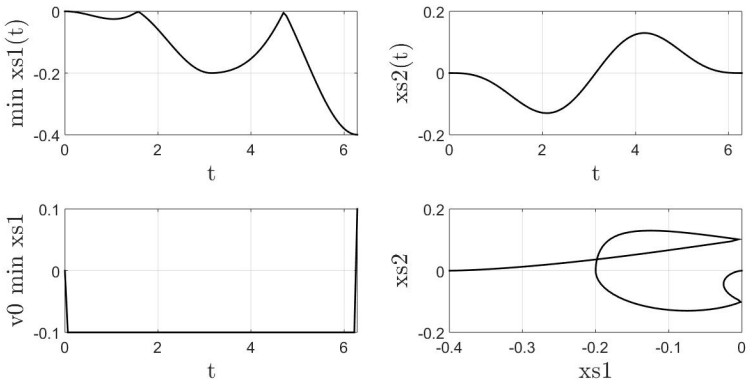

Fig. 33: 1) $\min x_1^s$; 2) x_2^s under acting of worst perturbation v^0 for $\min x_1^s$; 3) Worst perturbation v^0 for $\min x_1^s$; 4) Phase plane (x_1^s, x_2^s).

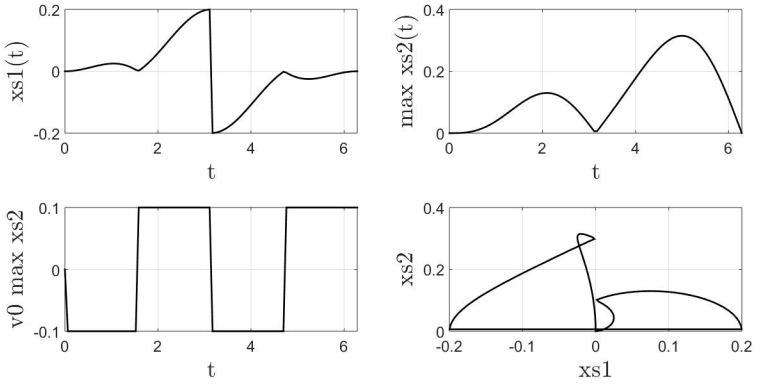

Fig. 34: 1) x_1^s under acting of worst perturbation v^0 for $\max x_2^s$; 2) $\max x_2^s$; 3) Worst perturbation v^0 for $\max x_2^s$; 4) Phase plane (x_1^s, x_2^s).

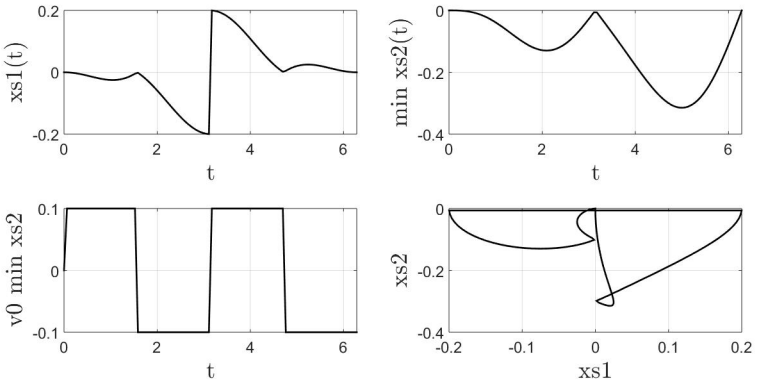

Fig. 35: 1) x_1^s under acting of worst perturbation v^0 for $\min x_2^s$; 2) $\min x_2^s$; 3) Worst perturbation v^0 for $\min x_2^s$; 4) Phase plane (x_1^s, x_2^s).

each individual point we find the maximum deviations in the coordinate x_1^s and x_2^s. Then the remaining points of the boundary of the reachable set are rebuilt using the conditional gradient method. The number of obtained points depends on the number of selected initial vectors c^T.

Thus, the boundary of the reachable set D_{t_1} can be constructed with any desired accuracy. For example, Fig. 36 illustrates results for period 2π divided into 10 points and using 100 initial vectors for each point. Fig. 37 illustrates results for same 10 points, but using 2500 initial vectors for each point. And on the Fig. 38 are presented results for period 2π divided into 20 points by using 2500 initial vectors for each point.

Using the above method was constructed the exact boundary of the reachable set D_{t_1} for $0 \leqslant t_1 \leqslant 2\pi$ for system (55). With an increase in the number of divided one period points to 100, can be seen the exact boundary of the reachable set D_{t_1} for nonlinear system (55).

The reachable set D_{t_1} for nonlinear system (55) is an area represented in the Fig. 39.

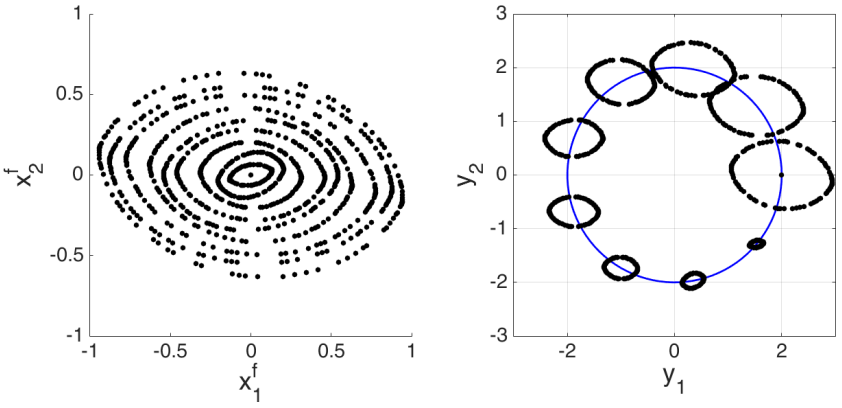

Fig. 36: For 10 points, 100 initial vectors: 1. Boundary points of D_{t_1} for $0 \leqslant t_1 \leqslant 2\pi$ for system (57). 2. Boundary points of D_{t_1} for $0 \leqslant t_1 \leqslant 2\pi$ for system (55).

.

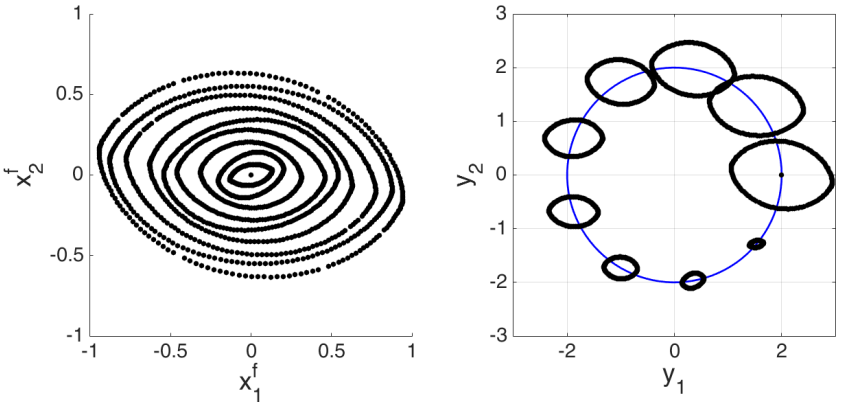

Fig. 37: For 10 points, 2500 initial vectors: 1. Boundary points of D_{t_1} for $0 \leqslant t_1 \leqslant 2\pi$ for system (57). 2. Boundary points of D_{t_1} for $0 \leqslant t_1 \leqslant 2\pi$ for system (55).

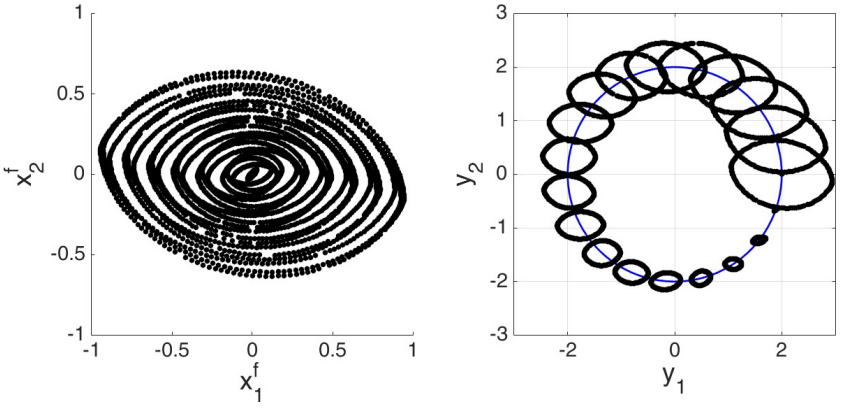

Fig. 38: For 20 points, 2500 initial vectors: 1. Boundary points of D_{t_1} for $0 \leqslant t_1 \leqslant 2\pi$ for system (57). 2. Boundary points of D_{t_1} for $0 \leqslant t_1 \leqslant 2\pi$ for system (55).

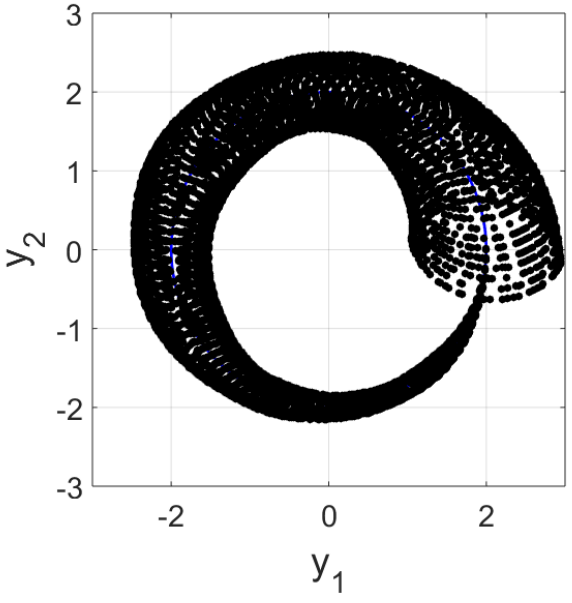

Fig. 39: Reachable set D_{t_1} for $0 \leqslant t_1 \leqslant 2\pi$ for system (55).

Refinement: the integral for the Van der Pol model without using the above method, has the following form

$$X_f(t) = \begin{pmatrix} e^{-\mu t}\cos(t) & \sin(t) \\ -e^{-\mu t}(\cos(t)+\sin(t)) & \cos(t) \end{pmatrix},$$

$$X_f^{-1}(s) = \begin{pmatrix} \frac{e^{\mu s}\cos(s)}{\mu\cos(s)\sin(s)+1} & -\frac{e^{\mu s}\sin(s)}{\mu\cos(s)\sin(s)+1} \\ \frac{\mu\cos(s)+\sin(s)}{\mu\cos(s)\sin(s)+1} & \frac{\cos(s)}{\mu\cos(s)\sin(s)+1} \end{pmatrix}.$$

Using the general solution

$$x_i^f(t_1) = \int_0^{t_1} e_i^T X_f(t_1)\cdot X_f^{-1}(s) b ds \quad i = 1,2$$

the maximum and minimum deviations in coordinates x_1^f and x_2^f are obtained:

$$\max_{v\in V} x_1^f(t_1) = \delta_1 \int_0^{t_1} \left| \frac{-e^{-\mu t_1}\cos(t_1)\cdot e^{\mu s}\sin(s) + \sin(t_1)\cdot\cos(s)}{\mu\cos(s)\sin(s)+1} \right| ds,$$

$$\max_{v\in V} x_2^f(t_1) = \delta_1 \int_0^{t_1} \left| \frac{e^{-\mu t_1}(\mu\cos(t_1)+\sin(t_1))\cdot e^{\mu s}\sin(s)+\cos(t_1)\cdot\cos(s)}{\mu\cos(s)\sin(s)+1} \right| ds.$$

The resulting formulas have a more complicated form then (58) - (59), the integrated function cannot be represented as the product of two functions, one of which depends on (t_1) and other on (s). Thus, the value of t_1 each time will need firstly substitute into the integrated function and only after that calculate the integral (which is also calculated numerically, because this integral cannot be calculated analytically).

2.4 Solution of the problem of inverse transition from the region of attraction of periodic attractor to the region of attraction of point attractor in bistable system

To solve the inverse transition problem, we need to turn to the bistable system (44) with two attractors. One of them is an

asymptotically orbitally stable limit cycle $y^0(t) = (y_1^0(t), y_2^0(t))$ and another one is a point attractor - stable focus (y_1^0, y_2^0). The region of attraction of a point attractor is denoted by A^* and it is bounded by a limit cycle, asymptotically orbitally stable in inverse time. The focus is located inside of the orbit of limit cycle $y^0(t)$. All points that do not belong to A^*, belonging to the domain of attraction of a periodic attractor, denoted $B^* = B \cup C$ (Fig. 40).

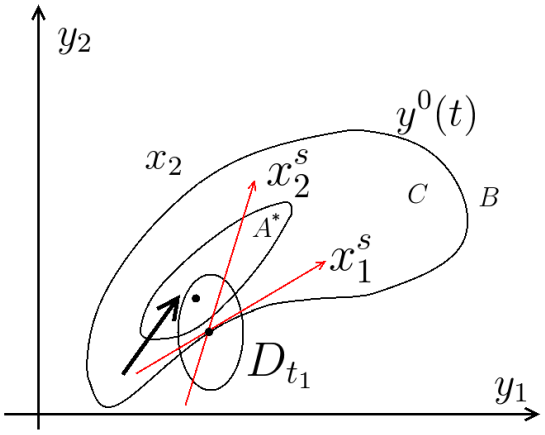

Fig. 40: Phase portrait of the bistable system (44).

The problem of the inverse transition in the system is that, with the same initial conditions, system must move from the region of attraction of a periodic attractor, to the region of attraction of a point attractor. One of the solutions is an option to add a permanent perturbation to the system (44) and work with system (45).

Algorithm for solving the problem of inverse transition:

1. From the nonlinear system (45) we make a transition to the system in variations

$$\dot{x} = A(t)x + bv(t), \tag{60}$$

by coordinates $x_i = y_i - y_i^0(0),\ i = 1,2,\ A = \left(\frac{\partial f^0(y_1^0(t), y_2^0(t)}{\partial y_i}\right)$ and by perturbation $b = \left(\frac{\partial (f^0(y)+bv)}{\partial v}\right)$ in the neighborhood of an orbitally stable limit cycle $(y_1^0(t), y_2^0(t))$.

2. Then we apply the algorithm of construction of reachable set D_{t_1}. Here t_1 - time of acting of permanent perturbation on the system.

3. Finally, we must compare the region of attraction of a point attractor A^* with the reachable set D_{t_1}. In contrast to the case of a direct transition, where we looked for points D_{t_1} that did not belong to A^*, here we are interested in the opposite. If set A^* and set D_{t_1} have commune points, then the problem of the inverse transition can be solved.

Numeric example of this algorithm and the solution of the problem of inverse transition in the Model of Hodgkin-Huxley with modifications of Soto-Alexandrov will be presented further in paragraph 3.3.

ANALYSIS AND SYNTHESIS OF THE MODEL OF HODGKIN-HUXLEY OF THE PRIMARY AFFERENT NEURON WITH MODIFICATIONS OF SOTO - ALEXANDROV

3.1 Analysis of the Model of Hodgkin - Huxley with modifications of Soto-Alexandrov of the second order. Application of the theorem of Andronov-Leontovich.

One of the main components of the human bionavigation system is a vestibular mechanoreceptor [54]. Let us consider the output block of the mechanoreceptor, namely, primary afferent neuron (or afferent nerve fiber). The main activity of the nerve fiber is the current generation as a response to the mechanical displacement of the hair cell cilias [25]. The study of the vestibular apparatus and, in particular, afferent primary neuron, makes it possible to solve the following practical problems:

- maintenance a stable upright stance for aged people [35];
- advanced flight simulation for training pilots in flight simulators [67];
- stabilization of the gaze during extreme flight situations [67].

Therefore, there is a huge interest to study the main physical parameters of the vestibular mechanoreceptor. The first mathematical model of the vestibular afferent neuron was introduced by Alan Hodgkin and Andrew Huxley in 1952 [41]. Further on, the initial Hodgkin-Huxley

model was enhanced by a series of experiments on the rats. These experiments were conducted in the Sensory Neurophysiology Laboratory headed by Dr. Enrique Soto [6]. In contrast with other models ([39, 56]), the model of Hodgkin-Huxley with modifications of Soto-Alexandrov is based in experimentally defined physiological parameters obtained from mammalian vestibule. The modified model includes a new coordinate related to the inactivation parameter of the potassium current, whose dynamics is described by the Kolmogorov equation for the Markov processes [52, 53] with a discrete number of states.

The explicit form of the simplified and modified Hodgkin-Huxley model is given by:

$$\begin{cases} C_{\rm m}\dfrac{dV}{dt} = I_{\rm syn} + \gamma_1 v_1(t) - g_{\rm L}(V - V_L) - g_{\rm K}n^4 h_{\rm K}(V - V_{\rm K}) - \\ \qquad\qquad - g_{\rm Na}(m_\infty(V))^3(C(V) - n)(V - V_{\rm Na}), \\ \dfrac{dn}{dt} = \dfrac{n_\infty(V) - n}{\tau_{\rm n}(V)}Q_{10}. \end{cases} \tag{61}$$

These equations are some modifications of the original Hodgkin - Huxley equations with consideration of experimental data [12] and the temperature factor Q.

The main physical parameters of the system (61) are given below:

V is the neuron action potential [mV];

$I_{\rm syn}$ is a constant value of the synaptic current $[\mu{\rm A}/{\rm cm}^2]$;

$v_1(\cdot) \in V = \{v(\cdot) \in KC|\ |v(t)| \leqslant \delta_1 < 1\}$ is a galvanic current (control or perturbation);

$I_{\rm Na}$ and $I_{\rm K}$ are the mean sodium and potassium currents respectively:

$$I_{\rm Na} = g_{\rm Na}(m_\infty(V))^3\ (C(V) - n)(V - V_{\rm Na}),$$
$$I_{\rm K} = g_{\rm K}n^4 h_{\rm K}(V - V_{\rm K}).$$

The second equality in (61) is the Kolmogorov probability

equation for a Markov process having two discrete states, namely, open (or active) and closed (inactive) [6, 53]. The $n(t)$ is a probability of the presence of potassium current activation particle in the potassium channels; h_{K} is a parameter that describes the process of the potassium current inactivation particles; g_{Na} and g_{K} denote the maximum conductances of the sodium and potassium channels respectively.

The functional parameters are of the form:

$m_\infty(V) = \dfrac{1}{1+e^{-\frac{V+33.8}{5.2}}}$	parameter of activation I_{Na}
$h_{\mathrm{Na}_\infty}(V) = \dfrac{1}{1+e^{\frac{V+60.5}{9.9}}}$	parameter of inactivation I_{Na}
$n_\infty(V) = \dfrac{1}{1+e^{-\frac{V+35}{5}}}$	parameter of activation I_{K}
$\tau_n(V) = \dfrac{68}{e^{-\frac{25+V}{15}}+e^{\frac{V+30}{20}}}$	time constant of I_{K} activation process
$Q_{10} = a^{\frac{T-T_0}{10}}$	temperature factor
$C(V) = n_\infty(V) + h_{\mathrm{Na}_\infty}(V)$	integral constant at fixed V

The numerical parameters in use are given in the Table 1.

Analyzing the isocline intersections of system (61) and the stability of singular points (for $v_1(t) \equiv 0$), one concludes that the Andronov-Hopf bifurcation point [19] is $I_{\mathrm{syn}} = 1.1476$ [μA/cm^2] and the bifurcation interval with two attractors is $I_{\mathrm{syn}} \in [0.9100, 1.1476)$ [12]. Hence, the system expressed by (61) is a bistable system with the

Parameter	Value	Units
C_{m}	1	$\mu\mathrm{F}/\mathrm{cm}^2$
V_{Na}	52	$m\mathrm{V}$
V_{K}	-84	$m\mathrm{V}$
V_{L}	-63	$m\mathrm{V}$
g_{Na}	2.3	$m\mathrm{S}/\mathrm{cm}^2$
g_{K}	2.4	$m\mathrm{S}/\mathrm{cm}^2$
g_L	0.03	$m\mathrm{S}/\mathrm{cm}^2$
h_K	0.7329	1
a	3	1
T	37	$^\circ C$
T_0	20	$^\circ C$
I_{syn}	$0-150$	$\mu\mathrm{A}/\mathrm{cm}^2$
γ_1	0.5	1

Table 1: Numerical parameters of the Modified Model of Hodgkin - Huxley

values of I_{syn} belonging to this interval (Fig. 41).

In the left neighborhood of the bifurcation interval there is an asymptotically stable focus; in the right neighborhood therein, we have a globally asymptotically orbitally stable limit cycle. On the bifurcation interval $I_{\mathrm{syn}} \in [0.9100, 1.1476)$ the stable focus is situated within the limit cycle (Fig 42). We shall use the Andronov-Leontovich theorem to analyze the system (61) [68].

Consider a bistable nonlinear system

$$\begin{cases} \dot{y}_1 = f_1(y_1, y_2, \mu), \\ \dot{y}_2 = f_2(y_1, y_2, \mu), \end{cases} \tag{62}$$

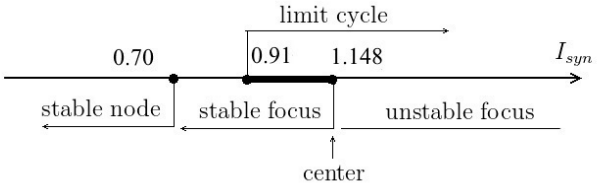

Fig. 41: Analysis of critical points of the system (61), bold line - the interval of bifurcation.

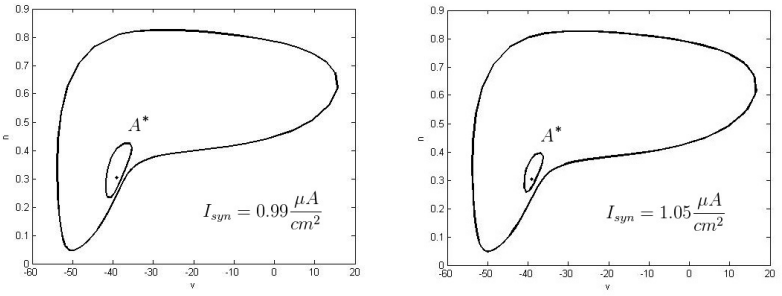

Fig. 42: Regions of attraction of stable focus A^* and globally asymptotically orbitally stable limit cycle for $I_{\rm syn} = 0.99$ [μA/cm^2] and $I_{\rm syn} = 1.05$ [μA/cm^2].

where $\mu = 0$ is a point of bifurcation of Andronov-Hopf. Then, for $\mu = 0$, the system (62) has a point of equilibrium with only imaginary characteristic exponents. Therefore, the roots of the characteristic equation $\lambda_{1,2}$ in the neighborhood of this point can be rewritten as:

$$\lambda_{1,2} = \alpha(\mu) \pm i\beta(\mu),$$

where $\alpha(\mu)$ and $\beta(\mu)$ are C^1-smooth functions of μ and

$$\alpha(0) = 0, \quad \beta(0) > 0.$$

By the theorem of reduction of system in the neighborhood of the equilibrium point y^0 [68], system (62) can be presented in the form

$(x = y - y^0)$:

$$\begin{cases} \dot{x}_1 = \alpha(\mu)x_1 - \beta(\mu)x_2 + G_1(x_1, x_2, \mu), \\ \dot{x}_2 = \beta(\mu)x_1 + \alpha(\mu)x_2 + G_2(x_1, x_2, \mu), \end{cases} \tag{63}$$

where $G_{1,2}$ are C^2-smooth functions.

Theorem of Andronov - Leontovich:

If the first value of Lyapunov $L_1 > 0$ for the system (63), then for small $\mu > 0$ state of equilibrium (v_0, n_0) unstable (unstable focus) and all trajectories leave a small neighborhood of the origin (in our case they are getting closer to the asymptotically stable by Poincaré limit cycle). When $\mu < 0$, state of equilibrium is stable (stable focus). Its region of attraction bounded by a periodic orbit with diameter $\sim \sqrt{-\mu}$, which is contracted to (v_0, n_0) for $\mu = 0$ and asymptotically stable by Poincaré in inverse time limit cycle [68].

Consider unperturbed $(v_1(t) \equiv 0)$ system (61) in the neighborhood of the bifurcation point $I_{\text{syn}} = I^*_{\text{syn}} + \Delta I_{\text{syn}}$, where $\Delta I_{\text{syn}} = \mu$, $I^*_{\text{syn}} = 1.1476$ $[\mu\text{A/cm}^2]$ and $\mu \in [-\mu_0, \mu_0]$, $0 < \mu_0 \ll 1$, $\mu_0 = 0.001$ (Table 2).

Making transition $(v, n) = y = Sx$, where

$$S = \begin{pmatrix} s_{11} & s_{12} \\ s_{21} & s_{22} \end{pmatrix} = \begin{pmatrix} \frac{\partial f1}{\partial v} - \alpha(\mu) & -\beta(\mu) \\ \frac{\partial f2}{\partial v} & 0 \end{pmatrix},$$

we shall obtain a new system in the neighborhood of the equilibrium point (Table 3):

$$\dot{x} = S^{-1} f(Sx) = F(x). \tag{64}$$

For $\mu \in [-0.001, 0.001]$, the third-order Taylor series

Table 2: Numerical calculus of critical points (v^0, n^0) and functions $\alpha(\mu)$, $\beta(\mu)$ for system (61) in the neighborhood of bifurcation point $I^*_{\text{syn}} = 1.1476$ $[\mu\text{A/cm}^2]$.

I_{syn}	μ	v^0	n^0	$\alpha(\mu)$	$\beta(\mu)$
1.1466	-0.0010	-38.6777	0.3240	-0.00016	0.3369
1.1467	-0.0009	-38.6775	0.3240	-0.00013	0.3369
1.1468	-0.0008	-38.6773	0.3240	-0.00011	0.3369
1.1469	-0.0007	-38.6771	0.3240	-0.00009	0.3369
1.1470	-0.0006	-38.6768	0.3240	-0.00006	0.3369
1.1471	-0.0005	-38.6766	0.3240	-0.00004	0.3369
1.1472	-0.0004	-38.6763	0.3240	-0.00001	0.3369
1.1473	-0.0003	-38.6760	0.3241	-0.00007	0.3371
1.1474	-0.0002	-38.6758	0.3241	-0.00005	0.3371
1.1475	-0.0001	-38.6755	0.3241	-0.00002	0.3371
1.1476	**0**	**-38.6749**	**0.3241**	**0**	**0.3371**
1.1477	0.0001	-38.6747	0.3241	0.00007	0.3371
1.1478	0.0002	-38.6746	0.3241	0.00009	0.3371
1.1479	0.0003	-38.6745	0.3241	0.00010	0.3371
1.1480	0.0004	-38.6742	0.3241	0.00013	0.3371
1.1481	0.0005	-38.6739	0.3241	0.00016	0.3371
1.1482	0.0006	-38.6737	0.3242	0.00008	0.3373
1.1483	0.0007	-38.6734	0.3242	0.00012	0.3373
1.1484	0.0008	-38.6731	0.3242	0.00015	0.3373
1.1485	0.0009	-38.6729	0.3242	0.00017	0.3373
1.1486	0.0010	-38.6726	0.3242	0.00021	0.3373

Table 3: Transition matrices S and critical points (x_1^0, x_2^0) for different values μ.

μ	s_{11}	s_{12}	s_{21}	s_{22}	x_1^0	x_2^0
-0.001	0.2984	-0.3369	0.0131	0	24.7328	136.7069
0	0.2983	-0.3371	0.0131	0	24.7381	136.6524
0.001	0.2987	-0.3373	0.0131	0	24.7479	136.6070

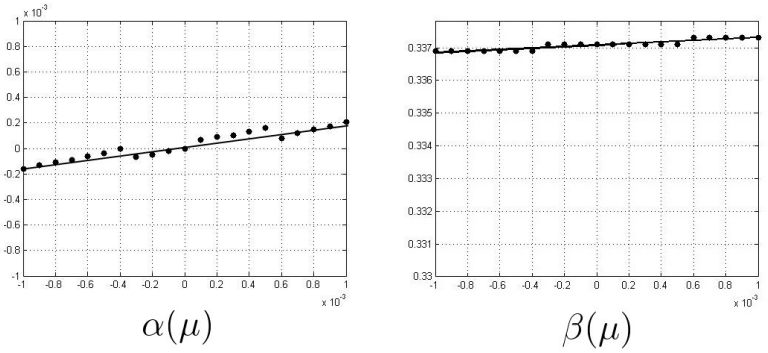

Fig. 43: Functions $\alpha(\mu)$ and $\beta(\mu)$.

decomposition of the system (64) gives

$$\begin{cases} \dot{x}_1 = \alpha(\mu)x_1 - \beta(\mu)x_2 + 0.0032x_1^2 - 0.003x_1x_2 - 0.0009x_2^2 - \\ \quad -0.0001x_1^3 + 0.0003x_1^2x_2 - 0.0003x_1x_2^2 + 0.0001x_2^3; \\ \dot{x}_2 = \beta(\mu)x_1 + \alpha(\mu)x_2 + 0.0248x_1^2 + 0.0334x_1x_2 - 0.0366x_2^2 + \\ \quad +0.0005x_1^3 + 0.0021x_1^2x_2 - 0.004x_1x_2^2 + 0.002x_2^3; \end{cases} \tag{65}$$

$\alpha(\mu)$ and $\beta(\mu)$ are presented at Fig. 43.

According to the formulas of calculation of the first Lyapunov value [30] for the system (65) in a small neighborhood of the point $\mu = 0$, the first value of Lyapunov is equal to $L_1 = 0.0195 > 0$. Explicitly, the

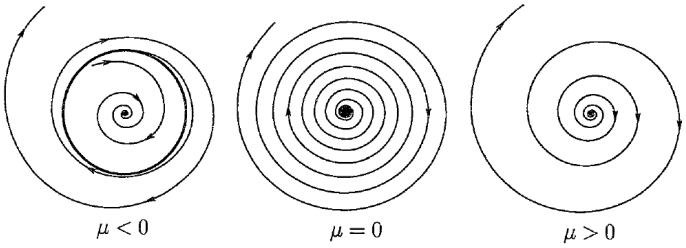

Fig. 44: Loose of stability by stable focus in the coordinate origin under the bifurcation of Andronov-Hopf [68].

details of this value calculation is given in Appendix A.

Eventually, when $\mu < 0$, equilibrium state is stable (stable focus). It's region of attraction is bounded by the periodic orbit of the diameter $\sim \sqrt{-\mu}$, which is contracting to (v_0, n_0) for $\mu = 0$ and it is an asymptotically stable by Poincaré in inverse time limit cycle.

3.2 Analysis of the Model of Hodgkin-Huxley with modifications of Soto-Alexandrov of the third order

The original Model of Hodgkin-Huxley with modifications of Soto-Alexandrov is the ninth order differential equations system. However, in the work [6] it was justified that the ninth-order system can be reduced to the third order one. Besides of that, the third-order system could be presented in the form of the second order equations system [8]. Here, we

shall study a system of third order having the form:

$$\begin{cases} C_{\rm m}\dfrac{dV}{dt} = I_{\rm syn} + \gamma_1 v_1(t) - g_{\rm L}(V - V_L) - g_{\rm K} n^4 h_{\rm K}(V - V_{\rm K}) - \\ \qquad\qquad - g_{\rm Na}(m_\infty(V))^3 (C(V) - n)(V - V_{\rm Na}), \\ \dfrac{dn}{dt} = \dfrac{n_\infty(V) - n}{\tau_{\rm n}(V)} Q_{10}, \\ \dfrac{dh_k}{dt} = \dfrac{h_{k\infty}(V) - h}{\tau_{h_k}(V)} Q_{10}, \end{cases} \tag{66}$$

$v_1(\cdot) \in V = \{v(\cdot) \in KC |\ |v(t)| \leqslant \delta_1 < 1\}$ is a galvanic current (control or perturbation), V is the membrane potential, n and h_k are the probabilities, which in physiology have the meaning of the potassium current activation and inactivation respectively, $h_{k\infty}(V)$ and $\tau_{h_k}(V)$ are explicitly given by

$$h_{k\infty}(V) = \frac{0.96408 - 0.7329}{1 + e^{\dfrac{V + 33.87968}{10.24986}}} + 0.7329,$$

$$\tau_{h_k}(V) = \frac{1250}{e^{-\dfrac{V + 15}{15}} + e^{\dfrac{V + 25}{10}}} + 500.$$

Other physical parameters fully correspond to those that were taken into account when considering the second-order system (61).

The system (66) for $v_1(t) \equiv 0$ is solved using numerical integration procedures such as Runge-Kutta methods. Specifically, we have used the **ode23** function which is the principal MATLAB instrument for solving nonstiff ordinary differential equations. The numerical integration of system (66) requires an indication of the corresponding parameters and initial conditions, which are given below:

- $I_{\rm syn} \in [0\ -\ 70]$ [μA/cm^2];
- $[V^0\ \ n^0\ \ h_k^0] = [-45\ \ 0.1\ \ 0.73]$ are the initial conditions for integration in the direct time (t);

- $[V^0_{inv}\ n^0_{inv}\ h^0_{k,inv}] = [-39\ 0.3\ 0.88]$ are the initial conditions for integration in the inverse time ($\tau = -t$);
- 500 [ms] is the integration time for both direct (t) and inverse (τ) integration processes;
- 15000 of integration points are used during both direct (t) and inverse (τ) integration.

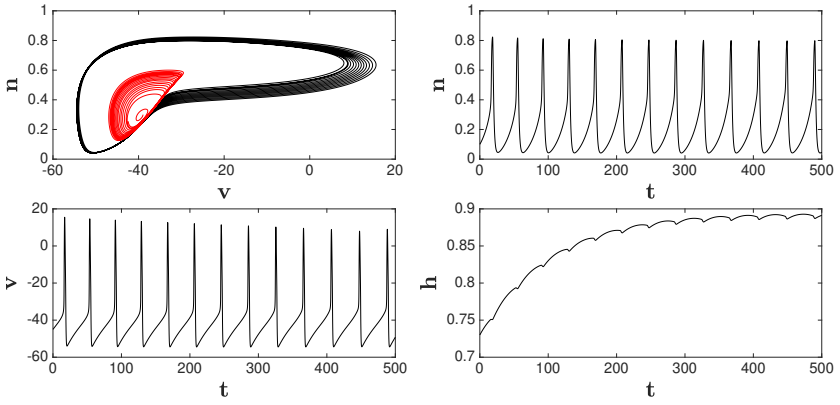

Fig. 45: Results of integration of the system (66) in surface by using $I_{\text{syn}} = 0.99\ [\mu\text{A/cm}^2]$.

Integration of the system (66) in the direct time t gives the limit cycle that is asymptotically orbitally stable in direct time. The resulting cycle is demonstrated in the upper left panel of Figure 45 and in Figure 46; it is marked with outer black solid curve. Along with the presence of a limit cycle, system (66) has a stable point attractor. Therefore, point $I_{\text{syn}} = 1.3325\ [\mu\text{A/cm}^2]$ is the bifurcation of Andronov-Hopf point. The corresponding critical point has the following values: $V_0 = -38.65,\ n_0 = 0.325,\ h_{k0} = 0.875$.

Analyzing the critical points for other values of the synaptic parameter, we obtain the bifurcation interval of the system (66). When

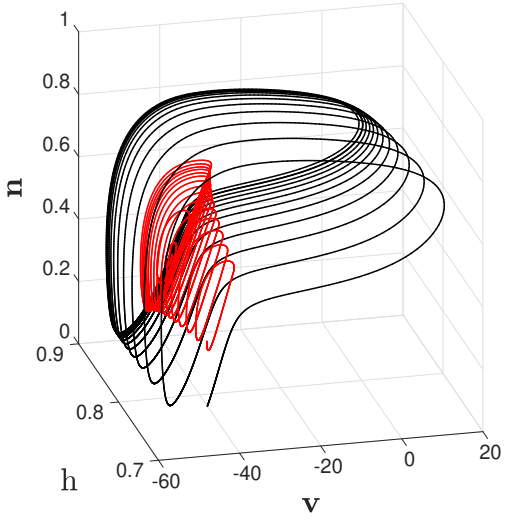

Fig. 46: Results of integration of the system (66) in three-dimensional space, the outer solid line (black) represents a periodical solution in direct time; the inner curve (red) denotes a periodical solution in inverse time, which is the boundary of the region of attraction for stable focus; here $I_{\text{syn}} = 0.99\ [\mu\text{A}/\text{cm}^2]$.

the synaptic current I_{syn} belongs to the interval $[0.92;\ 1.333]$, there are two attractors present in the system, namely, a point attractor and a periodical one.

Roots of the characteristic equation of the system (66) in the neighborhood of the point attractor have the form:

$$\begin{aligned} \lambda_1 &= -a, \\ \lambda_{2,3} &= -b \pm ic, \end{aligned} \tag{67}$$

a, b, c are positive real numbers. Therefore, this point attractor is the stable focus (Fig. 47).

The region of attraction of this stable focus is bounded by the asymptotically orbitally stable in the inverse time (τ) limit cycle (top-

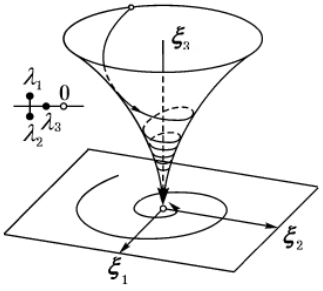

Fig. 47: The schematic interpretation of the stable focus trajectories [22].

left panel of Figure 45 and Figure 46, red solid line inside the black one).

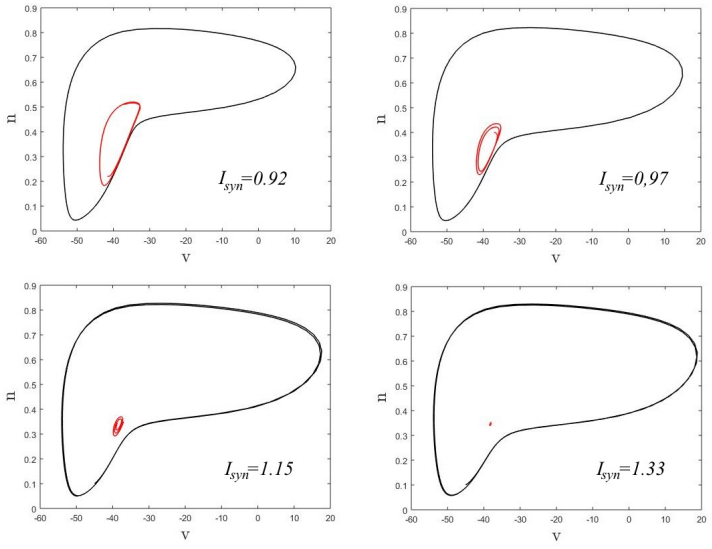

Fig. 48: Limit cycles of the system (66) for different values of the synaptic current. The inner cycle represents the integration of the same system in the inverse time; the outer one denotes the integration results in direct time.

There is an obvious interest for studying the attraction regions

of point and periodic attractors for different values of the synaptic parameter. In particular, for $I_{\text{syn}} = 0.92$ [μA/cm^2], $I_{\text{syn}} = 0.97$ [μA/cm^2], $I_{\text{syn}} = 1.15$ [μA/cm^2], and $I_{\text{syn}} = 1.33$ [μA/cm^2], the results of (66) integration in direct and inverse time are presented in Figure 48. Apparently, the region of attraction of the point attractor decreases with an increase of the synaptic current. It means that the probability of the system transitioning to the pulse generation mode increases. It should be noted that a similar behavior is observed for the second-order system [20, 46].

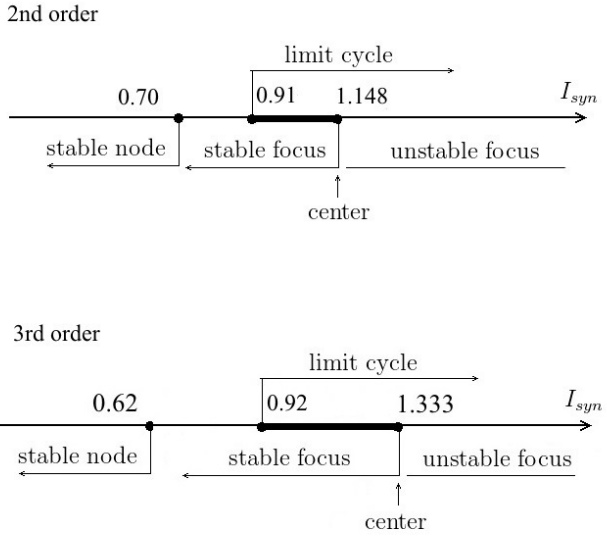

Fig. 49: Comparison of the intervals of bifurcation for models of Hodgkin-Huxley of 2nd and 3rd order.

Comparing the numerical results of the behavior of second and third order systems, respectively, we obtain qualitatively identical results. The only difference is that for a third-order system, the length of the bifurcation interval is longer. A graphical interpretation of these

results is presented in Figure 49.

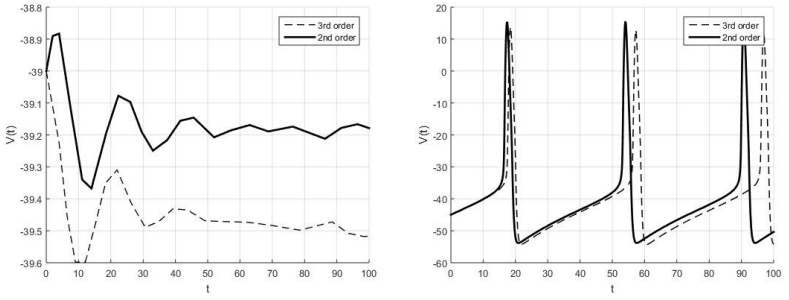

Fig. 50: Comparison of the second-order (solid line) and third-order (dashed line) systems integration. The left panel represents the membrane potential $V(t)$ with the initial conditions lying in the region of attraction of a stable focus. The right panel shows the same integration result with initial conditions that correspond to the region of attraction of a limit cycle.

Next, we proceed to a comparison of the numerical parameters of the membrane potential V obtained for the second and third order systems, respectively. The left panel of Figure 50 represents the results of integration of second (solid line) and third-order (dashed line) systems correspondingly having initial conditions that belong to the region of attraction of the point attractor. The right one shows results that corresponds to initial conditions of the region of attraction of the limit cycle. In practice, this result describes the generation of current pulses in the primary afferent neuron. As it is seen from these graphs, the solutions for both systems are qualitatively identical.

Figure 51 represents sodium and potassium currents in the models of second (dashed line) and third-order (solid line) respectively. Top graph pair $(I_{\mathrm{Na}}(t),\ I_{\mathrm{K}}(t))$ is built for synaptic current equal to 0.91 $[\mu\mathrm{A}/\mathrm{cm}^2]$. For the second-order system, this value of synaptic parameter

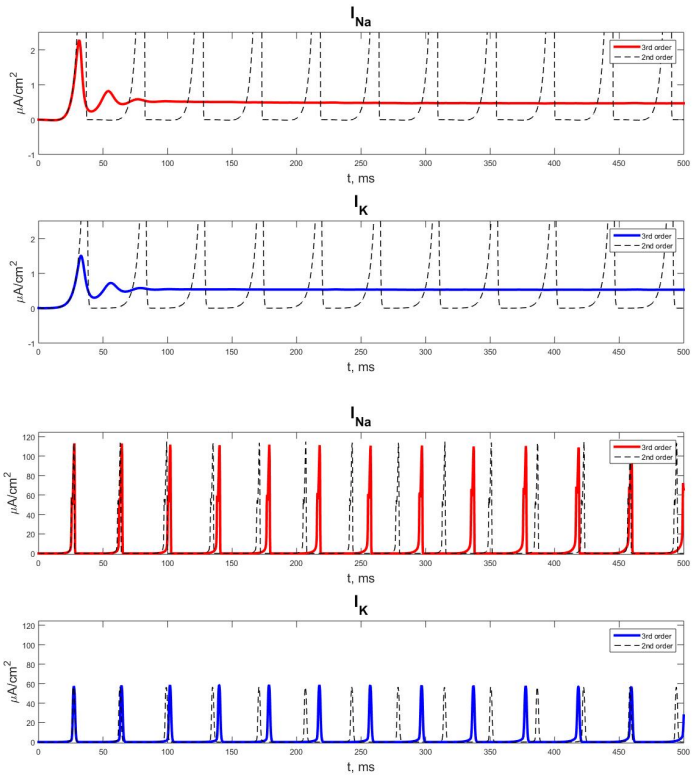

Fig. 51: The sodium and potassium currents comparison for the nonlinear systems of second (dashed line) and third order (solid line) correspondingly; the results are given for $I_{\text{syn}} = 0.91$ and 0.99 $[\mu\text{A}/\text{cm}^2]$.

belongs to the bifurcation interval, so the system is already in the pulse-generating mode. However, system of third order cannot generate current spikes for $I_{\text{syn}} < 0.92$ $[\mu\text{A}/\text{cm}^2]$.

The bottom pair in Figure 51 correspond to the synaptic parameter of 0.99 $[\mu A/cm^2]$ which already belongs to the bifurcation interval for both systems. A comparative characteristic of the frequencies for second and third order systems with the different values of the synaptic current is presented in Table 4.

	Second order system		Third order system	
I_{syn}, $[\mu A/cm^2]$	Spikes number in 500 ms	Frequency, [Hz]	Spikes number in 500 ms	Frequency, [Hz]
0.91	11	22	–	–
0.99	14	28	13	26
1.10	17	34	16	32
2	34	68	33	66
5	63	126	63	126
10	82	164	82	164
50	≈ 100	≈ 200	≈ 100	≈ 200

Table 4: Comparison of the sodium and potassium current frequencies in the case of second and third-order systems.

Summarizing the results obtained by integrating of second and third-order systems, we can conclude following:

- the qualitative results for synaptic current I_{syn}, membrane potential V, sodium I_{Na} and potassium I_{K} currents are the same;
- quantitatively, there is a small difference in the bifurcation intervals (the third-order system has longer bifurcation interval) and the frequencies of sodium and potassium currents; at certain values of I_{syn} the second-order system generates slightly more spikes than third-order one.

Unimprovable estimation of reachable set for point attractor of the third order system (66)

In solving robust stability problems, constructing an estimation of the reachable set is very important [71], [10].

Equating the right sides of the system (66) to zero (for $v_1(t) \equiv 0$)

and solving equations, we found one critical point $y^0 = (V_0, n_0, h_0)^T$. For $I_{\text{syn}} = 0.99\ \frac{\mu A}{cm^2}$ it is $V_0 = -39.5571,\ n_0 = 0.2867,\ h_0 = 0.8797$.

In the neighborhood of the critical point we construct a system in variations by coordinates $x = y - y^0$ and by parameter $v_1(t) \not\equiv 0$

$$\dot{x} = Ax + bv_1(t), \tag{68}$$

where

$$A = \begin{bmatrix} 0.2033 & -12.0735 & -0.7207 \\ 0.0127 & -0.3103 & 0 \\ -0.0001 & 0 & -0.0088 \end{bmatrix},\ b = \begin{bmatrix} 1 \\ 0 \\ 0 \end{bmatrix}.$$

We solve the characteristic equation

$$\det(\lambda E_3 - A) = \lambda^3 + 0.1158\lambda^2 + 0.0911\lambda + 0.0008 =$$

$$= \lambda^3 + a_1\lambda^2 + a_2\lambda + a_3 = 0$$

and find the eigenvalues $\lambda_i,\ i = 1, 2, 3$ of the matrix A

$$\lambda_1 = -0.0087,\ \lambda_{2,3} = -0.0536 \pm 0.2954i.$$

By classification of stability of points [22], a critical point y^0 is a stable focus.

According to [3] matrix A is observable since

$$\det(b, Ab, A^2b) \neq 0.$$

Therefore it could be presented in the form of a Frobenius matrix A_{Fr} [4]

$$A_{Fr} = \begin{bmatrix} 0 & 1 & 0 \\ 0 & 0 & 1 \\ -a_3 & -a_2 & -a_1 \end{bmatrix} = \begin{bmatrix} 0 & 1 & 0 \\ 0 & 0 & 1 \\ -0.0088 & -0.0911 & -0.1158 \end{bmatrix}.$$

The system (68) changes into the system

$$\dot{\xi} = A_{Fr}\xi + e_3 v_1(t) \tag{69}$$

by transition $x = C\xi$.

Here

$$C = (b, Ab, A^2b) \cdot \begin{bmatrix} a_2 & a_1 & 1 \\ a_1 & 1 & 0 \\ 1 & 0 & 0 \end{bmatrix} = \begin{bmatrix} 0.0027 & 0.3191 & 1 \\ 0.0001 & 0.0127 & 0 \\ -0.00001 & -0.00005 & 0 \end{bmatrix}.$$

The article [71] presents a detailed algorithm of constructing an unimprovable estimation of the reachable set in the neighborhood of the stable focus for a third-order system. The first step in the application of this algorithm is a separation of the system (69) into two independent subsystems, using transition

$$\xi = Dz, \quad D = \begin{bmatrix} 1.0093 & 1.1997 & 11.2020 \\ 0.0087 & 1 & 0 \\ 0 & 0.0087 & 1 \end{bmatrix}.$$

Thus, the system (69) changes by the two independent subsystems of the first and second order

$$\dot{z_1} = -0.0087z_1 + 11.2020v_1(t) \tag{70}$$

and

$$\begin{cases} \dot{z_2} = z_3; \\ \dot{z_3} = -0.0901z_2 - 0.1071z_3 + v_1(t). \end{cases} \tag{71}$$

For any $|v_1(t)| \leqslant \delta_1 = 0.1$ the result of solution of the maximum deviation problem for the system of first order (70) is the interval

$$z_1(t) \in [-128.7586, 128.7586]. \tag{72}$$

Solution of the maximum deviation problem for the system of second order (71) is a limit cycle (Fig. 52)

$$\begin{cases} z_2(t) = \mp 5.1132e^{-0.0536t}(\cos(0.2954t) + 0.1813\sin(0.2954t)) \pm 1.1099; \\ z_3(t) = \pm 1.5595e^{-0.0536t}\sin(0.2954t). \end{cases} \tag{73}$$

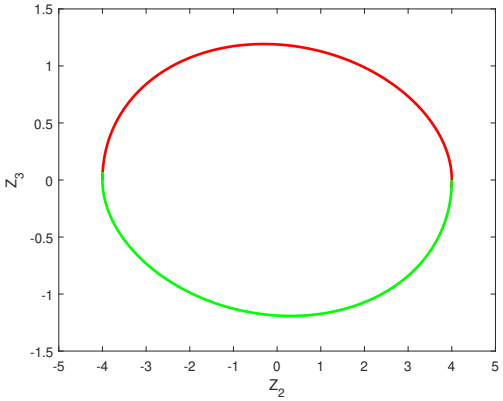

Fig. 52: Limit cycle of the subsystem (71).

The authors of the article [71] propose to combine these two solutions and to construct an unimprovable estimation of the reachable set for a third-order system (69) in the form of a cylinder. The height of this cylinder is a segment (72), the base is a limit cycle (73).

The inverse transition to the coordinates of the nonlinear system (66) is carried out by

$$y = CDz + y^0.$$

Thus, the presented cylinder is an unimprovable estimation of the reachable set of a system in variations (69) in the neighborhood of a stable focus. That is, under the influence of a constantly acting perturbation $v_1(t)$, the system (69) cannot move beyond the boundary of this cylinder.

3.3 Solution of the problem of inverse transition for model of the second order

Consider the possibility of galvanic stimulation of the afferent primary neurons (APN) activity of the vestibular apparatus. In the

standby mode of the mechanical stimulus this activity corresponds to the presence of two attractors (within the modified model of Hodgkin-Huxley): the periodic attractor and point attractor located inside of the periodic one.

In practice, solution of the problems, related to the transitions between point and periodic attractors, make possible realization of the following applications:

a) the galvanic imitation of a vestibule-ocular reflex (VOR) on a flying-dynamic stand of reference type with limited resources. The existing dynamic stands without any galvanic stimulation do not allow the dynamic simulation of VOR due to restricted roll angles;

b) the improvement of the pilot's gaze stabilization quality during extreme flight situations.

The solution of the direct transition problem was obtained within the mathematical model of APN [46] and [11].

The solution of the inverse transition problem was obtained in the experiment carried out on the Gough–Stewart platform having six degrees of freedom [67]. The mathematical interpretation of the realized experiment shall be presented below.

To solve the inverse transition problem, we shall use the theory, presented in Chapter 2, and construct the reachable set D_{t_k} for the system in variations (74). Further on, we shall consider the possible intersection of two domains – the region of attraction of a periodic attractor of the nonlinear system (61), and the reachable set D_{t_k} of the system in variations (74).

We consider the nonlinear system, given by Eq. (61), with a

functional inclusion of the form $\gamma_1 P(t) = v(t)$:

$$v(\cdot) \in V = \{v_1(\cdot) \in KC: \quad 0 \leqslant v(t) \leqslant \gamma_1\delta_1 \text{ for } t \in (0, t_1 < \infty),$$
$$v \equiv 0 \text{ for } t > t_1\}.$$

Periodical solutions $(v^0(t), n^0(t))$ were obtained as the results of the system (61) integration by using ***ode45*** function in Matlab (Figs. 53 and 54) with the following parameters:

- initial condition for the potential $V(t)$

$$v^0 = -40.55\ [mV]$$

- initial condition for the probability $n(t)$

$$n^0 = 0.2$$

- period of the oscillating system (61), therefore and time of integrating also

$$T = 35.2\ [ms]$$

- synaptic current of the system (61)

$$I_{\text{syn}} = 1\ \left[\frac{\mu A}{cm^2}\right]$$

- perturbation presence parameter

$$\gamma_1\delta_1 = 0.1$$

In the neighborhood of the periodic solution $(v^0(t), n^0(t))$ the system is variations was constructed. The origin of system's coordinates is moving along the orbit of the periodic attractor as follows:

$$\dot{x} = A(t)x + bv(t). \tag{74}$$

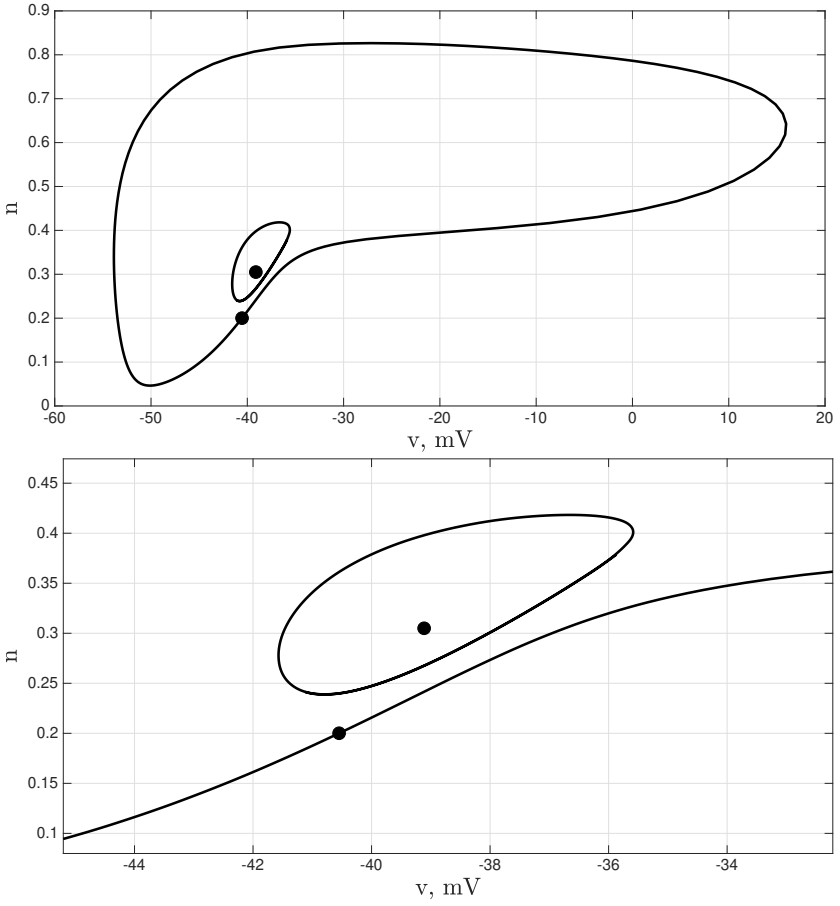

Fig. 53: Numerical integration of the system (61): phase plane

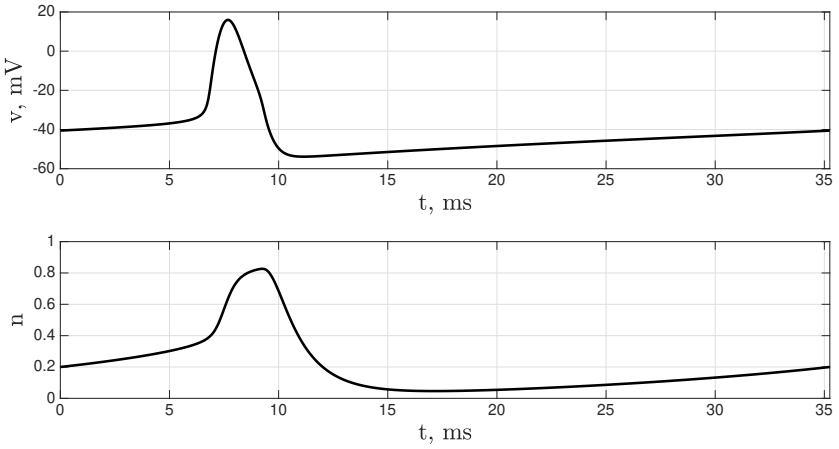

Fig. 54: Numerical integration of the system (61): time dependence

The explicit form of the parameters in (74) is given by:

$$\begin{aligned} b &= (1,0)^T, \\ y^0(t) &= (v_i^0(t), n_i^0(t)), \\ A(t) &= \left(\frac{\partial f_i(y^0(t))}{\partial y_i}\right) = \begin{pmatrix} a_{11}(t) & a_{12}(t) \\ a_{21}(t) & a_{22}(t) \end{pmatrix}. \end{aligned}$$

It should be emphasized that matrix $A(t)$ is a periodical one $A(t + T) = A(t)$.

To construct the limit cycle, the whole integration interval $[0, T]$ was divided by 1000 sub-intervals; consequently, we get the pair of points $[v_i^0(t_i), n_i^0(t_i)]$ for each sub-interval.

The next step is to obtain matrix $A(t)$ by finding the partial derivatives of the right hand side of the system (61) and substituting the corresponding values $[v_i^0(t_i), n_i^0(t_i)]$ into them. Since the orbit of the periodical attractor is found numerically, the matrix $A(t)$ has the form of the numerical data arrays. In other words, without having the explicit analytical formula of $y^0(t)$, the matrix $A(t)$ cannot be obtained in the

analytical form too.

For the integration of the system (74) it is necessary to construct a spline approximation of the matrix $A(t)$ at each sub-interval (Fig. 55).

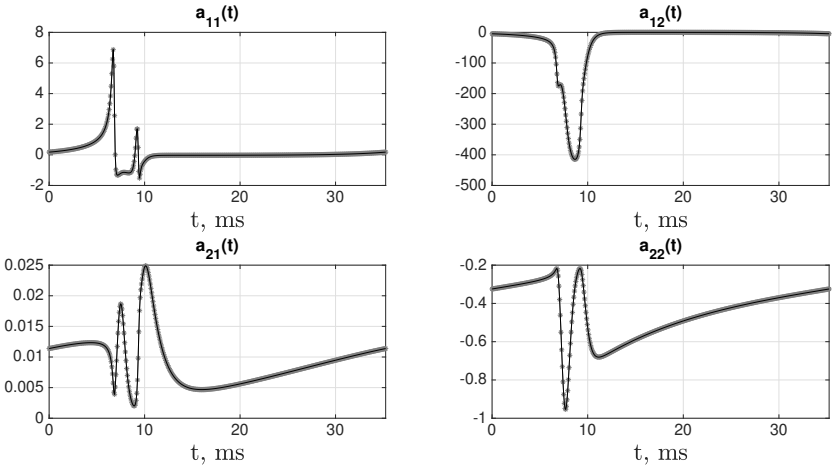

Fig. 55: Numerical representation (solid line) and approximation (asterisk markers) of the matrix $A(t)$

The normalized fundamental matrix of solutions $X_f(t)$ is found by integrating the system $\dot{X}_f = A(t)X_f$ with the initial conditions $X_f(0) = E_2$ (Fig. 56).

The matrix of the monodromy $X_f(T)$ is a matrix having constant numerical values unlike fundamental matrix $X_f(t)$, where $0 \leq t \leq T$. The eigenvalues of monodromy matrix $X_f(T)$ are $\rho_1 = 1$, $\rho_2 = 1.7 \cdot 10^{-5}$ respectively; the corresponding eigenvectors are

$$s^1 \approx \begin{pmatrix} 0.058 \\ -0.998 \end{pmatrix}, \qquad s^2 \approx \begin{pmatrix} -0.028 \\ 0.999 \end{pmatrix}.$$

According to the theory of Chapter 2, we construct a special fundamental matrix $X_s(t) = X_f(t) \cdot S$, where matrix S has to satisfy

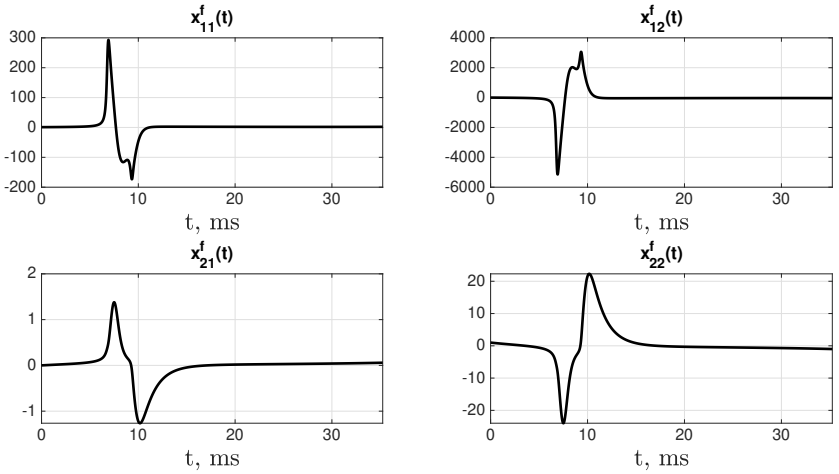

Fig. 56: Numerical representation of the normalized fundamental matrix $X_f(t)$

the condition $S^{-1}X_f(T)S = \mathrm{diag}(1, e^{\frac{1}{T}\ln|\rho_2|t})$. Obviously, the simplest way to find one of the explicit expressions for S is to use the matrix of eigenvectors $S = (s^1, s^2)$.

According to [34], the special matrix $X_s(t)$ can be represented as:

$$X_s(t) = \Phi_s(t)\ \mathrm{diag}\left(1, e^{\frac{1}{T}\ln|\rho_2|t}\right),$$

where $\Phi_s(t)$ is a real bounded T-periodic continuously differentiable (2×2)-matrix.

Consequently, $\Phi_s(t)$ is

$$\Phi_s(t) = X_s(t)\cdot\begin{pmatrix}1 & 0\\ 0 & e^{\frac{1}{T}\ln|\rho_2|t}\end{pmatrix}^{-1}.$$

Numerical representations and spline approximations of matrices $\Phi_s(t)$ and $\Phi_s^{-1}(s)$ are shown in Figs. 57-58. Initially, in the neighborhood of the point $t \approx 11$ ms the $\det(\Phi_s) \to 0$. Therefore, to avoid the numerical singularity of the Φ_s matrix, the method of adding a small

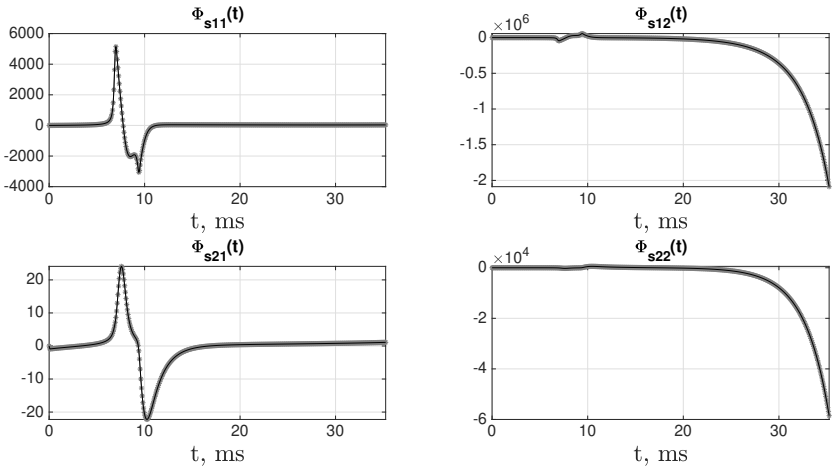

Fig. 57: Numerical representation (solid line) and its approximation (asterisk markers) of the matrix $\Phi_s(t)$

constant is applied. Hence, we use the following scheme to calculate the inverse of the matrix Φ_s (Fig. 59):

$$\mathrm{inv}(\Phi_s) \equiv (\Phi_s + 0.1E_2)^{-1}.$$

The similar method is applied recently to avoid the singularity problem during the calculation the form-factor of elementary cube for the macroscopic Fourier component [45].

However, we get one point, the value of which is more than 20 times the values of other points. Therefore, the extreme value (for $t \approx 11$ ms) can be excluded from the (Φ_s) data without loss of generality. Figure 59 represents the final result for the inverse of Φ_s matrix excluding the point of singularity (asterisks markers). Further on, to integrate $\max x_1^s$, $\min x_1^s$, $\max x_2^s$, and $\min x_2^s$ data arrays it is necessary to find the third-order spline approximation of $\mathrm{inv}(\Phi_s)$ matrix; the similar procedure (cubic spline approximation) was used previously to find the analytical form of $A(t)$ matrix. The final approximation result is also presented in

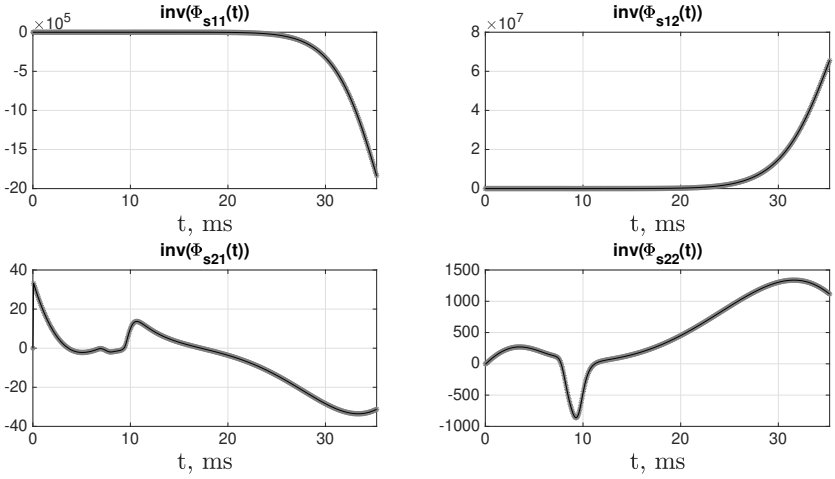

Fig. 58: Numerical representation (solid line) and its approximation (asterisk markers) of the inverse matrix $\Phi_s^{-1}(t)$

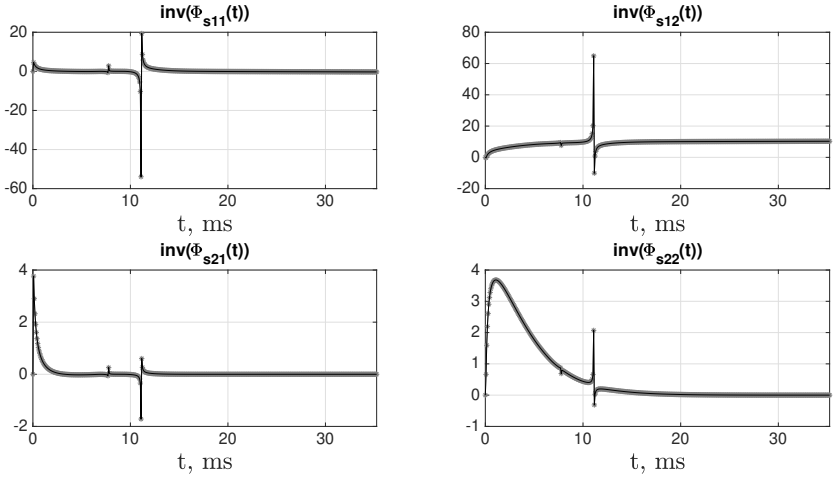

Fig. 59: Numerical representation (solid line) and its approximation (asterisk markers) of the inverse matrix $(\Phi_s(t) + 0.1 \cdot E_2)^{-1}$

Fig. 59 (solid line).

To construct the reachable set D_{t1}, it is first necessary to find

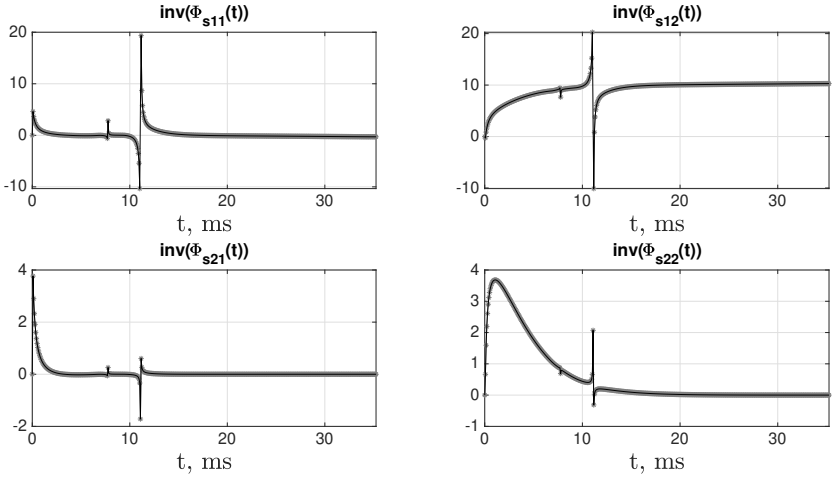

Fig. 60: Numerical representation (solid line) and approximation (asterisk markers) of the inverse matrix $(\Phi_s(t) + 0.1 \cdot E_2)^{-1}$; excluded one point of singularity at $t \approx 11$ ms

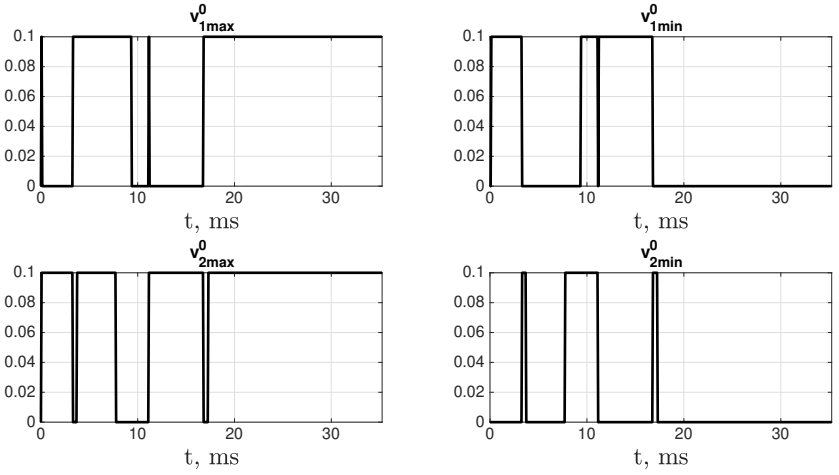

Fig. 61: Worst perturbations for $\max x_1^s$, $\min x_1^s$, $\max x_2^s$, and $\min x_2^s$.

the maximum and minimum deviations of the coordinates x_1^s and x_2^s. Therefore, the four extreme points are found; the corresponding worst perturbations $v^0_{1max}(s)$, $v^0_{2max}(s)$, $v^0_{1min}(s)$ and $v^0_{2min}(s)$ are presented

in Fig. 61.

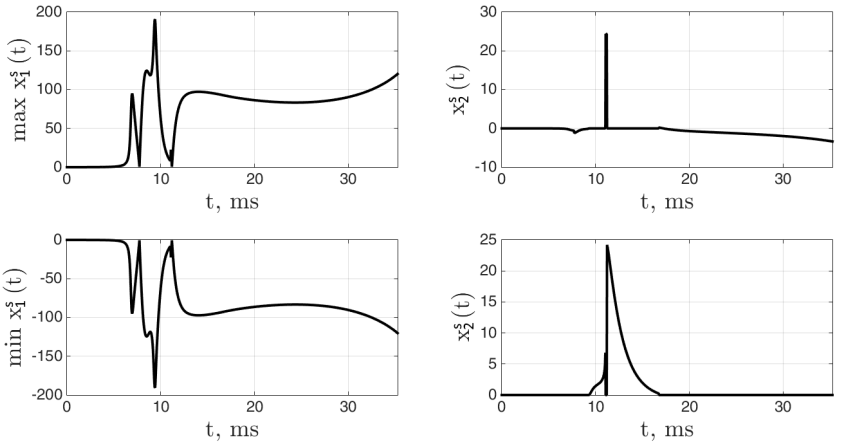

Fig. 62: Maximal and minimal deviations of $x_1^s(t)$.

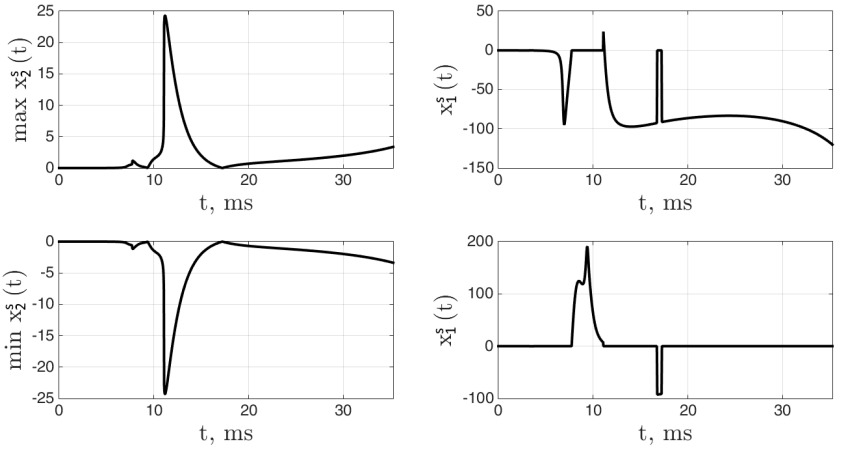

Fig. 63: Maximal and minimal deviations of $x_2^s(t)$.

The results of integration for $\max x_1^s$, $\min x_1^s$, $\max x_2^s$, and $\min x_2^s$ are presented in Figs. 62 and 63 respectively.

We shall use the conditional gradient method, described in Sec. 1.5, to construct remaining boundary points of reachable set D_{t_1}.

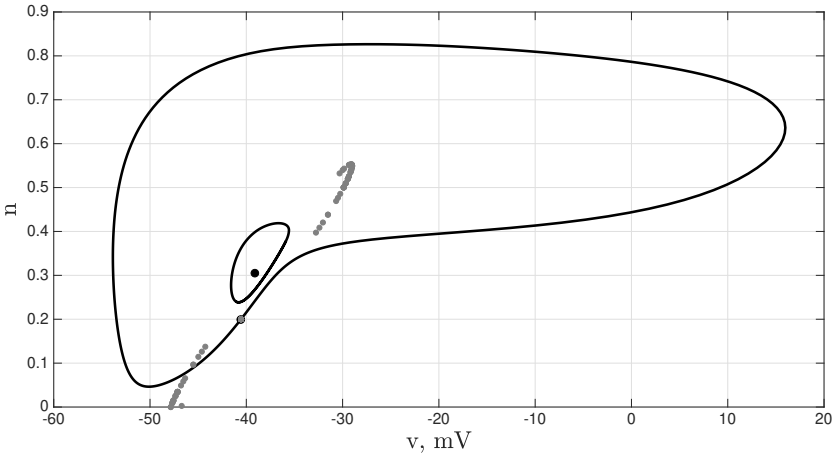

Fig. 64: Reachable set D_{t_1} for 100 initial vectors.

All boundary points were calculated in coordinates (x_1^s, x_2^s) first; then, we use the following transformation

$$(x_1^f, x_2^f) = (x_1^s, x_2^s) \cdot S^{-1},$$

with the matrix S^{-1} given by

$$S^{-1} = \begin{pmatrix} 33.1927 & 0.9305 \\ 33.1496 & 1.9297 \end{pmatrix},$$

to switch back into the coordinates (x_1^f, x_2^f) of the normalized fundamental matrix $X_f(t)$.

To find the boundary points of D_{t_1} in terms of coordinates (V, n), corresponding to the nonlinear system (61), we use the following translation

$$V = x_1^f + V^0,$$
$$n = x_2^f + n^0.$$

Within the described method, the quantity of boundary points straightforwardly depends on the chosen number of initial vectors. For

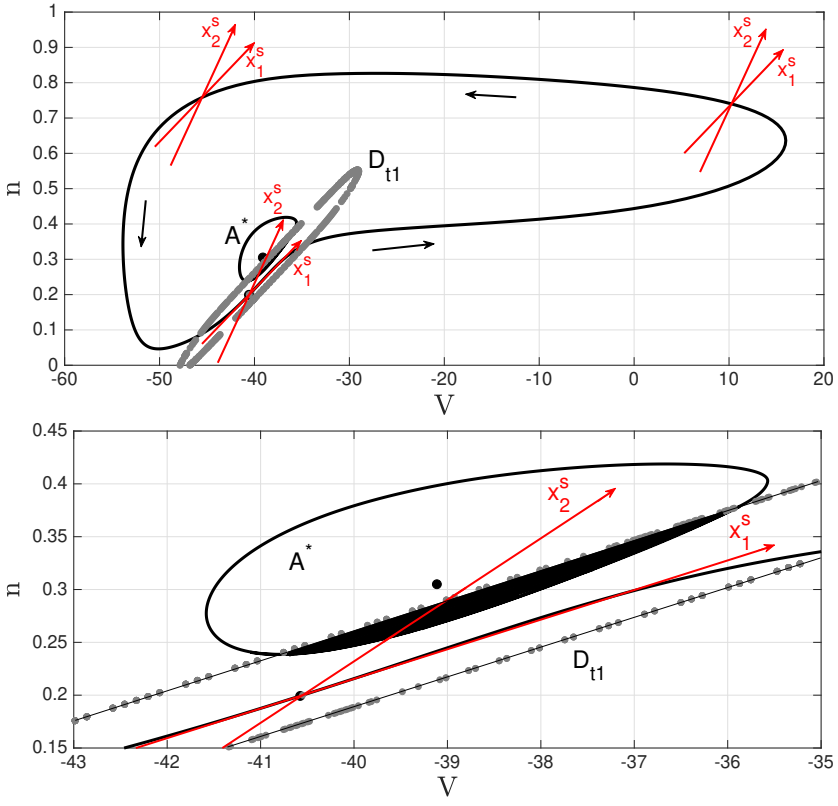

Fig. 65: Reachable set D_{t_1} for 250000 initial vectors.

example, having considered 100 initial vectors the following result for D_{t_1} is obtained (Fig. 64).

However, for the solution of the inverse transition problem it is rather insufficient, because the intersection of the reachable set D_{t_1} and the set of attraction of point attractor A^* cannot be analyzed. Hence, the number of initial vectors should be increased cardinally. As an example, by considering 250 000 initial vectors, one gets the boundary of the reachable set D_{t_1} more precisely (Fig. 65).

Obviously, Fig. 65 shows that reachable set D_{t_1} has a non-empty intersection (painted black set) with the region of attraction

of a point attractor A^*. As a very important consequence, there is exist a possibility of inverse transition. **System (61) can make the transition from the region of attraction of the periodic attractor (pulse generation state) to the region of attraction of the point attractor (relaxing mode) precisely at $t_1 = 35.2$ ms**.

In practice, such a possibility of the inverse transition with a small amplitude of galvanic correction of primary afferent neurons was shown in the work [67].

FUNCTIONAL SCHEME OF GALVANIC CORRECTOR OF THE VESTIBULAR APPARATUS

The practical realization of presented algorithm is a prototype of galvanic stimulator the designed and fabricated within the frame of current scientific investigation. The main schematic and operational parameters of the galvanic corrector prototype are listed below. All results were obtained in collaboration with Dr. Anatolii Konovalenko.

The problem of galvanic simulation can be expressed briefly in purely electrical control of human eye vision without any mechanical stimulation involved. As the particular example, the galvanic stimulation can be used to reduce reaction time during space station maintenance.

The solution of the galvanic stimulation problem makes possible realization of: a) galvanic imitation of a vestibule-ocular reflex (VOR) on the stand of a reference type with tilt angles that do not allow the dynamic simulation of the VOR; b) improvement of the quality of stabilization of the pilot's eye in extreme flight situations.

The theoretical results of a galvanic simulation solution require a specific waveform of electrical signal at the electrodes connected to the human head. There are few investigated electrode connection schemes, nevertheless, for each scheme the predefined quantity of electric current is required. Already known practical implementations of the galvanic correctors used the voltage source driven by voltage. As long as the impedance between the electrodes connected to galvanic stimulator is not changing it is a reliable approach. However, within stress conditions (space flight manual control, jet maneuvering at high angular velocity) an impedance of human head is a variable function that depends on

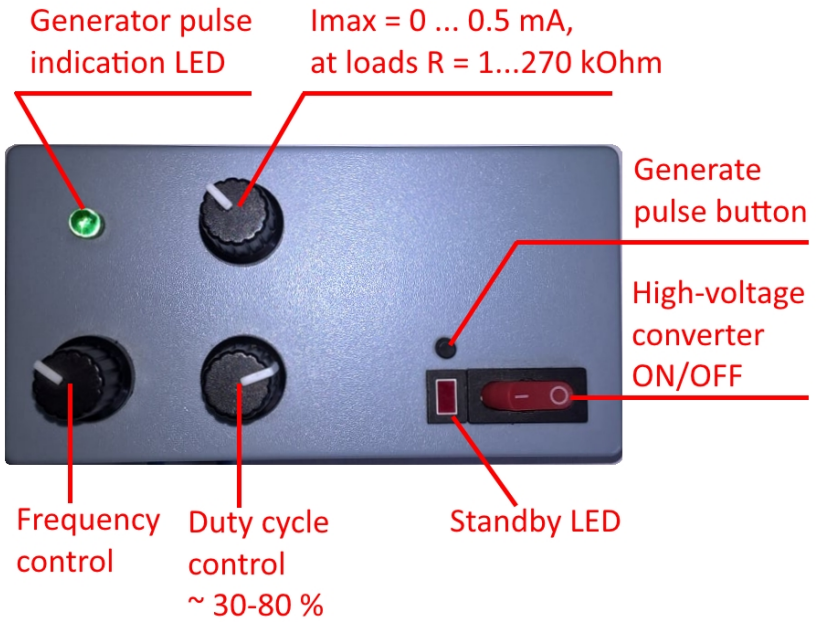

Fig. 66: Front panel of the galvanic corrector of the vestibular apparatus for solution of problem of inverse transition.

many parameters. Practically it means that electrical impedance of the load (which is in our case a head of the pilot) is floating within a wide range; fluctuations are up to one order of magnitude of the electrical resistance. Being connected to the voltage source the voltage profile at load shows drastic difference from one of the signal generator output. As the voltage profile and, correspondingly, current flowing is not the same as optimal, the galvanic stimulation is useless and could be even harmless.

In order to overcome discrepancy between the desired electrical signal and one between electrodes we propose to use the current source generator driven by voltage. The principal difference (comparing to the voltage source generator) is that current source delivers fixed current

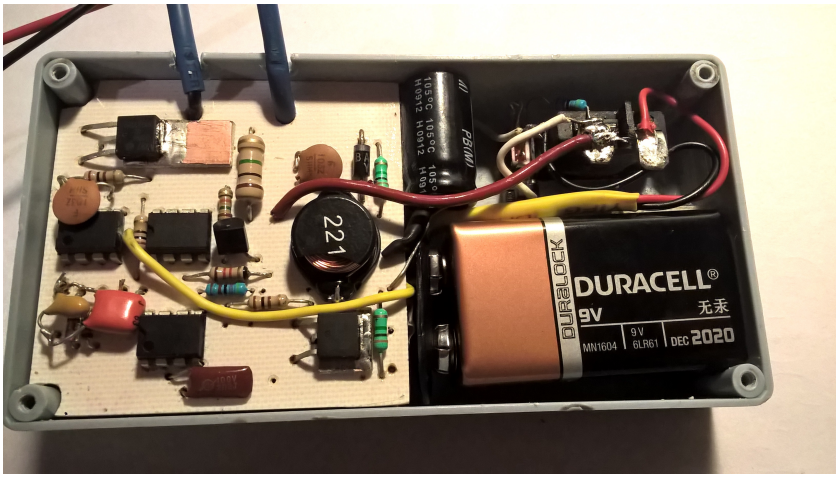

Fig. 67: Rear panel of the galvanic corrector of the vestibular apparatus for solution of problem of inverse transition.

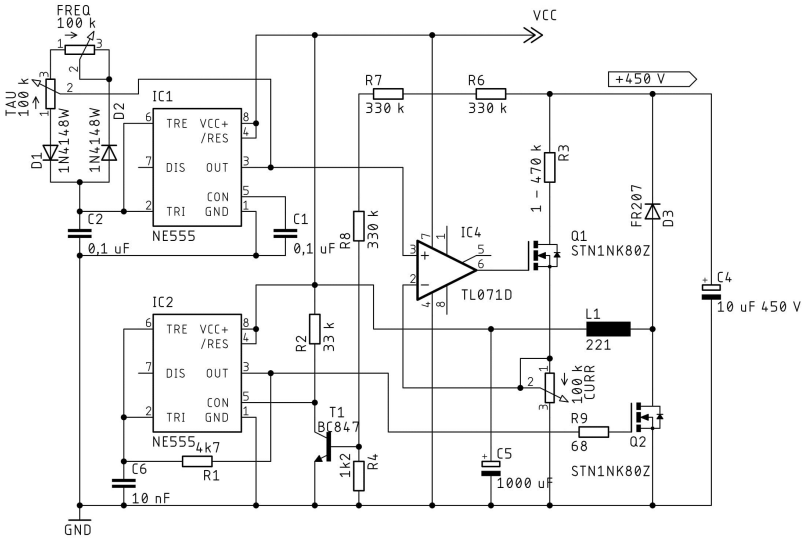

Fig. 68: Functional electrical scheme of the galvanic corrector of the vestibular apparatus for solution of problem of inverse transition.

quantity at any load within the specified range. Experiments show that anode-cathode impedance of a human head are between 10 $k\Omega$ - 470 $k\Omega$. Current feeding method ensures that the current profile at load will be exactly the same as the source one.

The core idea of designed prototype is to deliver square-wave pulses to the electrodes (anode and cathode) connected to the head of a pilot. Designed square wave generator is capable to work at high impedances, technically speaking it is **current source driven by voltage**.

The corrector itself consists of 3 principal blocks:

- High-voltage converter (9V - 270 V).
- Square wave generator with adjustable frequency and duty cycle (**30-80** % of period) adjustable by corresponding potentiometers.
- Pulse peak current limiter (**0 - 0.5 mA**, adjustable by potentiometer) for anode-cathode impedances **1-270 k**Ω.

Device is capable to feed the high impedance **floating** load with square pulses (user-defined frequency and duty cycle) with the **maximum limited** current. At any anode-cathode impedance within specified range the maximal current **should not** exceed 0-0.5 mA.

Experiment

The prototype of galvanic corrector was used during experiment in the Laboratory of Mathematical Modeling and Dynamic Systems at Department of Applied Mechanics and Control of Moscow State University in October of 2018 (Fig. 69).

The objective of the experiment is to improve the stabilization of the pilot's gaze using galvanic stimulation. The pilot sits on the moving Stewart platform, which has six degrees of freedom. The motion of such a

Fig. 69: Experimental setup in laboratory of Mathematical Modeling and Dynamic Systems, MSU, 2018.

platform is governed by various algorithms for the dynamic imitation of aircraft flights. In this experiment, the algorithm of the flight trajectory includes coordinated turn maneuvers, described in [67] and [40]. During these maneuvers, the pilot keeps his sight on a fixed point on the screen.

Two series of experiments were held, with and without galvanic stimulation. Fig. 70 presents the results of the experiment. Panel A of Fig. 70 illustrates the gaze stabilization without galvanic stimulation. As one can see, the function "Eye - Vertical" increases during time. Thus, there is a delay in gaze stabilization.

Panel B represents the results obtained with galvanic stimulation (GVS). The "Eye - Vertical" function is close to zero function. It means that the galvanic stimulation corrects the pilot's sight stabilization.

We conclude that stabilization of the pilot's gaze improves in the

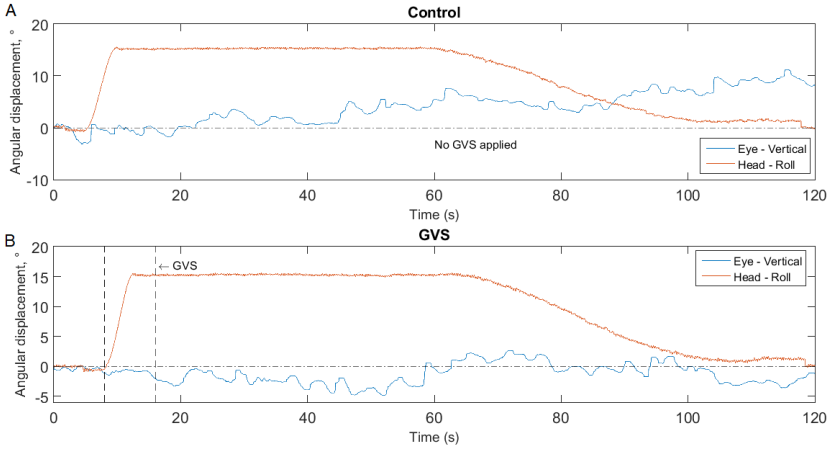

Fig. 70: Experimental results, obtained in [40].

presence of galvanic stimulation. Thus, it is necessary to have a practical functional scheme of the galvanic corrector for the vestibular activity of pilot's in the programmed flight-dynamic stands.

CONCLUSIONS

The author of the thesis obtained several theoretical, numerical and practical results:

1. Definition of the reachable set for a linear system with variable periodic coefficients is given. In addition, the properties of this reachable set were defined and proved (Section 1.1).

2. The algorithm of construction of the reachable set for a linear system, built in the neighborhood of periodical solution of the nonlinear system, is developed (Sections 2.1-2.2). The application of this algorithm for the model of Van der Pol yields the results for two systems, a linear and non-linear, respectively (Section 2.3). The reachable sets for linear system were constructed at fixed points of time. The reachable set for the periodical attractor of perturbed nonlinear system during one period of motion was obtained as union of a sequence of reachable sets for linear system. Besides, it was shown that the statement of the robust stability problem for a periodic attractor is incorrect when the infinitely acting perturbation belongs to the class of piece-wise continuous functions (Section 2.1).

3. The criterion of possibility of solution of the inverse transition problem for a second-order system was determined (Section 2.4) and applied for the modified second-order model of Hodgkin-Huxley (Section 3.3).

4. The numerical analysis of the modified Hodgkin-Huxley models of the second and third order demonstrates that qualitatively both systems have same behavior. The cylindrical estimation of the reachable set for point attractor of the third-order system was found (Section 3.2).

5. The first Lyapunov constant for the second order modified Hodgkin-Huxley model was calculated. Its numerical value allows to employ the Andronov-Leontovich theorem. As the consequence, the analytical evidence of severe loss of stability by focus is given (Section 3.1).

6. The functional scheme and the corresponding electric circuit diagram for a galvanic corrector is given (Chapter 4). Such a device is used to imitate a vestibule-ocular reflex of a pilot during its training on flight simulator (Stewart platform) with limited tilt angles [40]. Besides, the galvanic corrector, based on provided circuit diagram, improves the quality of pilot's gaze stabilization in extreme flight situations.

This work is of interest for specialists working in the field of movement simulations. Specifically, it allow to obtain new solutions for the problem of constructing reachable sets for controlled or perturbed linear systems with periodic coefficients. Moreover, the provided here results allow to solve the problem of approximation of the reachable set in a neighborhood of the limit cycle for a nonlinear system. The solution of these theoretical problems gives rise to various practical applications such as the galvanic correction of the activity vestibular apparatus of the human.

All results described in this thesis were presented in **articles**:

1) Alexandrov V. V., Alexandrova O. V., Konovalenko I. S., Tikhonova K. V. Perturbed stable systems on the plane, 1. Moscow State University Mechanics Bulletin. n. 5, 30-36 pp., 2016.

2) Alexandrov V. V., Alexandrova T. B., Konovalenko I. S., Tikhonova K. V. Perturbed stable systems on the plane, 2. Moscow State University Mechanics Bulletin. n. 1, 53-57 pp., 2017.

3) Sadovnichiy V. A., Alexandrov V. V., Alexandrova T.B., Vega R., Konovalenko I. S., Soto E., Tikhonova K.V., Gordillo-

Dominguez H. L., Gonzales O. About galvanic correction of the vestibular activity of the pilot in the visual control of flight. Moscow State University Mechanics Bulletin. n. 1. 34-41 pp. 2019.

4) Konovalenko I. S. On the construction of the reachable set in a neighborhood of a periodic attractor. Moscow State University Mechanics Bulletin, n. 3, 67-71 pp., 2020.

And the following **conferences**:

1) CIMA 2 (Congreso Internacional de Matematicas y sus Aplicaciones 2), September 2015, Puebla, Mexico: Alexandrov V., Temoltzi Avila R., Konovalenko I. The Robust stability of the absolutely oscillating systems.

2) CIMA 3 (Congreso Internacional de Matematicas y sus Aplicaciones 3), September 2016, Puebla, Mexico:
2.1. Konovalenko I., Alexandrov V. Two-dimensional perturbed stable systems.
2.2. Alexandrov V., Alexandrova T., Soto E., Vega R., Reyes Romero M., Konovalenko I., Gordillo Dominguez J.L. The correction of the vestibular activity: Mathematical problems and Space investigations.

3) Proceedings to the conference: Ideas and innovations, July 2018, Russian Academy of Engineering, Russia: Sadovnichiy V. A., Alexandrov V. V., Alexandrova T. B., Vega R., Konovalenko I. S., Soto E., Tikhonova K.V., Gordillo-Dominguez J.L., Gonzales O. On virtual reality technologies in outer space activities. n. 3. 8-15 pp.

4) Problems of mechanics and control, September 2018, Makhachkala, Russia: Alexandrov V. V., Alexandrova T. B., Konovalenko I. S., Sadovnichiy V. A., Soto E., Tikhonova K. V. Inertial mechanoreceptors and GVS technology of correction of their activity.

5) CIMA 6 (Congreso Internacional de Matematicas y sus

Aplicaciones 6), September 2019, Puebla, Mexico: Alexandrov V., Reyes Romero M., Konovalenko I., Gordillo Dominguez J.L. Transitions in a bistable dynamical system and applications for neural control of the vestibule-ocular system.

Appendix A First Lyapunov value

Explicit formulas for the first Lyapunov value were obtained by Bautin in 1949 [27] for system

$$\begin{cases} \dot{x} = ax + by + P_2(x,y) + P_3(x,y) + ..., \\ \dot{y} = cx + dy + Q_2(x,y) + Q_3(x,y) + ..., \end{cases} \tag{75}$$

where $ad - bc > 0,\ a + d = 0$ and

$$\begin{aligned} P_2(x,y) =& a_{20}x^2 + a_{11}xy + a_{02}y^2, \\ Q_2(x,y) =& b_{20}x^2 + b_{11}xy + b_{02}y^2, \\ P_3(x,y) =& a_{30}x^3 + a_{21}x^2y + a_{12}xy^2 + a_{03}y^3, \\ Q_3(x,y) =& b_{30}x^3 + b_{21}x^2y + b_{12}xy^2 + b_{03}y^3. \end{aligned}$$

Then

$$\begin{aligned} L_1 = -\frac{\pi}{4b\omega^3}\Big(& ac(a_{11}^2 + a_{11}b_{02} + a_{02}b_{11}) + ab(b_{11}^2 + a_{20}b_{11} + a_{11}b_{20}) + \\ & + c^2(a_{11}a_{02} + 2a_{02}b_{02}) - 2ac(b_{02}^2 - a_{20}a_{02}) - 2ab(a_{20}^2 - b_{20}b_{02}) - \\ & - b^2(2a_{20}b_{20} + b_{11}b_{20}) + (bc - 2a^2)(b_{11}b_{02} - a_{11}a_{20}) - \\ & - (a^2 + bc)\left[3(cb_{03} - ba_{30}) + 2a(a_{21} + b_{12}) + (ca_{12} - bb_{21})\right]\Big), \end{aligned}$$

where $\omega^2 = ad - bc$.

In the case when $a = d = 0,\ b = -\beta,\ c = \beta,\ \omega^2 = \beta^2$

$$\begin{aligned} L_1 = & -\frac{\pi}{4\beta}\Big(3(a_{30} + b_{03}) + (a_{12} + b_{21})\Big) - \\ & - \frac{\pi}{4\beta^2}\Big(2(a_{20}b_{20} - a_{02}b_{02}) - a_{11}(a_{02} + a_{20}) + b_{11}(b_{02} + b_{20})\Big). \end{aligned}$$

BIBLIOGRAPHY

1. Alexandrov V. V. To the problem of Bulgakov of perturbation's accumulation. Report of the USSR Academy of Sciences, Series Cybernetics. n. 3, 186 p., 1969.
2. Alexandrov V. V., Alexandrova O. V., Prikhodko I. P., Temoltzi-Avila R. Synthesis of autooscillations. Moscow State University Mechanics Bulletin. n. 3, 41-44 pp., 2007.
3. Alexandrov V. V., Bolotin Yu. V., Lemak S. S., Parusnikov N. A., Zlochevsky S. I., Guerrero Sanchez W.F. Introduction to control of dynamic systems. Puebla, - 239 p., 2009.
4. Alexandrov V. V., Boltyanskii V. G., Lemak S. S., Parusnikov N. A., Tikhomirov V. M. Optimization of the dynamics of controllable systems. – M. Moscow State University, 304 p., 2000.
5. Alexandrov V. V., Boltyansky V. G., Lemak S. S., Parusnikov N. A., Tikhomirov V. M. Optimal motion control. — M.: FIZMATLIT, 376 p., 2005.
6. Alexandrov V. V., Mikhaleva E. Yu., Soto E and Garcia Tamayo R. A modification of the Hodgkin-Huxley model for primary neurons of the vestibular apparatus. Moscow State University Mechanics Bulletin. n. 5, 21-24 pp., 2006.
7. Alexandrov V. V., Reyes Romero M., Sidorenko G. Yu., and Temoltzi-Avila R. Stability of controlled inverted pendulum under permanent horizontal perturbations of the supporting point. Moscow State University Mechanics Bulletin. n. 2, 41-48 pp., 2010.
8. Alexandrov V. V., Vázquez M. A. L. Á., Romero M. R., Alexandrova T. B., Tikhonova K. V., Vega R., Soto E. The

Correction of the Vestibular System Inertial Biosensors. XVI Congreso Latinoamericano de Control Automatico, CLCA 2014, UNAM, Mexico, 38 p., 2014.

9. Alexandrov V. V., Zhermolenko V. N. About absolute stability of the second order systems. Moscow State University Mechanics Bulletin. n. 5, 102-108 pp., 1972.

10. Alexandrov V. V., Zueva I. O., Sidorenko G. Yu. Robust stability of controlled systems of third order. Moscow State University Mechanics Bulletin. n. 1, 40-45 pp., 2014.

11. Alexandrov V. V., Alexandrova O. V., Konovalenko I. S., Tikhonova K. V. Perturbed stable systems on the plane, 1. Moscow State University Mechanics Bulletin. n. 5, 30-36 pp., 2016.

12. Alexandrov V. V., Alexandrova T. B., Angeles Vaskes A., Vega R., Reies Romero M., Soto E., Tikhonova K. V., and Shulenina N. E. An output signal correction algorithm for vestibular mechanoreceptors to simulate passive turns. Moscow State University Mechanics Bulletin. n. 5, 130-134 pp., 2015.

13. Alexandrov V. V., Alexandrova T. B., Konovalenko I. S., Tikhonova K. V. Perturbed stable systems on the plane, 2. Moscow State University Mechanics Bulletin. n. 1, 53-57 pp., 2017.

14. Alexandrov V. V., Krasilnikov I. E., Torres A. Absolute stability of one-dimensional oscillating systems. // In. Bulgakov's problem of the maximum deviation and its application. M .: Moscow State University, 48-57 pp., 1993.

15. Alexandrov V. V., Bugrov D. I., Zhermolenko V. N., Konovalenko I. S. The reachable set and robust stability of perturbed oscillatory systems. Moscow State University Mechanics Bulletin. 2021 (accepted to print).

16. Alexandrova O. V. The generalized resonance and limit cycle in the phase plane. Moscow State University Mechanics Bulletin. n. 1, 92-98 pp., 1993.

17. Althoff M. Manual of the Continuous Reachability Analyzer (CORA). Technische University of Munchen, 85748 Garching, Germany, 69 p., 2015.

18. Andronov A. A., Pontryagin L. S. Rough systems. Report for the Academy of Sciences of the USSR, T. 14, n. 5, 247-250 pp., 1937.

19. Andronov A. A., Vitt A. A., Haikin S. E. Theory of oscillations. – M. FIZMATLIT, 1959.

20. Angeles-Vázquez M. A. L. Tesis doctoral: Análisis matemático y computacional del modelo de Hodking Huxley modificado y simplificado. Puebla, Enero de 2016.

21. Arnold V. I. Geometric methods in the theory of ordinary differential equations. Izhevsk: Izhevsk Republican Typography, 400 p., 2000.

22. Arnold V. I. Ordinary differential equations. Methodical guide. M.: NAUKA, 272 p., 1984.

23. Arrowsmith D., Place C. M. Dynamical Systems: Differential Equations, Maps, and Chaotic Behaviour. Chapman and Hall/CRC, 330 p., 1992.

24. Atkinson K. E. An introduction to numerical analysis, 2nd ed. John Wiley & Sons, 712 p., 1989.

25. Bae Y. K., Barr M. M. Sensory roles of neuronal cilia: cilia development, morphogenesis, and function in C. elegans. Frontiers in bioscience: a journal and virtual library, 13, 5959, 2008.

26. Baier R., Gerdts M., and Xausa I. Approximation of reachable sets using optimal control algorithms. Numer. Algebra Control Optim., 519-548 pp., 2013.

27. Bautin N. N. Behavior of dynamic systems near boundaries of stability regions.- M.-L., Gostekhizdat, 1949.

28. Berger D. R., Schulte-pelkum J., Bulthoff H. H. Simulating believable forward accelerations on a stewart motion platform. Max Planck Institute for Biological Cybernetics, Technical Report n. 159, 18 p., 2007.

29. Blagodatskikh V. I. Introduction to optimal control (linear theory): a textbook for universities. - Moscow: Visch. shc., 239 p., 2001.

30. Bolotov M. I., Gonchenko S. V., Gonchenko A. S., Grines E. A., Kazakov A. O., Levanova T. A., Lukyanov V.I. Andronov-Hopf bifurcation for streams and mappings. Methodical guide. Nizhny Novgorod: Nizhny Novgorod State University, 73 p., 2017.

31. Bulgakov B. Accumulation of perturbations in linear oscillatory systems with constant parameters. Report for the Academy of Sciences of the USSR, T.51, n. 5, 339-342 pp., 1946.

32. Bulgakov B. Applied theory of gyroscopes. Gostekhizdat, 356 p., 1955.

33. Chilan C. M., Conway B. A. A reachable set analysis method for generating near-optimal trajectories of constrained multiphase systems. J. Optim. Theory Appl., 167-194 pp., 2015.

34. Demidovich B. P. Lectures on the mathematical theory of stability. – M. FIZMATLIT, 472 p., 1967.

35. Dionyssiotis Y. Analyzing the problem of falls among older people. International journal of general medicine, n. 5, 805 p., 2012.

36. Echeverria M. Apuntes de Ecuaciones Diferenciales. Dpto. de Mat., Univ. de Extremadura, 1074 p., 2016.

37. Elsgolts L. Differential equations and the calculus of variations. – M. MIR PUBLISHERS, 440 p., 1977.

38. Gayek J. E. Approximating reachable sets for a class of linear systems subject to bounded control. University of Arizona campus repository: Dissertation for Ph. D., October 1984.

39. Goldwyn J. H., Shea-Brown E. The what and where of adding channel noise to the Hodgkin-Huxley equations. PLoS computational biology, 7(11), e1002247, 2011.

40. Gordillo-Dominguez J. L. Tesis de Maestro en Ciéncias Físicas: Evaluación de calidad de algoritmos de simulación dinámica y estimulación galvánica vestibular. Puebla, Enero 2020.

41. Hodgkin A. L., Huxley A. F. A quantitative description of membrane current and its application to conduction and excitation in nerve. The Journal of physiology, 117(4), 500-544 pp., 1952.

42. Huttenlocher D. P., Klanderman G. A., Ruclidge W. Comparing images using the Hausdorff distance. Transactions on patterns analysis and machine intelligence, vol. 15, n 9, 1993.

43. Jordan D. W. and Smith P. Nonlinear Ordinary Differential Equations. Oxford University press. 525 p., 2007.

44. Kanatnikov A. N. Qualitative theory of ordinary differential equations. Methodical guide. Moscow: Moscow State Technical University of N. E. Bauman, 44 p., 2016.

45. Konovalenko A., Avendaño J. A. R., Blas A. M., Cervera F., Myslivets E., Radic S., and Perez-Rodriguez F. Nonlocal electrodynamics of homogenized metal-dielectric photonic crystals. Journal of Optics, 2019.

46. Konovalenko I. S. Master's Thesis: Robust Stability Of The Oscillating Systems With Permanent Perturbations. Puebla, December 2016.

47. Konovalenko I. S. On the construction of the reachable set in a neighborhood of a periodic attractor. Moscow State University Mechanics Bulletin. n. 3, 67-71 pp., 2020.

48. Lee E. B., Markus L. Foundations of optimal control theory. New York, Wiley, 576 p., 1967.

49. Leofante F., Schupp S., Abraham E., Tacchella A. Engineeering Controllers for Swarm Robotics via Reachability Analysis in Hybrid Systems. 33rd International ECMS European Conference on Modelling and Simulation, European Council for Modeling and Simulation, 407–413 pp., 2019.

50. Luo A. C. J., Lakeh A. B. Analytical solutions for period-m motions in a periodically forced van der Pol oscillator. Int. J. Dynam. Control, 99-115 pp., 2013.

51. Malkin I. Theory of Stability of Motion. Gostekhizdat, 1952.

52. Markov A. A. Rasprostranenie zakona bol'shih chisel na velichiny, zavisyaschie drug ot druga, Izvestiya Fiziko-matematicheskogo obschestva pri Kazanskom universitete, 2-ya seriya, T. 15, 135–156 pp., 1906.

53. Markov A.A. Extension of the limit theorems of probability theory to a sum of variables connected in a chain, reprinted in Appendix B of: R. Howard. Dynamic Probabilistic Systems, volume 1: Markov Chains. John Wiley and Sons, 1971.

54. Moser M.-B. and Moser E. I. The Nobel Prize in Physiology or Medicine 2014 for their discoveries of cells that constitute a positioning system in the brain, 2014.

55. Novikova A. O. Construction of Reachable Sets of Two-Dimensional Nonlinear Controlled System By The Pixel Method. Computational Mathematics and Modeling, 444–459 pp., 2016.

56. Ospeck M. Auditory Nerve Spike Generator Modeled as a Variable Attenuator Based on a Saddle Node on Invariant Circle Bifurcation. PloS one, 7(9), e45326, 2012.

57. Pecsvaradi T., and Narendra K. S. Reachable sets for linear dynamical systems. Information and Control, 319-344 pp., 1971.

58. Polyak B. T., Shcherbakov P. S. Robust stability and control. – M. Nauka, 303 p., 2002.

59. Pontryaguin L. S. Ordinary differential equations. – M. FIZMATLIT, 1974.

60. Prakash M. V. S., Mahindrakar A. D., Pasumarthy R. Computation of outer approximation to reachable set for cooperative systems: Application to an epidemic spreading model. 27th Mediterranean Conference on Control and Automation (MED), 2019.

61. Rasmussen M., Rieger J., and Webster K. N. Approximation of reachable sets using optimal control and support vector machines. J. Comput. Appl. Math., 68-83 pp., 2017.

62. Ree Chay T., Seek Lee Y.. How and Why Do Neurons Generate Complex Rhythms with Various Frequencies? Discrete Dynamics in Nature and Society, Vol. 2, 215-242 pp., 1998.

63. Riedl W., Baier R., Gerdts M. Optimization-based subdivision algorithm for reachable sets. Mathematics Subject Classification. 33 p., 2016.

64. Roublev I. V. A numerical algorithm for construction of three-dimensional projections for reachability sets. 8th IFAC Symposium on Nonlinear Control Systems University of Bologna, Italy, September 1-3, 2010.

65. Rote G. Computing the minimum Hausdorff distance between two point sets on a line under translation. Information Processing Letters 38, 123-127 pp., 1991.

66. Rucklidge W. Efficient Visual Recognition Using the Hausdorff Distance. Lecture Notes in Computer Science, vol 1173. Springer, Berlin, Heidelberg, 1996.

67. Sadovnichiy V. A., Alexandrov V. V., Alexandrova T.B., Vega R., Konovalenko I. S., Soto E., Tikhonova K.V., Gordillo-Dominguez H. L., Gonzales O. About galvanic correction of the vestibular activity of the pilot in the visual control of flight. Moscow State University Mechanics Bulletin. n. 1, 34-41 pp. 2019.

68. Shilnikov L. P., Shilnikov A., Turaev D. and Chua L. Methods of qualitative theory in nonlinear dynamics, Part I, Part II World Scientic, Singapore, 942 p., 2001.

69. Simiu E. Chaotic transitions in deterministic and stochastic dynamical systems, Princeton University Press, E.E.U.U., 224 p. 2002.

70. Temoltzi-Ávila R. Tesis de Maestro en Ciéncias Matemáticas: Síntesis de ciclos limite y auto oscilaciones estables. Puebla, Agosto 2007.

71. Temoltzi-Ávila R., Ávila-Pozos R., and Cruz-Castillo R. Estabilidad robusta en un sistema mecánico controlable. Padi Boletín Científico de Ciencias Básicas e Ingenierías del ICBI 5.9, 2017.

72. Tikhonov A. N., Vasil'eva A. B. and Sveshnikov A. G. Differential Equations. – M. FIZMATLIT, 1980.

73. Tran D. H., Yang Th. X., Luan Th., Nguyen V., Manzanas Lopez D., Xiang W., T Johnson T., Nguyen L. V., Musau P. Parallelizable Reachability Analysis Algorithms for Feed-Forward Neural Networks. Conference: FormaliSE 2019, Montreal, Canada, March 2019.

74. Ushakov V. N., Matviychuk A. R., Ushakov A. V. Numerical methods for construction reachability sets of dynamical systems.

Institute of Mathematics and Mechanics, Russian Academy of Sciences and Ural Federal University, Russia, 144-151 pp., 2012.

75. Zhermolenko V. N. Limit cycles on the phase plane. // In. Bulgakov's problem of the maximum deviation and its application. M .: Moscow State University, 35-48 pp., 1993.